9-24-2015 12:00 AM

Role of Cerebrovascular Abnormality in Neurodegenerative Disease and Subcortical Ischemic Disease: CT Perfusion and PET Imaging

Jun Yang
The University of Western Ontario

Supervisor
Ting-Yim Lee
The University of Western Ontario

Graduate Program in Medical Biophysics
A thesis submitted in partial fulfillment of the requirements for the degree in Doctor of Philosophy

Role of Cerebrovascular Abnormality in Neurodegenerative Disease and Subcortical Ischemic Disease: CT Perfusion and PET Imaging

(Thesis format: Integrated-Article)

by

Jun Yang

Graduate Program in Medical Biophysics

A thesis submitted in partial fulfillment

of the requirements for the degree of

Doctor of Philosophy

The School of Graduate and Postdoctoral Studies

The University of Western Ontario

London, Ontario, Canada

Abstract

Clinical studies indicate that about 30% ~ 50% of patients have cognitive impairment after the first or recurrent stroke. Ischemic injury, particularly subcortical lesions, caused by stroke has been demonstrated to further exacerbate cognitive impairment of Alzheimer's disease (AD) and vascular dementia. However, the mechanisms whereby cerebrovascular abnormalities contribute to neurodegeneration at early stage of disease and eventually to cognitive decline remain unclear. CT perfusion and positron emission tomography (PET) were used to investigate early mechanisms in a rat comorbid model of cerebral ischemia (CI) and β-amyloid (Aβ, a pathological hallmark of AD) toxicity, and in patients with small subcortical ischemic lesions.

Chapter 2 investigates the early hemodynamic disturbances within the first month after transient CI insult in the presence of Aβ toxicity in the comorbid rat model. CT perfusion revealed significantly lower cerebral blood flow (CBF) and blood volume (CBV) at acute phase due to the transient ischemia, and increased CBF and CBV in the ipsilateral striatum of CI+Aβ and CI groups at the first week post ischemia. These results suggest that CI is the primary driving factor of cerebrovascular abnormalities at early stage, and prolonged hyperperfusion and hypervolemia may imply reperfusion-related injury and downstream inflammation. Chapter 3 further addresses these questions with CT Perfusion-PET imaging.

Chapter 3 describes the temporal profiles of blood-brain barrier (BBB) disruption and neuroinflammation over 3 months after CI with and without concurrent Aβ toxicity in the comorbid rat model. CT perfusion showed significantly higher BBB permeability surface product (BBB-PS) in the ipsilateral striatum of CI+Aβ group at day 7, month 2 and 3, as compared to CI and sham group. PET imaging revealed the highest level of neuroinflammation

as reflected by the significantly increased ^{18}F-FEPPA uptake due to microglial activation in the striatal lesion of CI+Aβ group at day 7 and 14. The temporal features of these cererbrovascular and cellular changes may serve as early imaging biomarkers for development of cognitive impairment in high-risk patients post ischemic insult.

Chapter 4 investigates the temporal changes in BBB-PS and cerebral perfusion using CT perfusion over the first 3 months after small lacunar/subcortical stroke in patients. This longitudinal investigation suggests the chronic BBB leakage detected by CT perfusion may contribute to cognitive impairment and associated pathology in lacunar/subcortical stroke.

Overall, the imaging results presented in this thesis have demonstrated that BBB-PS, CBF, CBV and activated microglia can be used as imaging biomarkers for delineating the early pathogenic pattern and underlying contribution of cerebral ischemia to the disease development in the animal comorbid model and subcortical stroke patients.

Keywords

cerebral ischemia, β-amyloid toxicity, cerebral blood flow, cerebral blood volume, blood-brain barrier, microglia, neuroinflammation, subcortical/lacunar ischemic lesion, Alzheimer disease, cognitive impairment, positron emission tomography, CT perfusion

Co-Authorship Statement

The contents of Chapter 2 have been adapted from the original research manuscript entitled "Hemodynamic Effects of Combined Focal Cerebral Ischemia and Amyloid Protein Toxicity in a Rat Model: A Functional CT Study" published in *PLoS ONE*. 2014, 9(6): e100575 by J. Yang, C.D. d'Esterre, Z. Amtul, D.F. Cechetto and T.Y. Lee. D.F. Cechetto, T.Y. Lee and I were responsible for the design of the study, collecting and analyzing the data, and writing the manuscript. C.D. d'Esterre was responsible for editing the manuscript. Z. Amtul was responsible for performing the histology and editing the manuscript.

Chapter 3 has been adapted from the original research manuscript entitled "Breakdown of Blood-Brain Barrier and Neuroinflammation in a Rat Model of Combined Focal Cerebral Ischemia and Amyloid Protein Toxicity: A Longitudinal CT and PET Study" submitted to *Frontiers in Aging Neuroscience* by J. Yang, L. Morrison, L. Wang, N. Cockburn, D.F. Cechetto and T.Y. Lee. I was responsible for performing experiments and histology, collecting and analyzing the data, and writing the manuscript. T.Y. Lee and D.F. Cechetto were responsible for the study design and editing the manuscript. L. Morrison and L. Wang were responsible for technical assistance and data collection. N. Cockburn was responsible for producing the radiotracer used in the study.

Chapter 4 has been adapted from the original research manuscript entitled "Temporal Changes in Blood-Brain Barrier Permeability and Cerebral Perfusion in Lacunar/Subcortical Ischemic Stroke" submitted to *BMC Neurology* by J. Yang, C.D. d'Esterre, S. Ceruti, G. Roversi, A. Saletti, E. Fainardi and T.Y. Lee. I was responsible for collecting and analyzing the data, and writing the manuscript under supervision of E. Fainardi and T.Y. Lee. C.D. d'Esterre, E. Fainardi

and T.Y. Lee were responsible for the design of the study and editing the manuscript. S. Ceruti, G. Roversi and A. Saletti were responsible for collecting the clinical data.

Acknowledgements

The work contained within this thesis truly reflects a collaborative effort and support from a number of great scientists, physicians and associates. First and foremost, I would like to thank my supervisor, Dr. Ting-Yim Lee for his tremendous support during my PhD training, allowing me to search my own way while guiding me to the right direction at the same time. His passion and knowledge as well as dedication to both clinical and experimental work have always inspired me. It is a privilege to work with a scientist like him, giving me great opportunities to foster my independent thinking and problem-solving ability in research and science.

Furthermore, I also want to thank my advisory committee members, Dr. David Cechetto and Dr. Rob Bartha. They made a significant part for expanding my knowledge in the relevant field, and providing me with their insights, comments and encouragement. Particularly, I would like to show my appreciation for Dr. David Cechetto who gave me a learning opportunity in his lab and let me work with his excellent team. His expertise helped me address questions through multiple approaches.

In addition, I would like to thank all of the members in the Lee lab who assisted me in various aspects over the last six years. Dr. Christopher d'Esterre has made important contributions to my manuscript editing and provided helpful thoughts and conversations. I want to thank Laura Morrison, Jennifer Hadway and Lise Desjardins for their outstanding technical assistance in my experiments, which reflected their impressive professionalism and productivity. Thank you very much to Laura Morrison for always ensuring our experiments prepared and went smoothly, no matter nights and weekends. I also would like to thank Dr. Xiaogang Chen and Fang Su for their great help in image processing and registration. Moreover, I would like to

thank Drs. Errol Stewart, Aaron So and Yong Wang for all kinds of insightful discussions and encouragement. Lastly, I want to thank all the graduate students, summer students and colleagues in the Lee lab who have made my time at Robarts and UWO more enjoyable.

Beyond the Lee lab, I want to thank my collaborator and friend in Italy, Dr. Enrico Fainardi for collecting and sharing clinical imaging data with us. The collaborative research with him opens more channels for me to learn clinical knowledge of the diseases and to spark new ideas about my study. I also would like to thank Lynn Wang and Zareen Amtul from Dr. Cechetto's lab for their great assistance on immunohistochemistry.

Special thanks to Anne Leaist, who helped me tirelessly no matter the time of day. Her detailed, organized and hard work devoted to the group has made distinguished support for everyone in the lab. Her caring about everyone, meaningful conversations and friendship have helped me go through stresses and obstacles that I encountered in both my life and work.

Most importantly, I must say thank you to my parents and wife for their unconditional support and love in my life.

Epigraph

“When I was young, I observed that nine out of ten things I did were failures. So I did ten times more work.”

“Progress is impossible without change, and those who cannot change their minds cannot change anything.”

- George Bernard Shaw

Table of Contents

Abstract ····· **ii**

Co-Authorship Statement ····· **iv**

Acknowledgements ····· **vi**

Epigraph ····· **viii**

Table of Contents ····· **ix**

List of Tables ····· **xv**

List of Figures ····· **xvi**

List of Abbreviations ····· **xvii**

List of Appendices ····· **xx**

Chapter 1 ····· **1**

Introduction ····· **1**

1.1 Introduction ····· 1

1.2 Comorbidity of cerebrovascular disease and AD ····· 2

1.2.1 Comorbidity: prevalence and risk factors ····· 2

1.2.2 Impact of ischemic lesion on cognition ····· 4

1.3 Stroke and ischemic injury ····· 5

1.3.1 Causes, subtypes and symptoms of stroke ····· 5

1.3.2 Cerebral ischemia ····· 6

1.3.3 Disruption of blood-brain barrier ····· 8

1.3.4 Cerebrovascular abnormality in aged brains ····· 11

1.4 β-amyloid burden in aged brains ····· 12

1.4.1 Amyloid pathology and controversy about amyloid hypothesis ····· 13

1.4.2 Mechanism of Aβ neurotoxicity ····· 15

1.5 Effects of combined ischemic and amyloid injuries ····· 16

1.5.1 Inflammatory influence of CI and Aβ on the brain ····· 16

1.5.2 Activated microglia: a biomarker for imaging neuroinflammation in vivo? ····· 17

1.5.3 Animal comorbid model of cerebral ischemia and Aβ toxicity ····· 19

1.6 Medical imaging in cerebral ischemia and AD ····· 21

1.6.1 Positron emission tomography ····· 21

1.6.2 Magnetic resonance imaging ····· 24

1.6.3 CT perfusion imaging ····· 26

1.7 Research objectives ····· 31

1.8 References ····· 32

Chapter 2 ····· 52

Hemodynamic Effects of Combined Focal Cerebral Ischemia and Amyloid Protein Toxicity in a Rat Model: A Functional CT Study ····· 52

2.1 Introduction ····· 52

2.2 Methods and Materials ····· 54

2.2.1 Animals ····· 54

2.2.2 Surgical procedure ····· 54

2.2.3 CT perfusion scanning ····· 55

2.2.4 Image post-processing and analysis ····· 56

2.2.5 Immunohistochemistry ····· 56

2.2.6 Statistical analysis ····· 57

2.3 Results ····· 57

2.3.1 CTP functional maps ····· 57

2.3.2 Cerebral ischemia and hyperperfusion post ischemia ····· 59

2.3.3 Comparison of hemodynamics between Aβ+CI and Aβ alone model ····· 61

2.3.4 Vascular pathology after induced CI and Aβ ····· 63

2.4 Discussion ····· 64

2.5 Conclusion ····· 68

2.6 References ····· 69

Chapter 3 ····· 75

Breakdown of Blood-Brain Barrier and Neuroinflammation in a Rat Model of Combined Focal Cerebral Ischemia and Amyloid Protein Toxicity: A Longitudinal CT and PET Study ····· 75

3.1 Introduction ····· 75

3.2 Methods and Materials ····· 77

3.2.1 Animals and surgery ····· 77

3.2.2 CT perfusion study ····· 77

3.2.3 PET study ····· 78

3.2.4 Image analysis ····· 79

3.2.5 Immunohistochemistry ····· 79

3.2.6 Statistical analysis ····· 80

3.3 Results ····· 80

3.3.1 Changes in BBB permeability ····· 80

3.3.2 PET imaging of neuroinflammation ····· 82

3.3.3 Cerebral perfusion ····· 84

3.3.4 IgG leakage and microglial activation ····· 86

3.4 Discussion ····· 87

3.5 Conclusion ····· 91

3.6 References ····· 92

Chapter 4 ····· 98

Temporal Changes in Blood-Brain Barrier Permeability and Cerebral Perfusion in Lacunar/Subcortical Ischemic stroke ····· 98

4.1 Introduction ····· 98

4.2 Methods and Materials ····· 100

4.2.1 Subjects ····· 100

4.2.2 CT perfusion acquisition protocol and functional maps ····· 101

4.2.3 Image registration and analysis ····· 101

4.2.4 Statistical methods ····· 102

4.3 Results ····· 102

4.3.1 Patient data ····· 102

4.3.2 Temporal changes in blood-brain barrier permeability ····· 103

4.3.3 Cerebral hemodynamics ····· 105

4.4 Discussion ····· 107

4.5 Conclusion ····· 110

4.6 References ····· 111

Chapter 5 ····· 114

Conclusion and Future Work ····· 114

5.1 Summary ····· 114

5.2 Disturbances of cerebral perfusion ····· 115

5.3 Changes in BBB permeability/integrity ····· 116

5.4 Activation of microglia and neuroinflammation ····· 116

5.5 Clinical relevance and implications ····· 117

5.6 Future work ····· 118

5.6.1 Examination of cognitive performance ····· 118

5.6.2 Amyloid or tau imaging ····· 119

5.6.3 Long-term cognition and imaging study for patients with subcortical/lacunar lesions …… 120

5.7 References…… 121

Appendix A: Animal Ethics Approval for the work contained within Chapter 2 …… 122

Appendix B: Animal Ethics Approval for the work contained within Chapter 3…… 123

Appendix C: Human Ethics Approval for the work contained within Chapter 4 …… 124

Appendix D: Copyright Agreement…… 134

Appendix E: Absolute values of CBF and CBV …… 135

Curriculum Vitae …… 136

List of Tables

Table 4-1: Characteristics of patients with and without lacunar/subcortical lesion…… 103

List of Figures

Figure 1-1: Schematic of the blood-brain barrier in the neurovascular unit……...….. 9

Figure 1-2: Blood flow-scaled IRF, and arterial and tissue TDC curves……..... 29

Figure 2-1: Cerebral blood flow maps……. 58

Figure 2-2: Cerebral blood volume maps ……... 59

Figure 2-3: Evolution of striatal CBF and CBV over four-week period ……..... 60

Figure 2-4: Hemodynamic effects of Aβ+CI and Aβ alone models …….... 62

Figure 2-5: Histology of cerebral microvessels in control, CI and Aβ+CI groups…….. 63

Figure 3-1: Relative BBB-PS in the ipsilateral striatum of the three groups over the first 3 months…….. 81

Figure 3-2: Quantitative BBB-PS maps……... 82

Figure 3-3: Relative ^{18}F-FEPPA uptake in the ipsilateral striatum…….. 83

Figure 3-4: Relative CBF and CBV in the ipsilateral striatum…… 85

Figure 3-5: Immunohistochemistry of IgG leakage and activated microglia…….. 86

Figure 4-1: Blood-brain barrier permeability in the non-infarcted ipsilateral basal ganglia and thalamus……. 104

Figure 4-2: BBB-PS maps in a patient with a subcortical infarct in right putamen……..... 105

Figure 4-3: CBF and CBV in the non-infarcted ipsilateral basal ganglia and thalamus…….. 106

List of Abbreviations

Aβ	β-Amyloid protein
AD	Alzheimer's disease
AIF	Arterial input function
APP	Amyloid precursor protein
BBB	Blood-brain barrier
CAA	Cerebral amyloid angiopathy
CBF	Cerebral blood flow
CBV	Cerebral blood volume
CI	Cerebral ischemia
$CMRO_2$	Cerebral metabolic rate of oxygen
CNS	Central nervous system
COX-2	Cyclooxygenase-2
CSF	Cerebrospinal fluid
CT	Computed Tomography
CTP	Computed Tomography Perfusion
DWI	Diffusion weighted imaging

ET-1	Endothelin-1
^{18}F-FDG	F-18 labeled 2-fluoro-2-deoxy-d-glucose
GABA	Gamma-Aminobutyric Acid
IgG	Immunoglobulin
IL	Interleukin
IRF	Impulse Residue Function
LRP1	Low-density lipoprotein receptor related protein 1
MCAO	Middle cerebral artery occlusion
MCI	Mild cognitive impairment
MMP	Matrix metalloproteinases
MRI	Magnetic resonance imaging
mRS	modified Rankin Score
MTT	Mean transit time
NECT	Non-enhanced CT
NFT	Neurofibrillary tangles of tau protein
PET	Positron emission tomography
PS	Permeability surface area product

PWI	Perfusion weighted imaging
RAGE	Receptor for advanced end glycation products
ROI	Region of Interest
ROS	Reactive oxygen species
TDC	Time-density curve
TIA	Transient ischemic attack
TNF-α	Tumor necrosis factor-α
TSPO	Translocator protein
VCI	Vascular cognitive impairment
WML	White matter lesion

List of Appendices

Appendix A: Animal Ethics Approval for the work contained within Chapter 2 entitled "Hemodynamic Effects of Combined Focal Cerebral Ischemia and Amyloid Protein Toxicity in a Rat Model: A Functional CT Study"……..... 122

Appendix B: Animal Ethics Approval for the work contained within Chapter 3 entitled "Breakdown of Blood-Brain Barrier and Neuroinflammation in a Rat Model of Combined Focal Cerebral Ischemia and Amyloid Protein Toxicity: A Longitudinal CT and PET Study"…….. 123

Appendix C: Human Ethics Approval for the work contained within Chapter 4 entitled "Temporal Changes in Blood-Brain Barrier Permeability and Cerebral Perfusion in Lacunar/Subcortical Ischemic Stroke"……...… 124

Appendix D: Copyright Agreement……..... 134

Appendix E: Absolute values of CBF and CBV……..…….....135

Chapter 1

Introduction

1.1 Introduction

Cerebrovascular disease is recognized as a common cause of disability and functional impairment. Cerebrovascular lesions contribute to neuronal loss/degeneration and eventually cognitive decline. Particularly, stroke is a devastating cerebrovascular disease and the second leading cause of death in the world (1). In developed countries, about 75% of individuals above 65 years old could experience a stroke (1, 2). The proportion of stroke patients having permanent disability and cognitive deficits is estimated to be 30-50% (3-6). In United States and Canada, currently about 795,000 (7) and 315,000 people (8) respectively are affected by a new or recurrent stroke. Furthermore, current clinical evidence suggests that stroke is associated with Alzheimer's disease (AD) (9-12), a neurodegenerative disorder, which is found in over 70% of all dementia cases in the elderly population (13). With the increase in the elderly population, the prevalence of stroke and dementia also rises. One direct consequence of a large population with increasing stroke incidence is the escalated cost of treatment and rehabilitation.

Ischemic injury, particularly subcortical lesions caused by stroke has been demonstrated to further exacerbate cognitive impairment of AD and vascular dementia. However, the mechanisms whereby cerebrovascular abnormalities contribute to neurodegeneration at early stage of disease and eventually to cognitive decline remain unclear. In this thesis, CT perfusion and positron emission tomography (PET) were used to investigate early mechanism and temporal changes in cerebral perfusion, blood-brain barrier and neuroinflammation in a rat comorbid

model of cerebral ischemia (CI) and β-amyloid (Aβ, a pathological hallmark of AD) toxicity, and in patients with small subcortical ischemic lesions.

1.2 Comorbidity of cerebrovascular disease and AD

Many clinical and pathological studies have demonstrated that AD and cerebrovascular diseases such as ischemic stroke not only coexist, but also interact with or affect each other in the aging population. These two morbidities share some common vascular risk factors, and cerebrovascular pathology precedes and/or accompanies AD-related neurodegeneration (12, 14, 15). Regional reductions in cerebral blood flow (CBF) and glucose metabolism, which are typical indications of ischemia, are also frequently observed with cognitive impairment in prodromal AD (mild cognitive impairment, MCI) and AD subjects (16-19).

1.2.1 Comorbidity: prevalence and risk factors

Cerebrovascular lesions can be present in 30~50% of AD patients (9, 20, 21), and stroke accounts for a large portion of these lesions (22). Similarly, classical AD pathology, β-amyloid (Aβ) protein plaques and neurofibrillary tangles of tau protein (NFT), are present in 40% of vascular dementia patients (dementia due to vascular factors affecting the brain) (23). It is estimated that AD is three times more likely to occur in the elderly after a stroke episode or transient ischemic attack (24). Recent studies indicate that the presence of silent (asymptomatic) stroke doubled the risk of AD development in the age of 60-90 (25). These studies reported that subcortical ischemic and lacunar infarcts were associated with cognitive decline in AD patients (12, 15, 26-29). Particularly, the Nun study demonstrated that subcortical ischemic infarcts were

associated with a 20-fold higher risk to have dementia than the subjects without the concomitant cerebrovascular pathology (15). Furthermore, in rodent models, focal cerebral ischemia induces more APP expression (30, 31). On the other hand, AD patients have higher risks for developing stroke and cerebrovascular disease (32, 33). Cerebral amyloid angiopathy (CAA), which is seen in more than 80% of AD cases, is associated with a higher risk of microhemorrhage and stroke (34). AD and CAA are also associated with chronic blood-brain barrier/microvascular damage (35-37).

Some important vascular risk factors are shared by both stroke and AD. There is accumulating evidence that vascular risk factors associated with stroke can also contribute to the risks for developing AD and vascular dementia in age above 65 (11). Besides age, many epidemiological studies (Rotterdam study, Honolulu Asia aging study, Nun study, Framingham study, Uppsala, Sweden and Kuopio study, Chicago Health and Aging project, and others) have suggested that the risk factors for stroke, such as atherosclerosis, hypertension, atrial fibrillation, coronary artery disease, diabetes, smoking and high fat diet can substantially increase the probability of developing AD or other dementia (38). Among these risk factors, atherosclerosis, atrial fibrillation and hypertension are the three common causes of stroke in elderly. Carotid artery wall thickening and plaques due to atherosclerosis are strongly related to deterioration of cognitive function in late-onset AD (39). Longitudinal studies indicate that high systolic and diastolic blood pressure (hypertension) predicts cognitive dysfunction in AD at 15-25 years later (40, 41). Hypertension has also been shown to increase the risk of prodromal AD (40). Atrial fibrillation, a known risk factor for ischemic stroke, is also strongly linked to AD (42). All these vascular risk factors are commonly known to reduce CBF in the aged brain. For instance, atherosclerosis can reduce CBF (hypoperfusion) and cause silent stroke, which is involved in the

development of AD and white matter lesions (WMLs). Some longitudinal imaging studies reported significant CBF reductions in the temporal lobe and hippocampus in MCI patients who eventually converted to AD (17, 18, 43-45). MCI is considered a potential transitional phase between normal aging and dementia. Therefore, measurement of cerebral perfusion may be useful in predicting early disease progression.

1.2.2 Impact of ischemic lesion on cognition

Stroke impairs both motor and cognitive function. The risk of cognitive impairment after first ever stroke is twice as high as that in age-matched controls. With recurrent stroke this risk is even higher (46). Cognitive dysfunction among stroke patients is the most important cause for failure to resume daily independent life and prior occupation. The most common cognitive impairments post stroke are aphasia and hemispatial neglect. The other cognitive deficits include impaired working memory, information processing speed, attention and learning (6, 47, 48). The type and severity of cognitive symptoms can be different, depending on the location and size of the ischemic lesion and infarct. However, controversy does exist and some studies showed no association between cognitive dysfunction and size of lesion (49-51). In fact, some small lesions such as lacunar or subcortical ischemic infarcts may exert large long-term influence on cognition (15, 28, 50, 52), particularly in the presence of concurrent WMLs. The detrimental effect of lacunar and subcortical ischemic lesion on cognition is possibly due to the interruption of prefrontal and orbitofrontal cortical-subcortical circuits by the lesions (53, 54). These circuits are highly involved in executive function, working memory, language, attention regulation and mood, so the clinical symptoms can be loss of executive functioning and memory, deficiency in speech and attention, and depression. The anatomical regions involved in lacunar and subcortical

stroke include the striatum (i.e. caudate and putamen, a part of basal ganglia), thalamus, internal capsule, globus pallidus and surrounding white matter. In addition, hypoperfusion and hypometabolism in cortical areas and WMLs are commonly observed along with lacunar and subcortical ischemic lesions (53, 55, 56). It is difficult to determine the individual contribution of each type of lesion to the cognitive dysfunction because they commonly share the same risk factors and coexist in the affected brain (36). Nevertheless, the level of cognitive deterioration is linked to the extent and number of lacunar and subcortical ischemic lesions present (54). Therefore, more attention should be paid to temporal changes of cognitive function and cerebral vasculature in the presence of lacunar and subcortical ischemic lesions.

1.3 Stroke and ischemic injury

The human brain receives about 20% of cardiac blood output and consists of more than 100 billion neurons. Brain function depends on the coordinated activity of various neuronal networks which in turn depends on a continuous supply of oxygen and nutrients such as glucose by blood flow. In stroke, interruption of blood flow causes shortage of oxygen and nutrients to the brain, and then neurons start to lose bioactivity and eventually die in minutes if no reperfusion occurs (57).

1.3.1 Causes, subtypes and symptoms of stroke

Stroke is caused by interruption of blood flow to the brain or rupture of blood vessels in the brain. The majority of stroke is ischemic stroke, which accounts for about 85% of cases (58, 59). In ischemic stroke, blood vessels supplying the brain are completely or partially blocked by a

blood clot (1, 60). There are two types of blood clot, thrombus (caused by a clot that forms in an artery to the brain) and embolus (caused by a systemically developed clot that travels to the brain). In addition to a major ischemic stroke that leads to neurological symptoms and damages, transient ischemic attack (TIA or mini stroke) results in a brief episode of symptoms that resolve within 24 hours and is due to temporary blockage of cerebral blood vessels (61). The second type of stroke is hemorrhagic stroke, accounting for 15% of all stroke cases (59), where cerebral blood vessels leak or burst due to uncontrolled high blood pressure (hypertension) or abnormal structures (e.g. aneurysm). The bleeding disrupts the normal CBF and kills neurons by flooding the leakage region and releasing neurotoxic substances.

Clinical symptoms of stroke may manifest with focal weakness, reduced motor strength and coordination (ataxia), loss of sensory function (paralysis), and language/speech impairment (aphasia and dysarthria) (62). Neurological deficits include impaired cognition, visual disturbance, neglect, impaired skilled motor function (ideomotor apraxia) and aphasia (63). Hemi-spatial neglect (failure to respond to stimuli on the side contralateral to the stroke) typically occurs in more than 40% of patients with right hemispheric stroke, while aphasia (language impairment) occurs in 15% to one third of patients with left hemispheric stroke (64).

1.3.2 Cerebral ischemia

Cerebral ischemia (CI) is a condition that occurs when there is not enough blood flow to the brain to meet metabolic demand. CI leads to the lack of oxygen and glucose supply as well as neuronal death (65). There are two kinds of CI: (1) focal ischemia is confined to a specific region of the brain. Focal CI reduces blood flow to the particular brain region, increasing the risk of

neuronal death in the area. It can be either caused by thrombosis or embolism; (2) global ischemia can affect wide areas of the brain. For global ischemia, blood flow to the brain is severely interrupted or reduced. This is usually triggered by cardiac arrest. If adequate circulation is restored within a short period of time, symptoms may be transient. However, if there is a longer duration of global ischemia before reperfusion, brain damage can be permanent (irreversible).

In the ischemic cascade of CI, severe and prolonged reductions in CBF result in deprivation of oxygen and glucose delivery to the brain. As a result, a low level or absence of available glucose can lead to dramatic decline of ATP, which is the critical energy source for maintaining normal neuronal activity (66). Ionic perturbations and accumulation of toxic substances will occur after ATP is completely depleted. At first, the Na^+/K^+ transporter (pump), which is essential for activating signal propagation in axons, fails to maintain a normal Na^+/K^+ gradient due to depletion of ATP (67). The loss of Na^+/K^+ gradient and impairment of transporters can then cause a massive and rapid influx of Ca^{2+} and Na^+ into the cell and efflux of K^+ out of the cell (66, 68). The overload of intracellular Ca^{2+} greatly diminishes mitochondrial capacity of oxidative phosphorylation and in turn accelerates the breakdown of membrane phospholipids by activating phospholipases, thus degrading cell membrane and causing irreversible cell damages. In addition, the increase in intracellular Ca^{2+} induces the release of excessive glutamate, an excitatory neurotransmitter, which can stimulate Ca^{2+} permeable receptors to allow more Ca^{2+} to enter cells (69). This glutamate/Ca^{2+}-triggered excitotoxicity then initiates apoptosis and triggers the release of reactive oxygen species and other destructive mediators that lead to more cell damages (68, 69).

The hemodynamic disruption has a great impact on the destiny of ischemic tissue. A reduction of 20% in CBF diminishes protein synthesis and disrupts intracellular pH in the affected tissue (70). A CBF reduction over 50% greatly attenuates ATP synthesis and action potential of neurons (71). Severe CBF reduction over 80% can cause electrolyte imbalance and neuronal death observed in ischemic stroke (71). In the center of the ischemic area, the CBF can drop below 10% of normal perfusion (72, 73). Neurons in the center of ischemic area lose their bioactivity and will die eventually (74). This necrotic core is the infarct. Between infarct rim and normal brain tissue is the penumbra, where CBF drops to about 20-60% of normal perfusion (72). The tissue within the penumbra is functionally impaired but still maintains ionic homeostasis, so this area is potentially salvageable if reperfusion is established by interventional or drug treatment (75, 76). If CBF in the penumbra does not return to a level that meets the minimal energy demand of neurons, the infarct area can further expand to the penumbra (77).

1.3.3 Disruption of blood-brain barrier

The blood-brain barrier (BBB) is an important and unique structure of the brain. A major component of the BBB is a lipophilic layer of endothelial cells that form the wall of capillaries (78). The endothelial cells are connected with tight junctions to form the barrier which is further strengthened by the basal lamina, pericytes and astrocyte foot processes (Figure 1-1). The BBB acts as a selective diffusion/exchange barrier at the capillary level and maintains a constant and secure microenvironment for the functioning of the brain (79). Under normal physiological condition, the BBB only allows small molecules such as oxygen and carbon dioxide (via free diffusion) as well as metabolically important species such as glucose, pyruvate, lactate and

amino acids (through specific transporters) to cross the barrier and access the brain parenchyma. Water, sodium, other hydrophilic ions and large peptides cannot freely cross the BBB to enter the brain (78, 80). The surface area of the BBB is about 20 m^2 in the human adult brain (81), and as a part of neurovascular unit, it cooperates closely with pericytes and glial cells to regulate the exchange of substances in and out of the brain (82), which in turn affects BBB permeability.

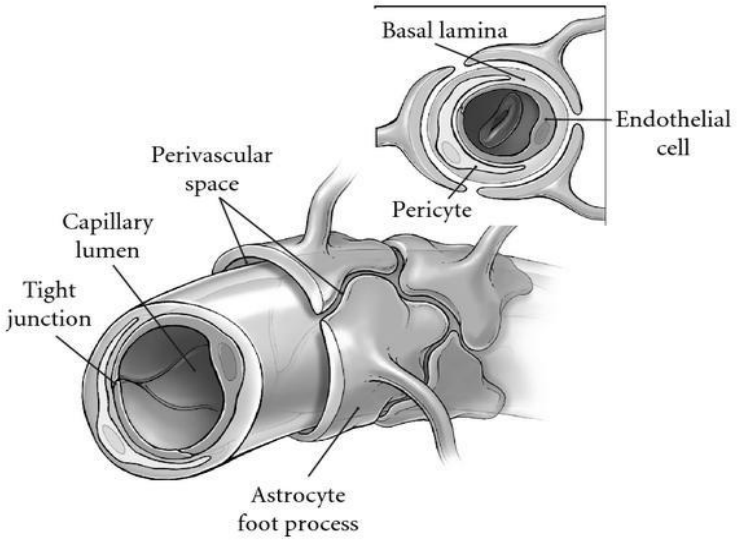

Figure 1-1: Schematic of the blood-brain barrier (BBB) in the neurovascular unit (83). The BBB consists of a layer of endothelial cells with tight junctions, surrounded by the basement membrane and pericytes. The functional integrity of the BBB is critically dependent on the basal lamina and endothelium, while pericytes and astrocytes regulate capillary blood flow and maintain/support vascular structure. Reprinted with permission.

Capillary barrier function is impaired or lost following focal CI (84, 85). This is due to ultrastructural alteration in endothelium-tight junction and loss of basal lamina (86, 87). After

loss of endothelial barrier function, as a result, vasogenic edema is induced as more water/fluid accumulates in the extravascular space of the brain (88-92). The blood plasma components such as albumin and immunoglobulins enter the brain via the leaky BBB, thus serving as a pathological indication of BBB leakiness. In addition, basal lamina, which prevents leakage of blood-borne elements into the surrounding cerebral tissue, is absent after CI (87), resulting in leaky BBB with increased permeability. The matrix of cerebral basal lamina contains laminin, collagen IV, fibronectin and other components. The expression of laminin and collagen IV is reduced after focal CI (87, 93, 94). Furthermore, extravasation of blood into the cerebral parenchyma (i.e. hemorrhagic transformation) of the ischemic lesion is observed in the region where the microvascular basal matrix is lost (94-96). Inflammatory responses following reperfusion can also cause damage to the cerebral microvessels by activating proteolysis of the microvascular matrix (97-99), thereby affecting BBB structure and permeability. The proteolysis is mediated by proteases such as matrix metalloproteinases MMP-2, MMP-3 and MMP-9. Several animal CI models have shown that these proteases contribute to the degradation of microvascular basal lamina matrix after middle cerebral artery occlusion (MCAO) (79, 100-103). In addition, the MCAO model in rats shows that microvascular permeability increases from day 3 to day 21 and peaks at day 7 after ischemia, particularly in the reperfused areas (104, 105). Taken together, the BBB is disrupted in CI, thus increased BBB permeability can serve as an imaging biomarker for predicting or explaining clinical outcome and brain damage (e.g. infarction, hemorrhage, white matter lesion or cerebral microvascular abnormality). Recent magnetic resonance imaging (MRI) and pathological studies show that increased BBB permeability and elevated level of cerebrospinal fluid (CSF) albumin are frequently found in patients with subcortical ischemic disease, lacunar stroke and leukoaraiosis (106-109). The

patients with hemorrhagic transformation and increased BBB permeability in the subcortical areas (white matter, basal ganglia and thalamus) tend to have poor functional outcome post stroke.

1.3.4 Cerebrovascular abnormality in aged brains

In the aged brain, a decrease of vessel density is frequently observed in subjects with ischemic stroke and AD (1, 35, 110). Pathologically, cerebral capillary degeneration is present in almost all AD brains in post-mortem studies. Morphologically, basement membrane of microvessels becomes thicker and capillary length is reduced in AD brains with cerebrovascular pathology (35). Arterioles and capillaries are tortuous and their lumen becomes narrow (35, 111). These morphological changes of cerebral vasculature are closely associated with subcortical lacunes, microbleeds and white matter abnormality (111), which are often detected by routine CT and FLAIR-based MRI. Lacunar stroke is caused by occlusion of small cerebral perforating arteries such as lenticulostriate artery, recurrent artery of Heubner or thalamoperforating artery. Most subcortical lacunes are clinically silent and usually manifest as gait problems and subtle cognitive dysfunction at acute state. However, recent research shows that lacunar and subcortical lesions actually have a larger impact on long-term cognitive deterioration and functional outcome than expected (15, 112-114), particularly for the lesions in the basal ganglia, thalamus and internal capsule (15). In addition, leukoaraiosis is one type of WML mainly caused by stenosis and hypoperfusion of multiple medullary arterioles. This arteriolar hypoperfusion leads to incomplete infarction of deep white matter, which manifests as periventricular and subcortical white matter hyperintensity on MRI (56). Moreover, CAA is mainly accumulated in the smooth

muscle cells of arterioles, thus causing vascular degeneration and stiffness. Aβ deposition in and around the vascular walls disrupts the basement membrane of arterioles and microvessels by upregulating matrix metalloproteinases (37).

Reduced vascular density and increased degeneration of vascular/capillary components can lead to regional hypoperfusion and BBB breakdown, which have been observed in patients with WMLs, subcortical ischemic lesions, AD and CAA (25, 36, 115). With advancing age, reduced CBF and compromised BBB function increase vulnerability of neurons and axons to ischemia. This may be a contributing mechanism of neurodegeneration in the early stage of AD and vascular dementia. Several animal studies have revealed that chronic cerebral hypoperfusion induces capillary abnormality, WMLs, microglia activation and memory impairment (115-121). Moreover, increased BBB permeability and extravasation of plasma proteins are found in patients with lacunar and subcortical ischemic lesions and WMLs, which are closely associated with cognitive impairment (106, 108, 109, 122, 123).

1.4 β-amyloid burden in aged brains

Alzheimer's disease and stroke are two contributing pathological factors to brain aging and cognitive dysfunction. Instead of acting separately, the two pathologies are frequently present in the same brain of elderly people (124). For instance, a connection between AD pathology and cerebrovascular disease is clearly demonstrated in the case of cerebral amyloid angiopathy, in which amyloid protein deposits in the blood vessels and adventitia, leading to cerebral microhemorrhage (125). In addition, the presence of silent stroke including subcortical ischemic and lacunar lesions can increase the risk of AD development and contribute to cognitive

impairment (12, 27, 126). In this section, the primary aim is to review an important neuropathological hallmark of AD, extracellular β-amyloid protein (Aβ), as well as its impact on the disease.

1.4.1 Amyloid pathology and controversy about amyloid hypothesis

The accumulation of Aβ aggregates around neurons is observed in the AD brain. However, the origin of Aβ, whether it is from the neuronal system or from other sources such as the blood pool, is still unclear. Aβ peptides are derived from a proteolytic cleavage of amyloid precursor protein (APP) by two enzymes, β- and γ-secretases (127). APP is highly expressed in the brain (128). Depending on the exact point of the cleavage by γ-secretase, three main forms/lengths of Aβ peptide are produced and individually contain 38-42 amino acids with molecular weight about 4.5 kDa. The three forms are Aβ38, Aβ40 and Aβ42, although the dominant Aβ peptides in the brain are Aβ40 and Aβ42 (129). In normal human CSF and plasma, the level of Aβ40 is respectively 10-fold and 1.5-fold higher than that of Aβ42 (130). However, Aβ42, the longer form of Aβ, is particularly prone to aggregate and produce toxic amyloid fibrils or oligomers than the more abundant Aβ40. In addition, recent studies suggest that soluble Aβ oligomer can be associated with synaptic dysfunction and cognitive impairment (131-134). The canonical amyloid hypothesis explains the development of AD, in which Aβ plays a central role (135). However, this hypothesis has one unexplained inconsistency which does not support the pathological role of Aβ plaques, that is, many elderly subjects can have Aβ plaques in the brain but do not show cognitive impairment (135). One plausible explanation, contrary to the amyloid hypothesis, is that Aβ plaque is the end-stage product of abnormal or sick neurons, rather than the cause of neurodegeneration. Furthermore, the vaccination trial against fibrillar Aβ (AN1792

trial) was halted due to meningoencephalitis in 6% of the patients in the treatment and no significant improvement on cognitive dysfunction (136, 137). Again, this result indicates that Aβ plaques may not be the therapeutic target as they may not be the real cause of cognitive dysfunction. Instead, further investigation is required to explain the source and pathogenic mechanism of soluble Aβ in the early stage of AD development (132, 135).

Familial AD (early onset subtype, 1~5% of AD cases) is related to genetic mutations (genes encoding APP, presenilin 1 and 2) producing excessive Aβ in the brain (129). The cause of most AD cases (late onset subtype) remains unclear but may be due to impaired clearance of soluble pre-fibrillar Aβ from the brain (138-141). For late-onset AD, the brain does not have increased Aβ production or APP overexpression, which is opposite to familial AD and transgenic animal models. Recent evidence demonstrates that amyloid load reaches a plateau early after onset of subtle clinical symptoms in AD patients and does not substantially increase in amount during clinical progression (142-145). In fact, the underlying pathogenic process of AD may begin many years before clinical signs appear. Therefore, the initial pathogenic event in the early stage of the disease must be a chronic and minimal perturbation to the neuronal system, without causing significant clinical symptoms. An alternative hypothesis is that the late-onset patients may have a failed clearance of toxic and soluble Aβ from the brain in the early stage due to deficient efflux transporters (e.g. LRP1, low-density lipoprotein receptor related protein 1) or increased influx transporters (e.g. RAGE, receptor for advanced end glycation products) for Aβ across BBB (146). As a result, Aβ starts to accumulate in the brain and exerts chronic effects on neurons. Reduced expression of LRP1, which clears Aβ from the brain, has been reported in the normal aged rodents and primates as well as in AD patients (139, 140, 146-149). Furthermore, elevated expression of RAGE in the cerebral microvessels of BBB is seen in AD brains, and this

leads to more Aβ entering the brain via RAGE (148, 150, 151). Aβ/RAGE interaction can further trigger downstream oxidative stress, neuroinflammation and release of endothelin-1 (ET-1) (146). However, the factors that trigger the changes in LRP1 or RAGE expression in AD are still not known. Aging and cerebrovascular diseases may be involved in up/down-regulation of LRP1 and RAGE, but more evidence is needed.

1.4.2 Mechanism of Aβ neurotoxicity

The exact mechanism of Aβ neurotoxicity is not known. However, mechanistic pathways have been proposed to elucidate the relationship between neuronal damage and Aβ. The first mechanism is Aβ-induced mitochondrial dysfunction. Some studies have found that exposure of rat neuronal mitochondria to Aβ leads to the decline in mitochondrial enzyme activity and the increase in mitochondrial membrane permeability (152-154). As a result, the dysfunctional mitochondria can swell and respiration is impaired, causing energy crisis such as the low cerebral glucose utilization seen in the AD brain. The second pathway for Aβ neurotoxicity is the induction of reactive oxygen species (ROS), which is also a consequence of mitochondrial dysfunction. Aβ has been shown to cause increased production of ROS and antioxidants may counteract Aβ-induced ROS (152). On the other hand, Aβ can also activate radical generating system in microglia (155, 156) and other cells (152, 157) in the brain by modulating specific NADPH oxidases. The induced ROS can cause downstream damages to membrane lipids and nucleic acids of neurons and other supportive cells to accelerate apoptosis.

1.5 Effects of combined ischemic and amyloid injuries

1.5.1 Inflammatory influence of CI and Aβ on the brain

It has been demonstrated that cerebral ischemic lesions can coexist with AD pathology such as Aβ and tau. Cerebral ischemia (CI) and Aβ together can exacerbate cognitive impairment by accelerating neurodegeneration in elderly subjects and animals (158-162). However, the underlying mechanism before occurrence of neurodegeneration and cognitive impairment is little known. One possible pathway contributing to the detrimental effects of CI and Aβ comorbidity is inflammation, which is the first reaction to tissue injury.

CI-induced inflammation can stimulate the release of multiple inflammatory mediators from neurovascular units in the affected area. Some locally produced cytokines such as interleukin-1β (IL-1β) and tumor necrosis factor-α (TNF-α) are released by activated microglial cells, astrocytes and endothelial cells (163). Cytokines are essentially small glycoproteins produced in response to immune activation and inflammation. In the diseased brain, cytokines act as inflammatory mediators and are primarily secreted by glial cells. Moreover, post-ischemia reperfusion can result in secondary damages to penumbral tissue (viable ischemic tissue surrounding the infarct) due to induced inflammation. In the reperfused area, ROS are released by inflammatory cells and accumulate locally (163). These ROS subsequently elicit the expression of pro-inflammatory proteins such as NF-κB and hypoxia inducible factor 1 (164). The upregulation of downstream TNF-α, IL-1β, nitric oxide synthase and cyclooxygenase-2 (COX-2) by NF-κB appears to exacerbate cerebral ischemic injury (163, 165). Among these cytokines and inflammatory mediators, TNF-α and IL-1β are substantially expressed by microglia in the AD brain. In-vitro studies using human microglia in the presence of Aβ42 show increased secretions of TNF-α and IL-1β (166-168), suggesting the role of Aβ in activating microglia-mediated inflammatory

reaction. The activated microglia can synthesize inflammatory cytokines to recruit more microglia, which further contribute to the production of ROS and neurodegeneration. In addition, COX-2 is highly expressed in neurons and microglia in response to Aβ toxicity and brain injury including ischemic stroke (167, 169). In post-mortem examinations of ischemic stroke patients, microglial COX-2 is upregulated in the ischemic area (163, 170). In the AD brain, the expression of COX-2 is elevated in the neurons of temporal cortex and hippocampus (171, 172), which are frequently involved in neurodegeneration and cognitive dysfunction. The increased level of COX-2 makes neurons vulnerable to glutamate excitotoxicity that leads to cell apoptosis. In CI+Aβ comorbidity, ischemic cerebral tissues can be more susceptible to excitotoxicity and ROS in the presence of Aβ. Together, these common inflammatory mediators from both AD and CI converge to increase neuronal damages by initiating a more intensive inflammatory response.

1.5.2 Activated microglia: a biomarker for imaging neuroinflammation in vivo?

Microglia is the resident macrophage of mature central nervous system (CNS) including the brain, spinal cord and optic nerve. They constitute 5-20% of the total brain glial cells (173). Microglial cells play a crucial role as immune phagocytic cells during inflammation and immune defence. They clear tissue debris, damaged cells, foreign antigens and microorganism. Normal or inactive microglia can be activated from resting state in response to various CNS injuries including CI, trauma, neurodegenerative diseases and infection (174). The activation of microglia after CI induces morphologic transformation and changes gene expression and functionality of the cells. They become enlarged with stout processes and convert to an amoeboid shape. Activated microglia also become more active and motile, which help them to proliferate and accumulate around a lesion such as ischemic penumbra. The extent of microglial

activation depends on duration and degree of the injury (175). Some studies show that in the animal brain with induced CI (e.g. MCAO model), microglia can transform into phagocytes and release a variety of inflammatory cytokines such as IL-1β and TNF-α as well as other neurotoxic molecules including ROS and prostanoids (163, 176, 177).

Microglial activation can be a cellular marker of neuroinflammation in ischemic stroke and neurodegenerative diseases such as AD. An increase in activated microglia is directly associated with a higher degree of brain damage because more tissue is involved in the neuroinflammation. For this reason, in-vivo imaging of activated microglia can be a valuable tool for assessing brain lesions and damages. One promising candidate for imaging activated microglia is a ligand binding to the peripheral benzodiazepine receptor (i.e. now renamed as translocator protein, TSPO). TSPO is an 18kD transmembrane protein located on the outer membrane of mitochondria (178). As a component of the outer mitochondrial membrane, TSPO plays a role in mediating mitochondrial functions including steroid synthesis, cholesterol transport and mitochondrial membrane permeability (179). In the brain, TSPO is mainly expressed in the outer mitochondrial membrane of activated microglia and reactive astrocytes (179, 180). Under the normal/healthy condition, TSPO expression is very low in the brain, compared to that in other organs (181, 182). The expression of TSPO after CI dramatically increases in response to the microglia-related neuroinflammation (183). Moreover, in the neurodegenerative AD brain, TSPO also significantly increases in affected areas with amyloid burden such as the temporal and parietal lobe (184, 185). Therefore, the upregulation of microglial TSPO in the brain can be considered as an inflammatory biomarker for in-vivo imaging with positron emission tomography (PET). Some recently developed TSPO-binding ligands such as PK11195, DPA714 and FEPPA are experimentally labelled with radioisotopes like ^{11}C or ^{18}F for PET imaging of the

activated microglia in CNS diseases (186). In animal models of CI, TSPO expression, detected by its radioactive ligands, increased predominantly in the activated microglia from acute phase up to 7-11 days after the insult, whereas the reactive astrocytes showed a delayed TSPO expression at later time and this could be related to the formation of astrocytic scar around the lesion (183, 187). In addition, transgenic animal models of AD showed an association between the increased level of microglia-expressing TSPO and elevated neuronal loss (188-190), whereas TSPO expression in astrocytes was associated with reduced neuronal damage (188). This evidence may imply the damaging effects of microglia but the protective effects of astrocytes on neurons, depending on intrinsic features of these inflammatory cells. The mechanism for the increased microglial TSPO level in the diseased CNS is not clear. Several studies reveal a correlation of increased PK11195/TSPO binding with the presence of inflammatory cytokines TNF-α and ILs (191-193). Nevertheless, PET imaging of TSPO in the activated microglia is useful for detecting and evaluating in-vivo neuroinflammation and associated neuronal damages.

1.5.3 Animal comorbid model of cerebral ischemia and Aβ toxicity

The coexistence of cerebral ischemic injury and neurodegeneration has been demonstrated in many studies. The combination of these two pathological processes may occur in ageing people and play an important role in causing chronic neuronal dysfunction, inflammation and eventually cognitive impairment or dementia (194). As discussed previously, the presence of ischemic lesions enhanced cognitive deficits in patients with AD pathology. Animal experimental models have found that cerebral ischemia upregulated (increased) the APP expression and enhanced the cleavage of APP to Aβ. In turn, Aβ can trigger the release of inflammatory mediators and cytokines such as TNF-α and interleukins, thus further contributing

to post-ischemia neuroinflammation and more neuronal damages. However, more work has to be done to elucidate the synergistic effects and mechanism of combined ischemic injury and AD pathology.

Several animal models combined both CI and AD pathology (mainly Aβ) together for the evaluation of pathological and cognitive changes. In these animal models, Aβ protein is injected into cerebral ventricles or hippocampus, and ischemia is induced by either endothelin-1 (ET-1, a potent vasoconstrictor) injection or MCAO (158, 162, 195-197). The common findings from these studies suggest that the combination of CI and Aβ toxicity can lead to significant memory impairment (i.e. using radial maze or similar test), increased levels of inflammatory mediators/cytokines and cells including microglia and astrocytes, more neuronal loss and larger infarcts. For this thesis, we used the previously established rat model of CI+Aβ created by Whitehead et al. This rat model combines ET-1-induced subcortical CI with cerebroventricular injection of soluble Aβ peptides (196). A small amount of ET-1 was injected into the center of the striatum, a part of basal ganglia in the subcortical area involved in memory, movement coordination and signal relay. The soluble Aβ protein was injected into the lateral ventricles in the brain, allowing infiltration of Aβ toxicity to the periventricular areas including the striatum. The characteristics of this model include spatial memory impairment and elevated level of neuroinflammation as well as neuronal damages (161). However, the previous investigation of this rat model did not explore in-vivo changes in cerebral perfusion, BBB integrity and neuroinflammation, which are considered as critical factors for functional/cognitive deficits at the early stage and may precede or accompany the development of substantial pathology. Therefore, investigation of cerebral perfusion and BBB integrity in this CI+Aβ model can reveal

the early vascular perturbations, which may explain the underlying contribution of cerebrovascular injury to neurodegeneration in AD.

1.6 Medical imaging in cerebral ischemia and AD

1.6.1 Positron emission tomography

Positron emission tomography (PET) is a functional imaging modality for diagnosis, monitoring and assessment of diseases using radiolabeled ligands. It has been widely used in measuring in-vivo metabolic and physiological activity and molecular function of the target tissue. The basic principle of PET imaging involves administration of a positron-emitting radionuclide (radioisotope) labeled ligand to the subject and subsequently imaging of the distribution of the radionuclide in vivo. Briefly, a positive electron, positron, is emitted from the radioisotope used to label the ligand which then annihilates with an electron in the surrounding tissue. This annihilation event emits two 511 keV gamma ray photons in opposite directions at 180° apart. The gamma rays are then detected by scintillation detectors in the PET scanner. Some common radioisotopes, ^{11}C, ^{15}O and ^{18}F are used to label different ligands which bind to specific targets in the tissue.

In the scenario of cerebral ischemia or stroke, disturbed CBF, oxygen metabolism, neuronal activity and microglial activation are the common physiological processes measured by PET imaging. CBF and cerebral metabolic rate of oxygen ($CMRO_2$), measured from PET imaging of ^{15}O-labeled water and oxygen, are used to identify the ischemic brain tissue which later becomes infarcted (198). Some PET studies reported that the severe decreases in both CBF and $CMRO_2$ (CBF < 12 mL/100g/min and $CMRO_2$ < 65 μmol/100g/min) could represent irreversible tissue

damage (i.e. infarction) (199-201). The extent of CBF and $CMRO_2$ disturbances has been used for differentiating irreversible damage from the viable penumbra, which has preserved $CMRO_2$ and CBF (202). Moreover, recently developed ^{11}C-flumazenil or ^{18}F-fluoroflumazenil binds to the central benzodiazepine gamma-aminobutyric acid (GABA) receptor in the cerebral cortex. These GABA neurons are sensitive to ischemia and can thus indicate early neuronal loss and identify the location of final infarct (203, 204). However, this ligand only binds to the GABA receptors in the cortex, and therefore cannot detect white matter lesions. Furthermore, inflammatory reaction in CI or stroke can be detected by PET imaging of microglial activation. As mentioned in the previous section, microglia-associated TSPO radiotracers (^{11}C-PK11195, ^{18}F-DPA714 or ^{18}F-FEPPA) have been used in human and animal studies. The ^{11}C-PK11195 studies found increased binding of the radiotracer in the rim of the ischemic core (205-208), and interestingly, also in some distant regions, especially in the subcortical white matter fibers (207, 209). This may indicate a secondary damage from the ischemia to the subcortical white matter. However, the non-specific binding property of ^{11}C-PK11195 (210), as the first generation neuroinflammatory tracer, can confound the observation in such cases. The second generation TSPO tracers, mostly radiolabeled with ^{18}F (e.g. FEPPA, PBR28 and DPA714), have better binding affinity, specificity and lipophilicity (for penetration of BBB), as compared to the prototypical ^{11}C-PK11195.

In the neurodegenerative AD brains, PET imaging has been applied in many studies focusing on early detection of the disease. Glucose hypometabolism, amyloid/tau protein and microglial activation are the primary targets of the radiotracers used in AD studies. The glucose analog compound, ^{18}F-labeled fluorodeoxyglucose (^{18}F-FDG) enables quantification of brain glucose metabolism. A number of studies using ^{18}F-FDG revealed the progressive decreases in

cerebral metabolic rate of glucose (CMRglc) in the hippocampus, parietotemporal and posterior cingulate cortex before appearance of clinical symptoms of AD (211, 212). Glucose hypometabolism correlates well with the decline in cognitive performance (142, 213). In addition, longitudinal studies have found that the regional glucose hypometabolism in the posterior cingulate cortex was the most sensitive marker in predicting MCI conversion to AD (214-216). Recently developed amyloid radiotracers such as ^{11}C-PiB and ^{18}F-AV45 have been used to identify MCI patients who have a greater risk of progressing to AD (217-221). However, cognitively normal subjects may also show ^{11}C-PiB uptake (218, 222), making it difficult to interpret whether these subjects are at-risk population or amyloid plaque is a common process in the aging brain rather than the neurodegenerative cause of the disease. ^{18}F-AV45 has non-specific binding in white matter nearly two-fold higher than ^{11}C-PiB (223). More recently, PET imaging of pathological tau protein with ^{18}F-THK523 and ^{11}C-PBB3 has shown promising binding to tau fibrils in animal models and AD patients (224-226), but the clinical usefulness of tau radiotracers for early detection of disease is yet to be fully investigated. Moreover, increased level of activated microglia in animal models and AD patients has been observed in both pathology and PET imaging. Significant ^{11}C-PK11195 binding was reported in the temporal, parietal cortex and hippocampus of AD patients, and correlated with lower cognitive performance scores but not with the amyloid load (184), suggesting that activated microglia is related to the AD progression.

In brains with coexisting ischemic injury and amyloid/Aβ pathology, which occurs in 30-50% of cognitively impaired elderly population, reliable biological targets for PET radiotracers are needed to study early mechanisms of the comorbidity. In the common pathological pathway of CI and Aβ toxicity, detecting neuroinflammation is a good step because histology in the animal

comorbid models has shown a stronger neuroinflammation in the first month after combined ischemic and Aβ insults were induced (161, 195, 196). In such cases, PET imaging using microglia-associated TSPO radiotracers can be useful for investigating inflammatory reaction caused by CI and Aβ. In comparison with histology, PET imaging can reveal in-vivo neuroinflammation related to the disease progression. However, the major limitation of PET studies is the requirement of an on-site cyclotron for producing and labeling radioisotopes because of the short half life of the tracer (^{15}O ~2 min, ^{11}C ~20 min). The distribution of radiotracers to remote medical centers is difficult unless a cyclotron is available nearby. With advances in biomarker discovery and development of novel radiotracers, the significance of ischemic injury and the mechanism in the comorbidity can be further elucidated in future research.

1.6.2 Magnetic resonance imaging

MRI is based on the principle that protons in the tissue have angular momentum which is polarized in a magnetic field. A pulse of radiofrequency can alter the energy state of protons. After the pulse is turned off, the protons return to their energy state, emitting a radiofrequency signal. This signal is measured by a receiver coil. Specific sequences can be designed by combining and manipulating gradients and pulses. Different sequences are sensitive to different tissue characteristics. Some MR sequences that are sensitive to structural or physiological changes have shown alternations in ischemic stroke or AD such as atrophy, edema or white matter hyperintensity. Diffusion weighted imaging (DWI) and perfusion weighted imaging (PWI) are commonly used to study functional/physiological changes in disease progression.

DWI has excellent sensitivity in detecting neuronal deficits caused by cerebral ischemia or stroke (227). It can measure the diffusion of water molecules, termed as apparent diffusion coefficient in DWI. In cerebral ischemia, as CBF declines below the critical level (~10mL/100g/min), the subsequent failure of energy dependent process such as the membrane Na^+/K^+ balance leads to cytotoxic edema (tissue swelling caused by excessive water diffusion into the cells). This is reflected as a decreased apparent diffusion coefficient and increased signal intensity on DWI. As a result, the signal hyperintensity in DWI represents edematous ischemic lesion that later may become an infarct. DWI has reported sensitivity of 95% and specificity of nearly 100% within 6 hours of stroke onset (228). It is usually used to study acute ischemia and is better than routine non-enhanced CT and T2-weighted MRI in identifying early ischemic lesions. However, DWI is rarely used for AD studies mainly because of the low spatial resolution and limited ability of detecting chronic lesions. Instead of DWI, AD studies use PWI to measure reductions in regional CBF or T1-weighted MRI to visualize hippocampal and temporal atrophy. In addition, subcortical ischemic lesions (e.g. lacunes) and WMLs can be detected by T2-weighted and fluid-attenuated inversion recovery (FLAIR)-MRI. Microbleeds can be detected by susceptibility-weighted imaging. Recent MRI studies indicated that the presence of lacunes or microbleeds was associated with AD and cognitive impairment (229-231).

PWI is based on the measurement of T2 or T2* decrease from the passage of an intravenously injected gadolinium contrast agent through the brain. The T2-weighted PWI, based on dynamic susceptibility contrast MRI (DSC-MRI), measures concentration of contrast agent such as gadolinium-DTPA by calculating the change in transverse relaxation rates from the rapid loss of MR T2 or T2* signal. MR images are serially acquired as contrast agent flows through the vascular system, and then signal intensity-time curve derived from the acquired images is

converted to a relative concentration-time curve for quantifying hemodynamic parameters such as CBF, CBV or mean transit time (MTT) (232). Besides DSC-MRI, arterial spin labeling (ASL-PWI) imaging, which does not require administration of gadolinium-based MR contrast agent, can also be used. ASL uses endogenous water molecules in the blood that is magnetically labeled as the contrast agent and produces quantitative maps of CBF. However, the main disadvantage of ASL is the low signal to noise ratio, therefore it cannot accurately measure low CBF. In clinical practices, PWI can measure CBF and CBV abnormality as well as prolonged MTT values in stroke. It is used together with DWI to identify the ischemic area at risk for infarction (PWI-DWI mismatch) (227). In AD studies, PWI has shown decreased CBF and CBV in the temporoparietal regions, but some recent studies reported hyperperfusion in the hippocampus, amygdale, anterior cingulate gyrus and basal ganglia in early AD and MCI patients, suggesting a regional compensation for neural damage in the transitional phase of the disease (233).

1.6.3 CT perfusion imaging

CT perfusion (CTP) or dynamic contrast-enhanced CT (DCE-CT) is an advanced functional CT imaging method that uses rapid acquisition of CT images after a bolus injection of intravenous contrast agent to image cerebral hemodynamics. In general, CTP requires the fast scanning speed of modern multi-detector CT scanners for continuously acquiring images (i.e. cine imaging mode) after iodinated contrast agent is infused through a peripheral vein. CTP can measure hemodynamic parameters such as CBF, CBV, MTT and permeability surface area product (PS) by analyzing temporal changes in attenuation in blood vessels and tissues from the arrival and washout of contrast agent. In actual practices, the increase in attenuation of the blood vessel and tissue after arrival of contrast agent is measured and expressed as enhancement in

Hounsfield unit (HU), which is linearly related to the iodine concentration within blood vessels and tissue. Based on different levels of the enhancement of the tissue, the physiological status can be reflected by hemodynamic parameters. In order to measure the enhancement any time after injection of contrast, baseline image intensity before contrast arrival is subtracted from image intensity after arrival of contrast agent. Using this subtraction technique, a time-enhancement or time-density/attenuation curve (TDC) of the tissue or blood vessel can be generated and analyzed with mathematical models to derive hemodynamic parameters such as CBF, CBV and MTT (232, 234, 235). The calculation of CBF, CBV and MTT makes use of the first phase (typically 45-60 s) after contrast injection because at this time frame the contrast agent is predominately intravascular. PS calculation makes use of the second phase (about 2-3 minutes after the first phase) which is dominated by the contrast leakage/passage from intravascular to extravascular space. Data in this prolonged phase (second phase) enables measurement of diffusion-driven microvascular permeability such as BBB permeability in the brain (236).

The arterial TDC is measured from cerebral arteries in the brain. However, due to the limited resolving power of CT, cerebral arteries are too small to be resolved. As a result, this underestimates the arterial input function (AIF). To avoid this partial volume averaging, a venous TDC measured from a large cerebral vein (superior sagittal sinus) is used to normalize the AIF by scaling the area of the AIF with that of venous TDC (234, 235). The corrected AIF can then be used for the calculation of CBF, CBV, MTT and PS.

Parametric maps of CBF, CBV, MTT and PS can be calculated and produced with commercially available CTP software. For this thesis, a mathematical deconvolution method was used in the CTP software (GE Healthcare) (235, 236). The tissue TDC of each pixel is

deconvolved against the arterial TDC (Figure 1-2B) which is obtained from an unaffected artery on the image (usually anterior cerebral artery, ACA) and corrected for partial volume averaging as discussed above. This deconvolution produces the blood flow-scaled impulse residue function (F·IRF) as illustrated in Figure 1-2A. The impulse residue function (IRF), which can be distinguished from the F·IRF calculated by deconvolution, describes the fraction of contrast agent that remains in the tissue over time following injection (237). CBF is calculated as the peak height of the F·IRF and CBV is the area under the F·IRF. MTT is the ratio of CBV/CBF, representing the mean time taken for blood (contrast) to exit from the draining vein after entry at the input arteries. The above condition applies when the BBB is intact. When the BBB becomes leaky as in stroke and possibly AD, the modified Johnson and Wilson model can be used to calculate PS in addition to CBF, CBV and MTT (238, 239). PS is related to blood flow and extraction fraction E via the Crone and Renkin relationship (239) as follows:

$$E = 1 - e^{-\frac{PS}{BF}}$$

This model separates BF and E, thus enabling the calculation of PS:

$$PS = -BF \cdot \ln(1 - E)$$

where E is the fraction of prolonged contrast enhancement in the IRF at the second phase, representing the portion of contrast agent leaking through a leaky BBB into the extravascular space after the first impulse response.

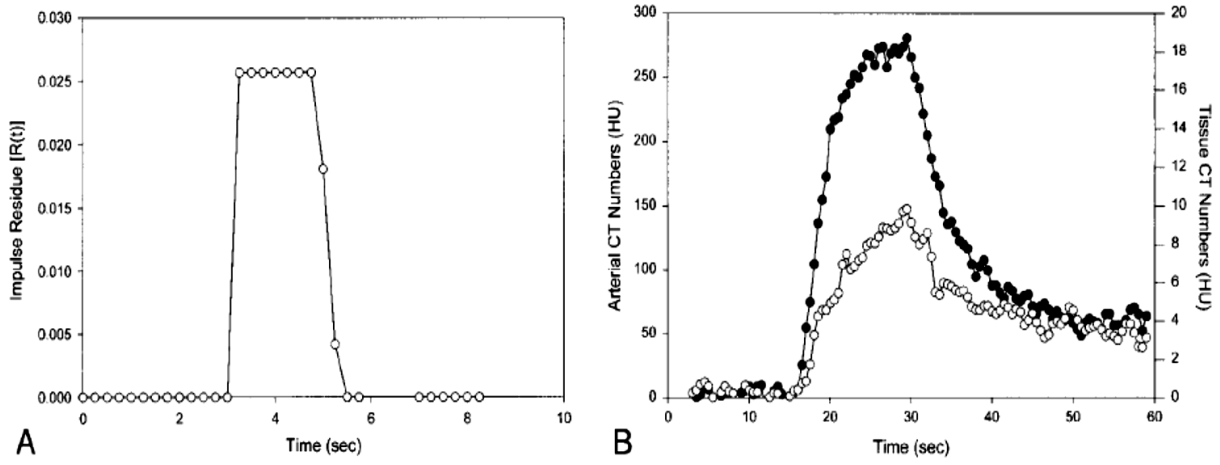

Figure 1-2: (A) a blood flow-scaled IRF as calculated from a deconvolution of arterial and tissue TDC. **(B)** example of arterial (closed circles) and tissue (open circles) TDC curves. Graphs reproduced from Cenic et al, 1999 (237). Reprinted with permission.

In ischemic stroke or CI, CTP has been applied to identify penumbra and infarct in the acute phase. CBF, CBV and MTT are commonly used to distinguish infarcted brain tissue from the penumbra. The hemodynamic characteristics of the penumbra include decreased CBF (ischemia), normal or elevated CBV (due to activation of vascular autoregulation) and elevated MTT, while infarct is indicated by decreased CBF and CBV along with increased MTT (240, 241). Some CTP studies have proposed CBF below 10 - 15mL/100g/min as the infarct (73, 242, 243) because of collapse of vascular autoregulation and thus irreversible tissue damage at this stage. However, decrease in CBV is more difficult to interpret, probably due to confounding factors such as locally released vasodilators (nitric oxide) or reactive hyperemia. For AD or vascular cognitive impairment (VCI), CTP so far has not been widely used. Recent CTP studies reported a correlation between regional hypoperfusion and cognitive decline in AD and VCI (244-246). As mentioned previously, AD and VCI patients have shown increased BBB permeability/leakage (BBB-PS) when subcortical ischemic lesions present. This gives an opportunity for CTP-derived BBB-PS to monitor microvascular dysfunction of the disease. With accumulating knowledge

about cerebrovascular lesion, CTP may become a promising modality for detection of abnormal cerebral perfusion and BBB leakage at the early stage.

The main advantages of CTP are wide availability, simplicity of acquisition and linear relationship between contrast concentration and signal intensity, as compared to MRI. CTP also has better spatial resolution than PET, which allows accurate delineation of region of interest (232, 247). However, the radiation dose (typically 2-3 mSv for a head CT scan) is the main concern of CTP compared to MRI. CTP has similar radiation dose to PET but limited brain coverage than both MRI and PET (247), which have whole brain coverage. More recently, the integrated PET-CT scanner enables acquisition of both anatomic and physiological information, and thus can be used to detect disturbances of cerebral perfusion and abnormal activity of cellular/molecular biomarkers in a single imaging session.

1.7 Research objectives

The work of this thesis focuses on two primary goals: (1) using CTP and PET to study the early mechanism of CI+Aβ in causing hemodynamic disturbance and neuroinflammation; and (2) using CTP to investigate the role of breakdown of BBB in subcortical CI or lesion. These goals were achieved by accomplishing the following objectives which include preclinical and clinical studies.

1. To investigate the abnormality of cerebral perfusion of CI in the presence of Aβ at the early stage of CI+Aβ comorbidity using CTP in an animal model

2. To reveal the temporal changes of BBB permeability/integrity over 3 months and assess the extent of BBB leakage with CTP and histology in the animal CI+Aβ model

3. To establish a pilot study for evaluation of ^{18}F-FEPPA in detecting in-vivo neuroinflammation induced by CI+Aβ comorbidity

4. To study the evolution of BBB permeability (BBB-PS) using CTP in patients with subcortical/lacunar ischemic lesions in the first 3 months post stroke, and compare to those without such lesions

5. Overall, to elucidate the contribution of cerebrovascular lesion/abnormality to the progression of CI+Aβ comorbidity and subcortical ischemic disease within the first 3 months post insult

1.8 References

1. Chen R-L, Balami JS, Esiri MM, Chen L-K, & Buchan AM (2010) Ischemic stroke in the elderly: an overview of evidence. *Nature Reviews Neurology* 6(5):256-265.
2. Feigin VL, Lawes CM, Bennett DA, & Anderson CS (2003) Stroke epidemiology: a review of population-based studies of incidence, prevalence, and case-fatality in the late 20th century. *The Lancet Neurology* 2(1):43-53.
3. Wade DT & Hewer RL (1987) Functional abilities after stroke: measurement, natural history and prognosis. *Journal of Neurology, Neurosurgery & Psychiatry* 50(2):177-182.
4. Greveson G, Gray C, French J, & James O (1991) Long-term outcome for patients and carers following hospital admission for stroke. *Age and Ageing* 20(5):337-344.
5. Patel MD, Coshall C, Rudd AG, & Wolfe CD (2002) Cognitive Impairment after Stroke: Clinical Determinants and Its Associations with Long-Term Stroke Outcomes. *Journal of the American Geriatrics Society* 50(4):700-706.
6. Tatemichi T, *et al.* (1994) Cognitive impairment after stroke: frequency, patterns, and relationship to functional abilities. *Journal of Neurology, Neurosurgery & Psychiatry* 57(2):202-207.
7. Lloyd-Jones D, *et al.* (2010) Heart disease and stroke statistics - 2010 update A report from the American Heart Association. *Circulation* 121(7):e46-e215.
8. Canada PHA (2011) *Tracking Heart Disease and Stroke in Canada – Stroke Highlights 2011*.
9. Breteler M (2000) Vascular involvement in cognitive decline and dementia: epidemiologic evidence from the Rotterdam Study and the Rotterdam Scan Study. *Annals of the New York Academy of Sciences* 903(1):457-465.
10. Helzner EP, *et al.* (2009) Contribution of vascular risk factors to the progression in Alzheimer disease. *Archives of neurology* 66(3):343-348.
11. Iadecola C (2010) The overlap between neurodegenerative and vascular factors in the pathogenesis of dementia. *Acta neuropathologica* 120(3):287-296.
12. Vermeer SE, *et al.* (2003) Silent brain infarcts and the risk of dementia and cognitive decline. *New England Journal of Medicine* 348(13):1215-1222.
13. Association As (2011) Alzheimer's Disease Facts and Figures. *Alzheimer's & Dementia* 7(2).

14. Kalaria RN (2012) Cerebrovascular Disease and Mechanisms of Cognitive Impairment Evidence From Clinicopathological Studies in Humans. *Stroke* 43(9):2526-2534.
15. Snowdon DA, *et al.* (1997) Brain infarction and the clinical expression of Alzheimer disease: the Nun Study. *JAMA* 277(10):813-817.
16. Craig-Schapiro R, Fagan AM, & Holtzman DM (2009) Biomarkers of Alzheimer's disease. *Neurobiology of disease* 35(2):128-140.
17. Hansson O, *et al.* (2009) Combined rCBF and CSF biomarkers predict progression from mild cognitive impairment to Alzheimer's disease. *Neurobiology of aging* 30(2):165-173.
18. Hirao K, *et al.* (2005) The prediction of rapid conversion to Alzheimer's disease in mild cognitive impairment using regional cerebral blood flow SPECT. *Neuroimage* 28(4):1014-1021.
19. Matsuda H (2001) Cerebral blood flow and metabolic abnormalities in Alzheimer's disease. *Annals of nuclear medicine* 15(2):85-92.
20. Jellinger KA & Attems J (2005) Prevalence and pathogenic role of cerebrovascular lesions in Alzheimer disease. *Journal of the neurological sciences* 229:37-41.
21. Heyman A, *et al.* (1998) Cerebral infarcts in patients with autopsy-proven Alzheimer's disease CERAD, part XVIII. *Neurology* 51(1):159-162.
22. Kokmen E, Whisnant J, O'Fallon W, Chu C-P, & Beard C (1996) Dementia after ischemic stroke A population-based study in Rochester, Minnesota (1960-1984). *Neurology* 46(1):154-159.
23. Ballard C, *et al.* (1999) Neuropathological substrates of dementia and depression in vascular dementia, with a particular focus on cases with small infarct volumes. *Dementia and geriatric cognitive disorders* 11(2):59-65.
24. Kalaria RN (2000) The role of cerebral ischemia in Alzheimer's disease. *Neurobiology of aging* 21(2):321-330.
25. Vermeer SE, Longstreth WT, & Koudstaal PJ (2007) Silent brain infarcts: a systematic review. *The Lancet Neurology* 6(7):611-619.
26. Kwan LT, *et al.* (1999) Effects of subcortical cerebral infarction on cortical glucose metabolism and cognitive function. *Archives of neurology* 56(7):809-814.

27. Song IU, Kim JS, Kim YI, Eah KY, & Lee KS (2007) Clinical significance of silent cerebral infarctions in patients with Alzheimer disease. *Cognitive and behavioral neurology* 20(2):93.
28. Wen HM, *et al.* (2004) Effect of white matter changes on cognitive impairment in patients with lacunar infarcts. *Stroke* 35(8):1826-1830.
29. Breteler M, *et al.* (1994) Cerebral white matter lesions, vascular risk factors, and cognitive function in a population-based study The Rotterdam Study. *Neurology* 44(7):1246-1246.
30. Hiltunen M, *et al.* (2009) Focal cerebral ischemia in rats alters APP processing and expression of Aβ peptide degrading enzymes in the thalamus. *Neurobiology of disease* 35(1):103-113.
31. Shi J, Yang SH, Stubley L, Day AL, & Simpkins JW (2000) Hypoperfusion induces overexpression of β-amyloid precursor protein mRNA in a focal ischemic rodent model. *Brain research* 853(1):1-4.
32. Ferrucci L, *et al.* (1996) Cognitive impairment and risk of stroke in the older population. *Journal of the American Geriatrics Society* 44(3):237-241.
33. Gale CR, Martyn CN, & Cooper C (1996) Cognitive impairment and mortality in a cohort of elderly people. *BMJ* 312(7031):608-611.
34. Biffi A & Greenberg SM (2011) Cerebral amyloid angiopathy: a systematic review. *Journal of Clinical Neurology* 7(1):1-9.
35. Brown WR & Thore CR (2011) Review: cerebral microvascular pathology in ageing and neurodegeneration. *Neuropathology and applied neurobiology* 37(1):56-74.
36. Wardlaw J, Sandercock P, Dennis M, & Starr J (2003) Is breakdown of the blood-brain barrier responsible for lacunar stroke, leukoaraiosis, and dementia? *Stroke* 34(3):806-812.
37. Hartz AM, *et al.* (2012) Amyloid-β contributes to blood–brain barrier leakage in transgenic human amyloid precursor protein mice and in humans with cerebral amyloid angiopathy. *Stroke* 43(2):514-523.
38. de la Torre J (2002) Alzheimer disease as a vascular disorder nosological evidence. *Stroke* 33(4):1152-1162.
39. Hofman A, *et al.* (1997) Atherosclerosis, apolipoprotein E, and prevalence of dementia and Alzheimer's disease in the Rotterdam Study. *The Lancet* 349(9046):151-154.

40. Kivipelto M, *et al.* (2001) Midlife vascular risk factors and late-life mild cognitive impairment A population-based study. *Neurology* 56(12):1683-1689.
41. Launer LJ, *et al.* (2000) Midlife blood pressure and dementia: the Honolulu–Asia aging study. *Neurobiology of aging* 21(1):49-55.
42. Ott A, *et al.* (1997) Atrial fibrillation and dementia in a population-based study The Rotterdam Study. *Stroke* 28(2):316-321.
43. Wang H, *et al.* (2009) Alterations in regional brain volume and individual MRI-guided perfusion in normal control, stable mild cognitive impairment, and MCI-AD converter. *Journal of geriatric psychiatry and neurology*.
44. Borroni B, *et al.* (2006) Combined 99m Tc-ECD SPECT and neuropsychological studies in MCI for the assessment of conversion to AD. *Neurobiology of aging* 27(1):24-31.
45. Kogure D, *et al.* (2000) Longitudinal evaluation of early Alzheimer's disease using brain perfusion SPECT. *Journal of nuclear medicine* 41(7):1155-1162.
46. Ivan CS, *et al.* (2004) Dementia after stroke the Framingham study. *Stroke* 35(6):1264-1268.
47. Kauhanen M, *et al.* (1999) Aphasia, depression, and non-verbal cognitive impairment in ischaemic stroke. *Cerebrovascular diseases* 10(6):455-461.
48. Madureira S, Guerreiro M, & Ferro J (2001) Dementia and cognitive impairment three months after stroke. *European Journal of Neurology* 8(6):621-627.
49. Lazar RM, Speizer AE, Festa JR, Krakauer JW, & Marshall RS (2008) Variability in language recovery after first-time stroke. *Journal of Neurology, Neurosurgery & Psychiatry* 79(5):530-534.
50. McMurtray AM, Liao A, Haider J, Licht E, & Mendez MF (2006) Cognitive performance after lacunar stroke correlates with leukoaraiosis severity. *Cerebrovascular diseases* 24(2-3):271-276.
51. Van Zandvoort MJ, De Haan EH, & Kappelle LJ (2001) Chronic cognitive disturbances after a single supratentorial lacunar infarct. *Cognitive and behavioral neurology* 14(2):98-102.
52. Pasquier F & Leys D (1997) Why are stroke patients prone to develop dementia? *Journal of neurology* 244(3):135-142.

53. Mori E (2002) Impact of subcortical ischemic lesions on behavior and cognition. *Annals of the New York Academy of Sciences* 977(1):141-148.
54. Román GC, Erkinjuntti T, Wallin A, Pantoni L, & Chui HC (2002) Subcortical ischaemic vascular dementia. *The Lancet Neurology* 1(7):426-436.
55. Capizzano AA, *et al.* (2004) White matter hyperintensities are significantly associated with cortical atrophy in Alzheimer's disease. *Journal of Neurology, Neurosurgery & Psychiatry* 75(6):822-827.
56. O'Brien JT, *et al.* (2003) Vascular cognitive impairment. *The Lancet Neurology* 2(2):89-98.
57. Powers WJ (1991) Cerebral hemodynamics in ischemic cerebrovascular disease. *Annals of neurology* 29(3):231-240.
58. Mohr J, *et al.* (1997) Etiology of stroke. *Stroke* 28(7):1501-1506.
59. Go AS, *et al.* (2014) Heart disease and stroke statistics -2014 update: a report from the American Heart Association. *Circulation* 129(3):e28.
60. van der Worp HB & van Gijn J (2007) Acute ischemic stroke. *New England Journal of Medicine* 357(6):572-579.
61. Johnston SC (2002) Transient ischemic attack. *New England Journal of Medicine* 347(21):1687-1692.
62. Yoon SS, Heller RF, Levi C, Wiggers J, & Fitzgerald PE (2001) Knowledge of stroke risk factors, warning symptoms, and treatment among an Australian urban population. *Stroke* 32(8):1926-1930.
63. Rathore SS, Hinn AR, Cooper LS, Tyroler HA, & Rosamond WD (2002) Characterization of incident stroke signs and symptoms findings from the atherosclerosis risk in communities study. *Stroke* 33(11):2718-2721.
64. Gottesman RF & Hillis AE (2010) Predictors and assessment of cognitive dysfunction resulting from ischaemic stroke. *The Lancet Neurology* 9(9):895-905.
65. Iadecola C (1999) Mechanisms of cerebral ischemic damage. *Cerebral Ischemia*, (Springer), pp 3-32.
66. Lo EH, Dalkara T, & Moskowitz MA (2003) Mechanisms, challenges and opportunities in stroke. *Nature Reviews Neuroscience* 4(5):399-414.

67. Dirnagl U, Iadecola C, & Moskowitz MA (1999) Pathobiology of ischaemic stroke: an integrated view. *Trends in neurosciences* 22(9):391-397.
68. Juurlink BH & Sweeney MI (1997) Mechanisms that result in damage during and following cerebral ischemia. *Neuroscience & Biobehavioral Reviews* 21(2):121-128.
69. Wood AJ, Brott T, & Bogousslavsky J (2000) Treatment of acute ischemic stroke. *New England Journal of Medicine* 343(10):710-722.
70. Hossmann KA (1994) Viability thresholds and the penumbra of focal ischemia. *Annals of neurology* 36(4):557-565.
71. Obrenovitch T, *et al.* (1988) Brain tissue concentrations of ATP, phosphocreatine, lactate, and tissue pH in relation to reduced cerebral blood flow following experimental acute middle cerebral artery occlusion. *Journal of Cerebral Blood Flow & Metabolism* 8(6):866-874.
72. Bandera E, *et al.* (2006) Cerebral blood flow threshold of ischemic penumbra and infarct core in acute ischemic stroke a systematic review. *Stroke* 37(5):1334-1339.
73. Murphy B, *et al.* (2006) Identification of penumbra and infarct in acute ischemic stroke using computed tomography perfusion–derived blood flow and blood volume measurements. *Stroke* 37(7):1771-1777.
74. Jones TH, *et al.* (1981) Thresholds of focal cerebral ischemia in awake monkeys. *Journal of neurosurgery* 54(6):773-782.
75. Jaffer H, Morris VB, Stewart D, & Labhasetwar V (2011) Advances in stroke therapy. *Drug delivery and translational research* 1(6):409-419.
76. Moustafa RR & Baron J (2007) Perfusion thresholds in cerebral ischemia. *Neurological Disease and Therapy* 93:21-35.
77. Ebinger M, *et al.* (2009) Imaging the penumbra–strategies to detect tissue at risk after ischemic stroke. *Journal of Clinical Neuroscience* 16(2):178-187.
78. Abbott NJ, Patabendige AA, Dolman DE, Yusof SR, & Begley DJ (2010) Structure and function of the blood–brain barrier. *Neurobiology of disease* 37(1):13-25.
79. Yang Y & Rosenberg GA (2011) Blood–brain barrier breakdown in acute and chronic cerebrovascular disease. *Stroke* 42(11):3323-3328.
80. Hawkins BT & Davis TP (2005) The blood-brain barrier/neurovascular unit in health and disease. *Pharmacological reviews* 57(2):173-185.

81. Begley DJ & Brightman MW (2003) Structural and functional aspects of the blood-brain barrier. *Progress in Drug Research* 61:39-78.

82. Sandoval KE & Witt KA (2008) Blood-brain barrier tight junction permeability and ischemic stroke. *Neurobiology of disease* 32(2):200-219.

83. Anderson VC, Lenar DP, Quinn JF, & Rooney WD (2011) The blood-brain barrier and microvascular water exchange in Alzheimer's disease. *Cardiovascular psychiatry and neurology* 2011:1-9.

84. Naganuma Y (1990) Changes of the cerebral microvascular structure and endothelium during the course of permanent ischemia. *The Keio journal of medicine* 39(1):26-31.

85. Petty M & Wettstein J (2001) Elements of cerebral microvascular ischaemia. *Brain Research Reviews* 36(1):23-34.

86. Dietrich WD, Busto R, & Ginsberg MD (1984) Cerebral endothelial microvilli: formation following global forebrain ischemia. *Journal of Neuropathology & Experimental Neurology* 43(1):72-83.

87. Hamann GF, Okada Y, Fitridge R, & del Zoppo GJ (1995) Microvascular basal lamina antigens disappear during cerebral ischemia and reperfusion. *Stroke* 26(11):2120-2126.

88. Ito U, Ohno K, Nakamura R, Suganuma F, & Inaba Y (1979) Brain edema during ischemia and after restoration of blood flow. Measurement of water, sodium, potassium content and plasma protein permeability. *Stroke* 10(5):542-547.

89. Kuroiwa T, Shibutani M, & Okeda R (1988) Blood-brain barrier disruption and exacerbation of ischemic brain edema after restoration of blood flow in experimental focal cerebral ischemia. *Acta neuropathologica* 76(1):62-70.

90. Neumann-Haefelin T, *et al.* (2000) Serial MRI after transient focal cerebral ischemia in rats dynamics of tissue injury, blood-brain barrier damage, and edema formation. *Stroke* 31(8):1965-1973.

91. Taniguchi M, *et al.* (2000) Induction of aquaporin-4 water channel mRNA after focal cerebral ischemia in rat. *Molecular brain research* 78(1):131-137.

92. Yang G-Y & Betz AL (1994) Reperfusion-induced injury to the blood-brain barrier after middle cerebral artery occlusion in rats. *Stroke* 25(8):1658-1664.

93. Fukuda S, *et al.* (2004) Focal cerebral ischemia induces active proteases that degrade microvascular matrix. *Stroke* 35(4):998-1004.

94. Rosell A, *et al.* (2008) MMP-9–Positive Neutrophil Infiltration Is Associated to Blood–Brain Barrier Breakdown and Basal Lamina Type IV Collagen Degradation During Hemorrhagic Transformation After Human Ischemic Stroke. *Stroke* 39(4):1121-1126.
95. Hamann GF, Okada Y, & del Zoppo GJ (1996) Hemorrhagic transformation and microvascular integrity during focal cerebral ischemia/reperfusion. *Journal of Cerebral Blood Flow & Metabolism* 16(6):1373-1378.
96. Heo JH, *et al.* (1999) Matrix metalloproteinases increase very early during experimental focal cerebral ischemia. *Journal of Cerebral Blood Flow & Metabolism* 19(6):624-633.
97. del Zoppo GJ, *et al.* (2007) Microglial activation and matrix protease generation during focal cerebral ischemia. *Stroke* 38(2):646-651.
98. Justicia C, *et al.* (2003) Neutrophil infiltration increases matrix metalloproteinase-9 in the ischemic brain after occlusion/reperfusion of the middle cerebral artery in rats. *Journal of Cerebral Blood Flow & Metabolism* 23(12):1430-1440.
99. Rosenberg GA (2002) Matrix metalloproteinases in neuroinflammation. *Glia* 39(3):279-291.
100. Gasche Y, *et al.* (1999) Early Appearance of Activated Matrix Metalloproteinase-9 After Focal Cerebral Ischemia in Mice: A Possible Role in Blood-Brain Barrier Dysfunction. *Journal of Cerebral Blood Flow & Metabolism* 19(9):1020-1028.
101. Romanic AM, White RF, Arleth AJ, Ohlstein EH, & Barone FC (1998) Matrix metalloproteinase expression increases after cerebral focal ischemia in rats inhibition of matrix metalloproteinase-9 reduces infarct size. *Stroke* 29(5):1020-1030.
102. Planas AM, Solé S, & Justicia C (2001) Expression and activation of matrix metalloproteinase-2 and-9 in rat brain after transient focal cerebral ischemia. *Neurobiology of disease* 8(5):834-846.
103. Wang CX & Shuaib A (2007) Critical role of microvasculature basal lamina in ischemic brain injury. *Progress in neurobiology* 83(3):140-148.
104. Durukan A, *et al.* (2009) Post-ischemic blood–brain barrier leakage in rats: One-week follow-up by MRI. *Brain research* 1280:158-165.
105. Lin C-Y, *et al.* (2008) Dynamic changes in vascular permeability, cerebral blood volume, vascular density, and size after transient focal cerebral ischemia in rats: evaluation with

contrast-enhanced magnetic resonance imaging. *Journal of Cerebral Blood Flow & Metabolism* 28(8):1491-1501.

106. Farrall AJ & Wardlaw JM (2009) Blood–brain barrier: ageing and microvascular disease–systematic review and meta-analysis. *Neurobiology of aging* 30(3):337-352.
107. Taheri S, *et al.* (2011) Blood–brain barrier permeability abnormalities in vascular cognitive impairment. *Stroke* 42(8):2158-2163.
108. Topakian R, Barrick T, Howe F, & Markus H (2010) Blood–brain barrier permeability is increased in normal-appearing white matter in patients with lacunar stroke and leucoaraiosis. *Journal of Neurology, Neurosurgery & Psychiatry* 81(2):192-197.
109. Wardlaw JM, *et al.* (2009) Lacunar stroke is associated with diffuse blood–brain barrier dysfunction. *Annals of neurology* 65(2):194-202.
110. Kalaria RN, Akinyemi R, & Ihara M (2012) Does vascular pathology contribute to Alzheimer changes? *Journal of the neurological sciences* 322(1):141-147.
111. Attems J & Jellinger KA (2014) The overlap between vascular disease and Alzheimer's disease–lessons from pathology. *BMC medicine* 12(1):206.
112. Benisty S, *et al.* (2009) Location of lacunar infarcts correlates with cognition in a sample of non-disabled subjects with age-related white-matter changes: the LADIS study. *Journal of Neurology, Neurosurgery & Psychiatry* 80(5):478-483.
113. Corbett A, Bennett H, & Kos S (1994) Cognitive dysfunction following subcortical infarction. *Archives of neurology* 51(10):999-007.
114. Norrving B (2003) Long-term prognosis after lacunar infarction. *The Lancet Neurology* 2(4):238-245.
115. de la Torre JC (2000) Cerebral hypoperfusion, capillary degeneration, and development of Alzheimer disease. *Alzheimer Disease & Associated Disorders* 14(1):S72-S81.
116. De Jong G, *et al.* (1999) Cerebral hypoperfusion yields capillary damage in the hippocampal CA1 area that correlates with spatial memory impairment. *Neuroscience* 91(1):203-210.
117. Ni J-w, Ohta H, Matsumoto K, & Watanabe H (1994) Progressive cognitive impairment following chronic cerebral hypoperfusion induced by permanent occlusion of bilateral carotid arteries in rats. *Brain research* 653(1):231-236.

118. Wakita H, Tomimoto H, Akiguchi I, & Kimura J (1994) Glial activation and white matter changes in the rat brain induced by chronic cerebral hypoperfusion: an immunohistochemical study. *Acta neuropathologica* 87(5):484-492.
119. Shibata M, Ohtani R, Ihara M, & Tomimoto H (2004) White matter lesions and glial activation in a novel mouse model of chronic cerebral hypoperfusion. *Stroke* 35(11):2598-2603.
120. Ueno M, Tomimoto H, Akiguchi I, Wakita H, & Sakamoto H (2002) Blood–brain barrier disruption in white matter lesions in a rat model of chronic cerebral hypoperfusion. *Journal of Cerebral Blood Flow & Metabolism* 22(1):97-104.
121. Shibata M, *et al.* (2007) Selective impairment of working memory in a mouse model of chronic cerebral hypoperfusion. *Stroke* 38(10):2826-2832.
122. Erickson MA & Banks WA (2013) Blood–brain barrier dysfunction as a cause and consequence of Alzheimer's disease. *Journal of Cerebral Blood Flow & Metabolism* 33(10):1500-1513.
123. Wardlaw JM, *et al.* (2013) Blood–Brain Barrier Permeability and Long-Term Clinical and Imaging Outcomes in Cerebral Small Vessel Disease. *Stroke* 44(2):525-527.
124. Gorelick PB, *et al.* (2011) Vascular contributions to cognitive impairment and dementia a statement for healthcare professionals from the American Heart Association/American Stroke Association. *Stroke* 42(9):2672-2713.
125. Smith EE & Greenberg SM (2009) β-amyloid, blood vessels, and brain function. *Stroke* 40(7):2601-2606.
126. de la Torre JC (2004) Is Alzheimer's disease a neurodegenerative or a vascular disorder? Data, dogma, and dialectics. *The Lancet Neurology* 3(3):184-190.
127. Selkoe DJ (1998) The cell biology of β-amyloid precursor protein and presenilin in Alzheimer's disease. *Trends in cell biology* 8(11):447-453.
128. Selkoe DJ (1994) Normal and abnormal biology of the beta-amyloid precursor protein. *Annual review of neuroscience* 17(1):489-517.
129. Selkoe DJ (2001) Alzheimer's disease: genes, proteins, and therapy. *Physiological reviews* 81(2):741-766.
130. Fagan AM, *et al.* (2006) Inverse relation between in vivo amyloid imaging load and cerebrospinal fluid Aβ42 in humans. *Annals of neurology* 59(3):512-519.

131. Lue L-F, *et al.* (1999) Soluble amyloid β peptide concentration as a predictor of synaptic change in Alzheimer's disease. *The American journal of pathology* 155(3):853-862.
132. Selkoe DJ (2008) Soluble oligomers of the amyloid β-protein impair synaptic plasticity and behavior. *Behavioural brain research* 192(1):106-113.
133. Wang J, Dickson DW, Trojanowski JQ, & Lee VM-Y (1999) The levels of soluble versus insoluble brain Aβ distinguish Alzheimer's disease from normal and pathologic aging. *Experimental neurology* 158(2):328-337.
134. Cleary JP, *et al.* (2005) Natural oligomers of the amyloid-β protein specifically disrupt cognitive function. *Nature neuroscience* 8(1):79-84.
135. Hardy J & Selkoe DJ (2002) The amyloid hypothesis of Alzheimer's disease: progress and problems on the road to therapeutics. *Science* 297(5580):353-356.
136. Robinson SR, Bishop GM, Lee H-g, & Münch G (2004) Lessons from the AN1792 Alzheimer vaccine: lest we forget. *Neurobiology of aging* 25(5):609-615.
137. Wisniewski T & Konietzko U (2008) Amyloid-β immunisation for Alzheimer's disease. *The Lancet Neurology* 7(9):805-811.
138. Kim J, *et al.* (2009) Overexpression of low-density lipoprotein receptor in the brain markedly inhibits amyloid deposition and increases extracellular Aβ clearance. *Neuron* 64(5):632-644.
139. Mawuenyega KG, *et al.* (2010) Decreased clearance of CNS β-amyloid in Alzheimer's disease. *Science* 330(6012):1774-1774.
140. Shibata M, *et al.* (2000) Clearance of Alzheimer's amyloid-β1-40 peptide from brain by LDL receptor–related protein-1 at the blood-brain barrier. *Journal of Clinical Investigation* 106(12):1489.
141. Zlokovic BV (2011) Neurovascular pathways to neurodegeneration in Alzheimer's disease and other disorders. *Nature Reviews Neuroscience* 12(12):723-738.
142. Engler H, *et al.* (2006) Two-year follow-up of amyloid deposition in patients with Alzheimer's disease. *Brain* 129(11):2856-2866.
143. Jack CR, *et al.* (2013) Tracking pathophysiological processes in Alzheimer's disease: an updated hypothetical model of dynamic biomarkers. *The Lancet Neurology* 12(2):207-216.

144. Villemagne VL, *et al.* (2013) Amyloid β deposition, neurodegeneration, and cognitive decline in sporadic Alzheimer's disease: a prospective cohort study. *The Lancet Neurology* 12(4):357-367.
145. Villemagne VL, *et al.* (2011) Longitudinal assessment of Aβ and cognition in aging and Alzheimer disease. *Annals of neurology* 69(1):181-192.
146. Zlokovic BV (2008) The blood-brain barrier in health and chronic neurodegenerative disorders. *Neuron* 57(2):178-201.
147. Deane R, *et al.* (2004) LRP/amyloid β-peptide interaction mediates differential brain efflux of Aβ isoforms. *Neuron* 43(3):333-344.
148. Deane R, Wu Z, & Zlokovic BV (2004) RAGE (Yin) versus LRP (Yang) balance regulates Alzheimer amyloid β-peptide clearance through transport across the blood–brain barrier. *Stroke* 35(11 suppl 1):2628-2631.
149. Sagare A, *et al.* (2007) Clearance of amyloid-β by circulating lipoprotein receptors. *Nature medicine* 13(9):1029-1031.
150. Deane R, *et al.* (2003) RAGE mediates amyloid-β peptide transport across the blood-brain barrier and accumulation in brain. *Nature medicine* 9(7):907-913.
151. Du Yan S, *et al.* (1996) RAGE and amyloid-β peptide neurotoxicity in Alzheimer's disease.
152. Abramov AY, Canevari L, & Duchen MR (2004) β-amyloid peptides induce mitochondrial dysfunction and oxidative stress in astrocytes and death of neurons through activation of NADPH oxidase. *The Journal of neuroscience* 24(2):565-575.
153. Casley C, Canevari L, Land J, Clark J, & Sharpe M (2002) β-Amyloid inhibits integrated mitochondrial respiration and key enzyme activities. *Journal of neurochemistry* 80(1):91-100.
154. Reddy PH & Beal MF (2008) Amyloid beta, mitochondrial dysfunction and synaptic damage: implications for cognitive decline in aging and Alzheimer's disease. *Trends in molecular medicine* 14(2):45-53.
155. Colton CA, Chernyshev ON, Gilbert DL, & Vitek MP (2000) Microglial contribution to oxidative stress in Alzheimer's disease. *Annals of the New York Academy of Sciences* 899(1):292-307.

156. Della Bianca V, Dusi S, Bianchini E, Dal Prà I, & Rossi F (1999) β-Amyloid Activates the O_2 Forming NADPH Oxidase in Microglia, Monocytes, and Neutrophils, A possible inflammatory mechanism of neuronal damage in Alzheimer's disease. *Journal of Biological Chemistry* 274(22):15493-15499.

157. Johnstone M, Gearing AJ, & Miller KM (1999) A central role for astrocytes in the inflammatory response to β-amyloid; chemokines, cytokines and reactive oxygen species are produced. *Journal of neuroimmunology* 93(1):182-193.

158. Iwasaki K, *et al.* (2006) Cerebral ischemia combined with β-amyloid impairs spatial memory in the eight-arm radial maze task in rats. *Brain research* 1097(1):216-223.

159. Lee MJ, *et al.* (2014) Synergistic effects of ischemia and β-amyloid burden on cognitive decline in patients with subcortical vascular mild cognitive impairment. *JAMA psychiatry* 71(4):412-422.

160. Marchant NL, *et al.* (2012) Cerebrovascular disease, beta-amyloid, and cognition in aging. *Neurobiology of aging* 33(5):1006. e1025-1006. e1036.

161. Whitehead SN, Cheng G, Hachinski VC, & Cechetto DF (2007) Progressive increase in infarct size, neuroinflammation, and cognitive deficits in the presence of high levels of amyloid. *Stroke* 38(12):3245-3250.

162. Amtul Z, *et al.* (2014) Comorbid Aβ toxicity and stroke: hippocampal atrophy, pathology, and cognitive deficit. *Neurobiology of aging* 35(7):1605-1614.

163. Huang J, Upadhyay UM, & Tamargo RJ (2006) Inflammation in stroke and focal cerebral ischemia. *Surgical neurology* 66(3):232-245.

164. Michiels C, Minet E, Mottet D, & Raes M (2002) Regulation of gene expression by oxygen: NF-κB and HIF-1, two extremes. *Free Radical Biology and Medicine* 33(9):1231-1242.

165. Schaller B & Graf R (2004) Cerebral ischemia and reperfusion: the pathophysiologic concept as a basis for clinical therapy. *Journal of Cerebral Blood Flow & Metabolism* 24(4):351-371.

166. Franciosi S, Choi HB, Kim SU, & McLarnon JG (2005) IL-8 enhancement of amyloid-beta (Aβ 1-42)-induced expression and production of pro-inflammatory cytokines and COX-2 in cultured human microglia. *Journal of neuroimmunology* 159(1):66-74.

167. Tuppo EE & Arias HR (2005) The role of inflammation in Alzheimer's disease. *The international journal of biochemistry & cell biology* 37(2):289-305.

168. Cameron B & Landreth GE (2010) Inflammation, microglia, and Alzheimer's disease. *Neurobiology of disease* 37(3):503-509.

169. Wang Q, Tang XN, & Yenari MA (2007) The inflammatory response in stroke. *Journal of neuroimmunology* 184(1):53-68.

170. Iadecola C, Forster C, Nogawa S, Clark HB, & Ross ME (1999) Cyclooxygenase-2 immunoreactivity in the human brain following cerebral ischemia. *Acta neuropathologica* 98(1):9-14.

171. Hoozemans JJ, Veerhuis R, Rozemuller AJ, Arendt T, & Eikelenboom P (2004) Neuronal COX-2 expression and phosphorylation of pRb precede p38 MAPK activation and neurofibrillary changes in AD temporal cortex. *Neurobiology of disease* 15(3):492-499.

172. Ho L, *et al.* (2001) Neuronal cyclooxygenase 2 expression in the hippocampal formation as a function of the clinical progression of Alzheimer disease. *Archives of neurology* 58(3):487-492.

173. Saijo K & Glass CK (2011) Microglial cell origin and phenotypes in health and disease. *Nature Reviews Immunology* 11(11):775-787.

174. Garden GA & Möller T (2006) Microglia biology in health and disease. *Journal of Neuroimmune Pharmacology* 1(2):127-137.

175. Nakajima K & Kohsaka S (2001) Microglia: activation and their significance in the central nervous system. *Journal of biochemistry* 130(2):169-175.

176. Gregersen R, Lambertsen K, & Finsen B (2000) Microglia and macrophages are the major source of tumor necrosis factor in permanent middle cerebral artery occlusion in mice. *Journal of Cerebral Blood Flow & Metabolism* 20(1):53-65.

177. Rothwell NJ (1999) Cytokines-killers in the brain? *The Journal of physiology* 514(1):3-17.

178. Chen M-K & Guilarte TR (2008) Translocator protein 18 kDa (TSPO): molecular sensor of brain injury and repair. *Pharmacology & therapeutics* 118(1):1-17.

179. Rupprecht R, *et al.* (2010) Translocator protein (18 kDa)(TSPO) as a therapeutic target for neurological and psychiatric disorders. *Nature reviews Drug discovery* 9(12):971-988.

180. Batarseh A & Papadopoulos V (2010) Regulation of translocator protein 18kDa (TSPO) expression in health and disease states. *Molecular and cellular endocrinology* 327(1):1-12.

181. Banati RB (2002) Visualising microglial activation in vivo. *Glia* 40(2):206-217.

182. Cosenza-Nashat M, *et al.* (2009) Expression of the translocator protein of 18 kDa by microglia, macrophages and astrocytes based on immunohistochemical localization in abnormal human brain. *Neuropathology and applied neurobiology* 35(3):306-328.

183. Thiel A & Heiss W-D (2011) Imaging of microglia activation in stroke. *Stroke* 42(2):507-512.

184. Edison P, *et al.* (2008) Microglia, amyloid, and cognition in Alzheimer's disease: An [11C](R) PK11195-PET and [11C] PIB-PET study. *Neurobiology of disease* 32(3):412-419.

185. Yokokura M, *et al.* (2011) In vivo changes in microglial activation and amyloid deposits in brain regions with hypometabolism in Alzheimer's disease. *European journal of nuclear medicine and molecular imaging* 38(2):343-351.

186. Chauveau F, Boutin H, Van Camp N, Dollé F, & Tavitian B (2008) Nuclear imaging of neuroinflammation: a comprehensive review of [11C] PK11195 challengers. *European journal of nuclear medicine and molecular imaging* 35(12):2304-2319.

187. Martín A, *et al.* (2010) Evaluation of the PBR/TSPO radioligand [18F]-DPA-714 in a rat model of focal cerebral ischemia. *Journal of Cerebral Blood Flow & Metabolism* 30(1):230-241.

188. Ji B, *et al.* (2008) Imaging of peripheral benzodiazepine receptor expression as biomarkers of detrimental versus beneficial glial responses in mouse models of Alzheimer's and other CNS pathologies. *The Journal of neuroscience* 28(47):12255-12267.

189. Maeda J, *et al.* (2011) In vivo positron emission tomographic imaging of glial responses to amyloid-β and tau pathologies in mouse models of Alzheimer's disease and related disorders. *The Journal of neuroscience* 31(12):4720-4730.

190. Venneti S, *et al.* (2009) PK11195 labels activated microglia in Alzheimer's disease and in vivo in a mouse model using PET. *Neurobiology of aging* 30(8):1217-1226.

191. Oh YJ, Francis JW, Markelonis GJ, & Oh TH (1992) Interleukin-1β and Tumor Necrosis Factor-α Increase Peripheral-Type Benzodiazepine Binding Sites in Cultured Polygonal Astrocytes. *Journal of neurochemistry* 58(6):2131-2138.

192. Trincavelli ML, *et al.* (2002) Upregulation of mitochondrial peripheral benzodiazepine receptor expression by cytokine-induced damage of human pancreatic islets. *Journal of cellular biochemistry* 84(3):636-644.

193. Rey C, *et al.* (2000) Up-regulation of mitochondrial peripheral benzodiazepine receptor expression by tumor necrosis factor alpha in testicular leydig cells: possible involvement in cell survival. *Biochemical pharmacology* 60(11):1639-1646.

194. Iadecola C & Gorelick PB (2003) Converging pathogenic mechanisms in vascular and neurodegenerative dementia. *Stroke* 34(2):335-337.

195. Li J, Wang YJ, Zhang M, Fang CQ, & Zhou HD (2011) Cerebral ischemia aggravates cognitive impairment in a rat model of Alzheimer's disease. *Life sciences* 89:86-92.

196. Whitehead SN, Hachinski VC, & Cechetto DF (2005) Interaction Between a Rat Model of Cerebral Ischemia and β-Amyloid Toxicity: Inflammatory Responses. *Stroke* 36(1):107-112.

197. Choi B-R, *et al.* (2011) Synergistic memory impairment through the interaction of chronic cerebral hypoperfusion and amlyloid toxicity in a rat model. *Stroke* 42(9):2595-2604.

198. Heiss W-D & Herholz K (1994) Assessment of pathophysiology of stroke by positron emission tomography. *European journal of nuclear medicine* 21(5):455-465.

199. Baron J, Bousser M, Comar D, Soussaline F, & Castaigne P (1981) Noninvasive tomographic study of cerebral blood flow and oxygen metabolism in vivo. *European neurology* 20(3):273-284.

200. Lenzi G, Frackowiak R, & Jones T (1982) Cerebral oxygen metabolism and blood flow in human cerebral ischemic infarction. *J Cereb Blood Flow Metab* 2(3):321-335.

201. Powers WJ, Grubb RL, Darriet D, & Raiehle ME (1985) Cerebral blood flow and cerebral metabolic rate of oxygen requirements for cerebral function and viability in humans. *Journal of Cerebral Blood Flow & Metabolism* 5(4):600-608.

202. Baron J-C (1998) Mapping the ischaemic penumbra with PET: implications for acute stroke treatment. *Cerebrovascular diseases* 9(4):193-201.

203. Heiss W-D, *et al.* (1997) Early detection of irreversibly damaged ischemic tissue by flumazenil positron emission tomography in cats. *Stroke* 28(10):2045-2052.

204. Heiss W-D, *et al.* (1998) Permanent cortical damage detected by flumazenil positron emission tomography in acute stroke. *Stroke* 29(2):454-461.

205. Sette G, *et al.* (1993) In vivo mapping of brain benzodiazepine receptor changes by positron emission tomography after focal ischemia in the anesthetized baboon. *Stroke* 24(12):2046-2057.

206. Ramsay S, *et al.* (1992) Monitoring by PET of macrophage accumulation in brain after ischaemic stroke. *The Lancet* 339(8800):1054-1055.

207. Gerhard A, Schwarz J, Myers R, Wise R, & Banati RB (2005) Evolution of microglial activation in patients after ischemic stroke: a [11 C](R)-PK11195 PET study. *Neuroimage* 24(2):591-595.

208. Schroeter M, *et al.* (2009) Neuroinflammation extends brain tissue at risk to vital peri-infarct tissue: a double tracer [11C]PK11195 and [18F]FDG-PET study. *Journal of Cerebral Blood Flow & Metabolism* 29(6):1216-1225.

209. Price CJ, *et al.* (2006) Intrinsic activated microglia map to the peri-infarct zone in the subacute phase of ischemic stroke. *Stroke* 37(7):1749-1753.

210. Ching ASC, *et al.* (2012) Current paradigm of the 18-kDa translocator protein (TSPO) as a molecular target for PET imaging in neuroinflammation and neurodegenerative diseases. *Insights into imaging* 3(1):111-119.

211. Mosconi L, *et al.* (2009) FDG-PET changes in brain glucose metabolism from normal cognition to pathologically verified Alzheimer's disease. *European journal of nuclear medicine and molecular imaging* 36(5):811-822.

212. Mosconi L (2005) Brain glucose metabolism in the early and specific diagnosis of Alzheimer's disease. *European journal of nuclear medicine and molecular imaging* 32(4):486-510.

213. De Leon M, *et al.* (2001) Prediction of cognitive decline in normal elderly subjects with 2-[18F] fluoro-2-deoxy-D-glucose/positron-emission tomography (FDG/PET). *Proceedings of the National Academy of Sciences* 98(19):10966-10971.

214. Drzezga A, *et al.* (2005) Prediction of individual clinical outcome in MCI by means of genetic assessment and 18F-FDG PET. *Journal of nuclear medicine* 46(10):1625-1632.

215. Minoshima S, *et al.* (1997) Metabolic reduction in the posterior cingulate cortex in very early Alzheimer's disease. *Annals of neurology* 42(1):85-94.
216. Drzezga A, *et al.* (2003) Cerebral metabolic changes accompanying conversion of mild cognitive impairment into Alzheimer's disease: a PET follow-up study. *European journal of nuclear medicine and molecular imaging* 30(8):1104-1113.
217. Forsberg A, *et al.* (2008) PET imaging of amyloid deposition in patients with mild cognitive impairment. *Neurobiology of aging* 29(10):1456-1465.
218. Pike KE, *et al.* (2007) β-amyloid imaging and memory in non-demented individuals: evidence for preclinical Alzheimer's disease. *Brain* 130(11):2837-2844.
219. Okello A, *et al.* (2009) Conversion of amyloid positive and negative MCI to AD over 3 years An 11C-PIB PET study. *Neurology* 73(10):754-760.
220. Fleisher AS, *et al.* (2011) Using positron emission tomography and florbetapir F 18 to image cortical amyloid in patients with mild cognitive impairment or dementia due to Alzheimer disease. *Archives of neurology* 68(11):1404-1411.
221. Doraiswamy PM, *et al.* (2012) Amyloid-β assessed by florbetapir F 18 PET and 18-month cognitive decline, A multicenter study. *Neurology* 79(16):1636-1644.
222. Klunk WE, *et al.* (2004) Imaging brain amyloid in Alzheimer's disease with Pittsburgh Compound-B. *Annals of neurology* 55(3):306-319.
223. Herholz K & Ebmeier K (2011) Clinical amyloid imaging in Alzheimer's disease. *The Lancet Neurology* 10(7):667-670.
224. Fodero-Tavoletti MT, *et al.* (2011) 18F-THK523: a novel in vivo tau imaging ligand for Alzheimer's disease. *Brain* 134(4):1089-1100.
225. Maruyama M, *et al.* (2013) Imaging of tau pathology in a tauopathy mouse model and in Alzheimer patients compared to normal controls. *Neuron* 79(6):1094-1108.
226. Suhara T, *et al.* (2014) In vivo tau PET imaging using [11C] PBB3 in Alzheimer's disease and non-Alzheimer's disease tauopathies. *Journal of nuclear medicine* 55(supplement 1):1824-1824.
227. Muir KW, Buchan A, von Kummer R, Rother J, & Baron J-C (2006) Imaging of acute stroke. *The Lancet Neurology* 5(9):755-768.
228. Lovblad K-O, *et al.* (1998) Clinical experience with diffusion-weighted MR in patients with acute stroke. *American journal of neuroradiology* 19(6):1061-1066.

229. Ayaz M, Boikov AS, Haacke EM, Kido DK, & Kirsch WM (2010) Imaging cerebral microbleeds using susceptibility weighted imaging: one step toward detecting vascular dementia. *Journal of Magnetic Resonance Imaging* 31(1):142-148.

230. Poels M, *et al.* (2012) Cerebral microbleeds are associated with worse cognitive function The Rotterdam Scan Study. *Neurology* 78(5):326-333.

231. Staekenborg SS, *et al.* (2009) Progression of mild cognitive impairment to dementia: contribution of cerebrovascular disease compared with medial temporal lobe atrophy. *Stroke* 40(4):1269-1274.

232. O'Connor J, *et al.* (2011) Dynamic contrast-enhanced imaging techniques: CT and MRI. *British Journal of Radiology* 84:S112–S120.

233. Chen W, *et al.* (2011) Advances in perfusion magnetic resonance imaging in Alzheimer's disease. *Alzheimer's & Dementia* 7(2):185-196.

234. Hoeffner EG, *et al.* (2004) Cerebral Perfusion CT: Technique and Clinical Applications 1. *Radiology* 231(3):632-644.

235. Lee T-Y (2002) Functional CT: physiological models. *Trends in biotechnology* 20(8):S3-S10.

236. Lee T, Purdie T, & Stewart E (2003) CT imaging of angiogenesis. *The quarterly journal of nuclear medicine* 47(3):171-187.

237. Cenic A, Nabavi DG, Craen RA, Gelb AW, & Lee T-Y (1999) Dynamic CT measurement of cerebral blood flow: a validation study. *American journal of neuroradiology* 20(1):63-73.

238. Johnson JA & Wilson TA (1966) A model for capillary exchange. *American Journal of Physiology* 210:1299-1303.

239. Lawrence KSS & Lee T-Y (1998) An adiabatic approximation to the tissue homogeneity model for water exchange in the brain: I. Theoretical derivation. *Journal of Cerebral Blood Flow & Metabolism* 18(12):1365-1377.

240. Lui Y, Tang E, Allmendinger A, & Spektor V (2010) Evaluation of CT perfusion in the setting of cerebral ischemia: patterns and pitfalls. *American journal of neuroradiology* 31(9):1552-1563.

241. Parsons MW (2008) Perfusion CT: is it clinically useful? *International Journal of Stroke* 3(1):41-50.

242. Nabavi DG, Cenic A, Henderson S, Gelb AW, & Lee T-Y (2001) Perfusion mapping using computed tomography allows accurate prediction of cerebral infarction in experimental brain ischemia. *Stroke* 32(1):175-183.

243. Eastwood JD, *et al.* (2002) CT Perfusion Scanning with Deconvolution Analysis: Pilot Study in Patients with Acute Middle Cerebral Artery Stroke. *Radiology* 222(1):227-236.

244. Streitparth F, *et al.* (2008) Diagnostic value of multislice perfusion CT in dementia patients. *Der Radiologe* 48(2):175-183.

245. Zimny A, *et al.* (2007) Does perfusion CT enable differentiating Alzheimer's disease from vascular dementia and mixed dementia? A preliminary report. *Journal of the neurological sciences* 257(1):114-120.

246. Zimny A, Leszek J, Kiejna A, & Sąsiadek M (2007) Analysis of correlation between the degree of cognitive impairment and the results of perfusion CT in patients with dementia. *Medical Science Monitor* 13(1):23-30.

247. Wintermark M, *et al.* (2005) Comparative overview of brain perfusion imaging techniques. *Stroke* 36(9):e83-e99.

Chapter 2

Hemodynamic Effects of Combined Focal Cerebral Ischemia and Amyloid Protein Toxicity in a Rat Model: A Functional CT Study

This chapter is adapted from the original research manuscript entitled "Hemodynamic Effects of Combined Focal Cerebral Ischemia and Amyloid Protein Toxicity in a Rat Model: A Functional CT Study" published in *PLoS ONE*. 2014, 9(6): e100575 by J. Yang, C.D. d'Esterre, Z. Amtul, D.F. Cechetto and T.Y. Lee.

2.1 Introduction

Stroke and Alzheimer's disease (AD) are the most common contributors to cognitive impairment in the population greater than 65 years of age (1). The pathogenic mechanisms of these two conditions not only overlap, but are also highly interactive (2). In fact, the presence of ischemic lesions or silent infarcts in persons with AD is associated with a greater decline in cognition (3-5). It is speculated that cerebral ischemia (CI) may accelerate AD disease progression (3-8).

For patients with moderate to severe stages of AD and vascular dementia, cerebral hypoperfusion is prevalent (9-12). Changes in cerebral blood flow (CBF) occur early in the pre-symptomatic stages of AD, much sooner than brain atrophy, tau and plaque pathology (10,13-15). Some subjects with mild cognitive impairment (MCI) also show a similar pattern of hypoperfusion, in the absence of substantial Aβ plaque (10,16). Animal studies have shown that CI can stimulate mRNA expression of amyloid precursor protein (APP) and APP proteolytic

processing to β-amyloid protein (Aβ), a central neuro-toxic/degenerative factor in AD pathogenesis (17,18). Disruption of the blood-brain-barrier (BBB) caused by CI may also increase the extravasation of soluble Aβ peptides, as well as its precursor APP, into the brain parenchyma, resulting in a neuroinflammatory reaction and Aβ plaque formation (19,20). In turn, Aβ accumulation can reduce brain capillary density and cause aberration of capillary structures, decreasing local cerebral perfusion (21-25). These hemodynamic changes may indicate neurovascular degeneration (26).

CT perfusion (CTP), a functional imaging modality involving intravenous injection of contrast agent, is currently used for the diagnosis of both acute stroke and brain tumors (27,28). CTP not only measures tissue perfusion but also vascular permeability, an indicator of BBB integrity. Moreover, this technique is more accessible and less expensive to perform in the clinic than single photon emission computed tomography (SPECT) and positron emission tomography (PET), the modalities currently used for studying dementia. CTP-derived CBF and cerebral blood volume (CBV) can clearly reveal the degree and site of ischemia in a relatively short scanning time with minimal invasiveness.

We sought to determine the potential negative hemodynamic effects of Aβ toxicity combined with CI. To mimic the clinical situation, an intra-cerebroventricular injection of $A\beta_{25-35}$ fragment, and unilateral striatal ischemic insult were conducted in an animal model (29,30). CTP imaging was performed to visualize and measure CBF and CBV, in conjunction with histology. We hypothesize that the combination of Aβ toxicity and CI will cause greater hemodynamic disruption compared to CI alone or control.

2.2 Methods and Materials

2.2.1 Animals

Male Wistar rats, weighing 250-300g, were obtained from Charles River (Montreal, Quebec). They were housed in separated cages in a room maintained at 23℃ with light from 7:00 to 19:00 hr, and had free access to food and water. All experimental procedures were approved by the Animal Use Subcommittee of the Canadian Council on Animal Care of our institution (protocol number: 2008-113). At end of the study, all animals were euthanized by administration of pentobarbital overdose (80 mg/kg) and perfused transaortically, first with 0.01M PBS and then followed by 4% paraformaldehyde (pH 7.4). The brains were carefully removed and cryoprotected in 30% sucrose at 4℃ before sectioning.

2.2.2 Surgical procedure

Rats were anesthetized with 2-2.5% isoflurane/medical air during surgery. A stereotaxic frame was used for all surgeries and body temperature was maintained at 37℃. The atlas of Paxinos and Watson was used for selecting the stereotactic coordinates for all injections. Small burr holes were drilled in the parietal bone at near-bregma locations to insert injection cannula (23-gauge). Rats were divided into 4 groups: (1) CI model: unilateral injection of 60pmol vasoconstrictor, endothelin-1 (ET) (Sigma-Aldrich, Oakville, ON) into right striatum (anterior/posterior (AP): +0.5mm relative to bregma, medial/lateral (ML): -3.0mm relative to bregma, and dorsal/ventral (DV): -5.0mm below dura); (2) Aβ+CI model: first bilateral injections of 50nmol $A\beta_{25-35}$ peptide (Bachem, Torrance, CA) into lateral ventricles (AP: -0.8mm relative to bregma, ML: ±1.4mm relative to bregma, and DV: -4.0mm below dura) followed by

the same unilateral ET injection into right striatum; (3) Amyloid alone model (Aβ alone): bilateral injections of 50 nmol $A\beta_{25-35}$ peptide into lateral ventricles was used as an internal control for comparison between Aβ+CI and Aβ alone model; (4) Sham-control: unilateral injection of 10μL of 0.9% w/v saline into right striatum as in the CI model. At the end of each injection, the cannula was left in-situ for 3 minutes before fully retracted. Once all the injections were completed, the wound was sutured and each rat received one dose of intramuscular buprenorphine (40mg/kg).

2.2.3 CT perfusion scanning

CTP studies were performed at pre-surgery baseline, 30min, 60min, 1 week and 4 weeks post-surgery on rats which were anesthetized with 1.5% isoflurane during the scans. Each CTP study started with an injection of iodinated contrast agent (Isovue-300, Bracco Diagnostics, Princeton, NJ) at a dose of 2.5mL/kg body weight into a tail vein at an infusion rate of 8mL/min while a clinical CT scanner (GE Healthcare, Waukesha, WI) continuously scanned coronal sections of the rat brain using the high resolution mode. The technical parameters used were FOV of 10cm, 80kVp, 300mA and 0.4s per rotation of the gantry. Each CTP acquisition consisted of two phases: 24 scans acquired every 1 second, and 12 scans acquired every 14.6 seconds. Sixteen image slices (1.25mm thick/slice) were scanned for each study. CBF and CBV maps were generated with the CT Perfusion software (GE Healthcare, Waukesha, WI) (31).

2.2.4 Image post-processing and analysis

The average maps of all acquired images of each CTP study were manually co-registered to a digital 3D atlas template of the rat brain (LONI rat brain atlas, UCLA, CA) by alignment of corpus callosum, lateral ventricles and cerebellum using Analyze v11.0 software (Mayo Clinic, Rochester, MN). Region of interests (ROIs) were defined in the striata of the same coronal slices of the brains from all experimental groups. Absolute values of CBF and CBV were obtained from the defined striatal ROIs. ROI data from each time point were then normalized in two ways: 1) either with its contralateral value for the groups with unilateral injection of ET and control to differentiate effects of Aβ+CI and CI from control, or 2) with its pre-surgery baseline value for the comparison between Aβ+CI and Aβ alone group.

2.2.5 Immunohistochemistry

Immunohistochemical staining was performed on serial, coronal sections of the entire brain and 35μm-thick sections were cut using a Tissue-Tek Cryo3 sliding microtome (Torrance, CA). Sections were then stained with laminin primary antibody (1:1000, rabbit anti-rat Laminin, Sigma-Aldrich). Laminin staining was used to measure numbers and diameters of microvessels. The stained brain sections were then examined using a light microscope (Leica DC-300, Heerbrugg, Switzerland). The results were expressed as the numbers of dilated microvessels per mm^2 of the striatum.

2.2.6 Statistical analysis

Normalized CBF and CBV between baseline and other time points were analyzed by using one-way ANOVA and Tukey's post hoc tests with a significance level of $p<0.05$. A two-group comparison of the hemodynamics between Aβ+CI and Aβ alone group for each time point, was assessed by t-test with $p<0.05$. All histological measurements were analyzed by using one-way ANOVA followed by Dunnett's post hoc tests with $p<0.05$. All values were presented as mean ± standard error of the mean (SEM).

2.3 Results

2.3.1 CTP functional maps

CTP-derived CBF and CBV maps at baseline, 30min, week 1 and week 4 post injection of one rat from each of the four groups are shown (Figure 2-1 and 2-2), respectively. Baseline CBF and CBV among all groups were not significantly different. In the CI group there was a large ischemic lesion at 30min post injection, which showed as large CBF and CBV defects in the functional maps. The Aβ+CI brain also showed a large hypoperfused lesion at 30min, mainly in the right striatum. Increased CBF (hyperperfusion) and CBV (hypervolemia) were observed at week 1 in both CI and Aβ+CI animals, but not in control. The animal with Aβ alone injection did not show significant changes of CBF and CBV from baseline over 4 weeks. No significant difference in CBF and CBV at week 4 was observed between CI and Aβ+CI group.

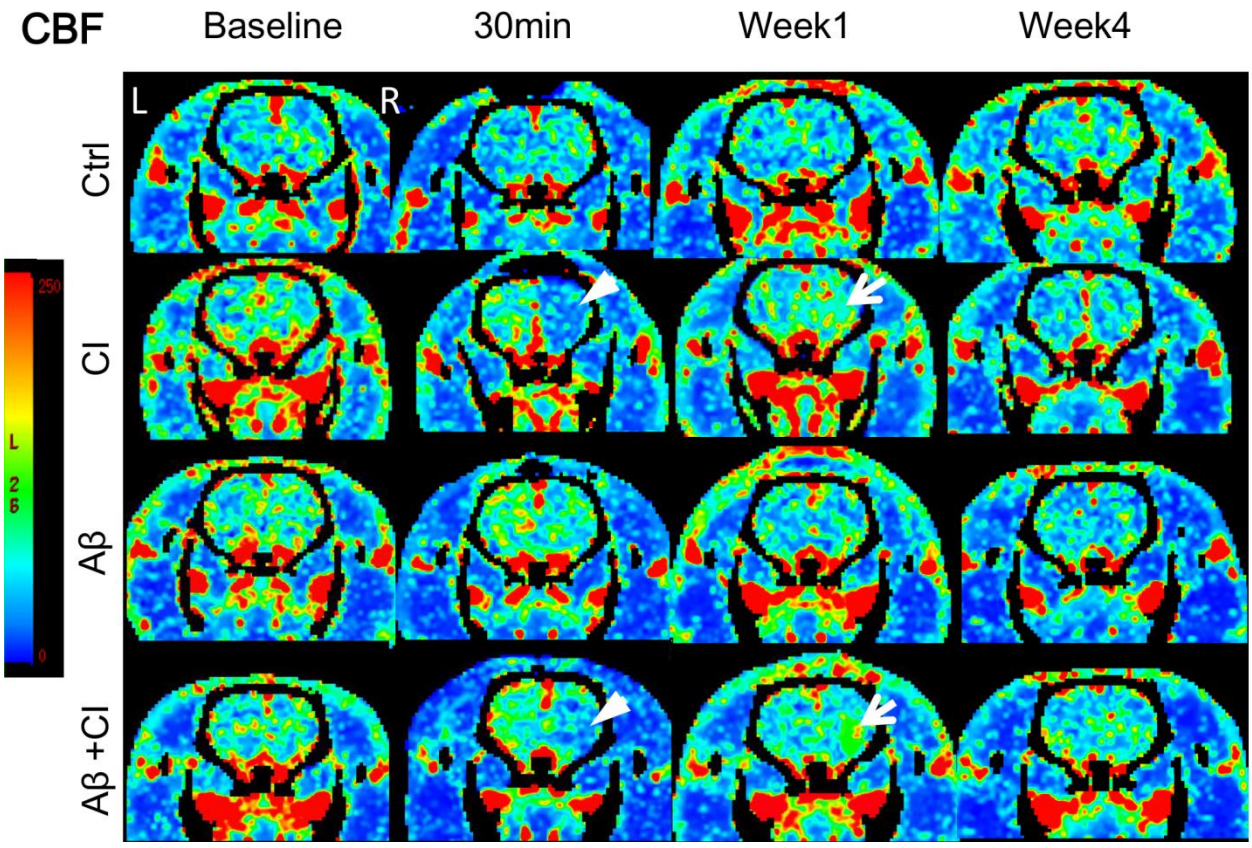

Figure 2-1: **Cerebral blood flow** maps at four time points in: control rat (1st row); CI rat (2nd row); Aβ alone rat (3rd row) and Aβ+CI rat (4th row). Baseline imaging was done before any injection. In CI and Aβ+CI brains, ischemia (white arrow head) and hyperperfusion (white arrow) in the right striatum were observed at 30 minutes and 1 week post injection, respectively. No significant change in CBF was observed over four weeks in control and Aβ alone rats, when compared to their baselines.

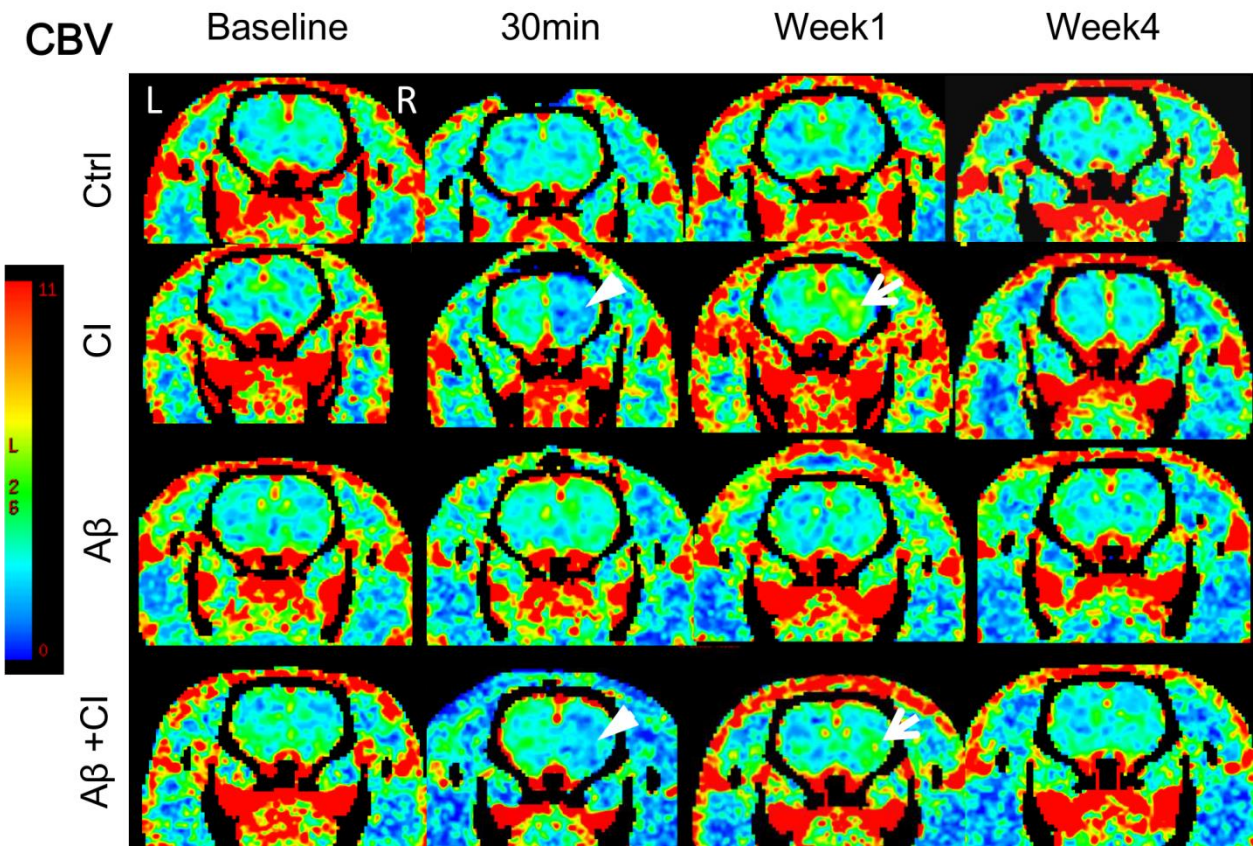

Figure 2-2: **Cerebral blood volume** maps at four time points in: control, CI, Aβ alone and Aβ+CI rat. Baseline imaging was done before any injection. In CI and Aβ+CI brains, similar to the CBF results, CBV deficit (white arrow head) and hypervolemia (white arrow) in the right striatum were observed at 30 minutes and 1 week post injection, respectively. Similar to the CBF maps, no significant CBV change was observed over four weeks in control and Aβ alone rats, when compared to their baselines.

2.3.2 Cerebral ischemia and hyperperfusion post ischemia

Relative CBF (rCBF) and CBV (rCBV) to the contralateral striatum in the control group (n=3) did not show significant differences between baseline and other time points (Figure 2-3a and 2-3b). In contrast, Aβ+CI (n=7) and CI (n=6) groups at the acute phase (30-60 minutes) had a significantly lower rCBF and rCBV in the right striatum when compared to their baseline

values as well as to control (p<0.05). At week 1, rCBF and rCBV increased significantly from baselines in the right striatum of the CI (p<0.05) and Aβ+CI (p<0.05) groups, but not in the control group. Furthermore, at week 4 only the combined Aβ+CI group showed a significantly higher rCBF and rCBV in the right striatum when compared to its baseline (p<0.05). However, no significant difference between Aβ+CI and CI group was seen over 4 weeks.

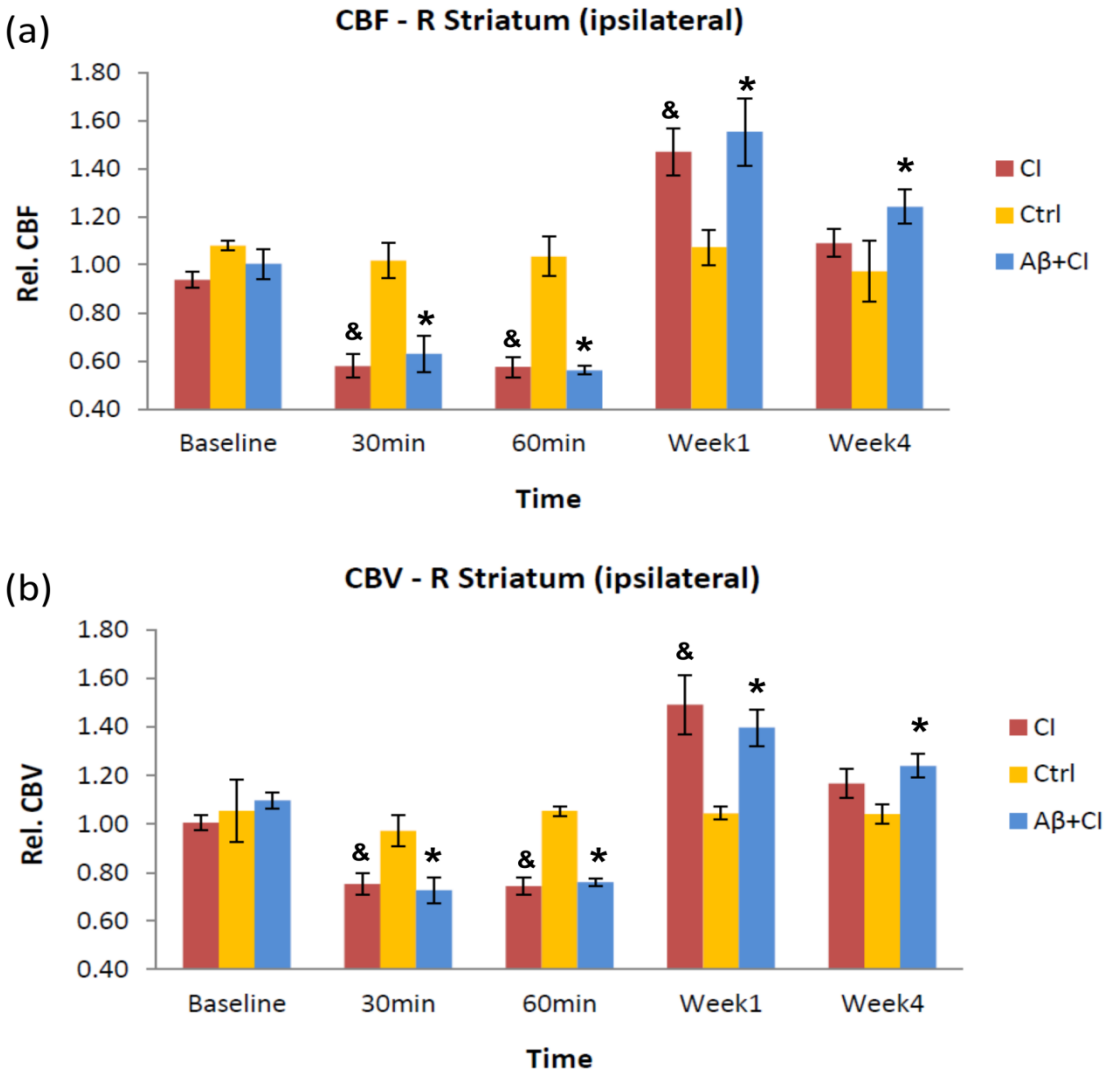

Figure 2-3: **Evolution of striatal CBF and CBV** over four-week period post injection. Absolute CBF and CBV in the right (ipsilateral) striatum at each time point from Aβ+CI, CI and control group were normalized by their contralateral values. (a), normalized (relative) CBF; (b),

normalized CBV. In Aβ+CI group (*, n=7), there were significant differences in CBF and CBV between baseline and those at other time points (30min, 60min, week 1 and week 4. $p<0.05$). Similar findings were shown in the CI group (&, n=6. $p<0.05$), except for week 4. No significant CBF and CBV difference from baseline was found in the control group (n=3). In addition, Aβ+CI and CI groups showed significantly lower CBF and CBV at acute phase and higher CBF and CBV at week 1 than control. However, no significant difference between Aβ+CI and CI group was seen over 4 weeks.

2.3.3 Comparison of hemodynamics between Aβ+CI and Aβ alone model

To differentiate hemodynamic effects caused by combined Aβ and CI to that by Aβ alone, ipsilateral (right striatum) CBF and CBV normalized by their baseline (pre-surgery) values between Aβ+CI and Aβ alone group were compared (Figure 2-4a and 2-4b). At 30-60 minutes and 1 week, but not 4 weeks post the insult, ipsilateral rCBF and rCBV in the striatal ROIs from Aβ+CI model (n=7) were significantly different from those from Aβ alone model (n=6). Aβ+CI group showed an opposite temporal changes in ipsilateral rCBF and rCBV to the Aβ group at the acute state ($p<0.01$) and week 1 ($p<0.05$). At the first week, hyperperfusion and hypervolemia were seen in the Aβ+CI group, but not in the Aβ group. At week 4 the hyperperfusion and hypervolemia in the Aβ+CI group had subsided to be statistically non-significant from its baseline. Interestingly, from week 1 to week 4, ipsilateral rCBF and rCBV of Aβ+CI group decreased much faster than those of Aβ alone group (-36 ± -11% versus -6 ± -9% for CBF; -20 ± -7% versus -2 ± -6% for CBV).

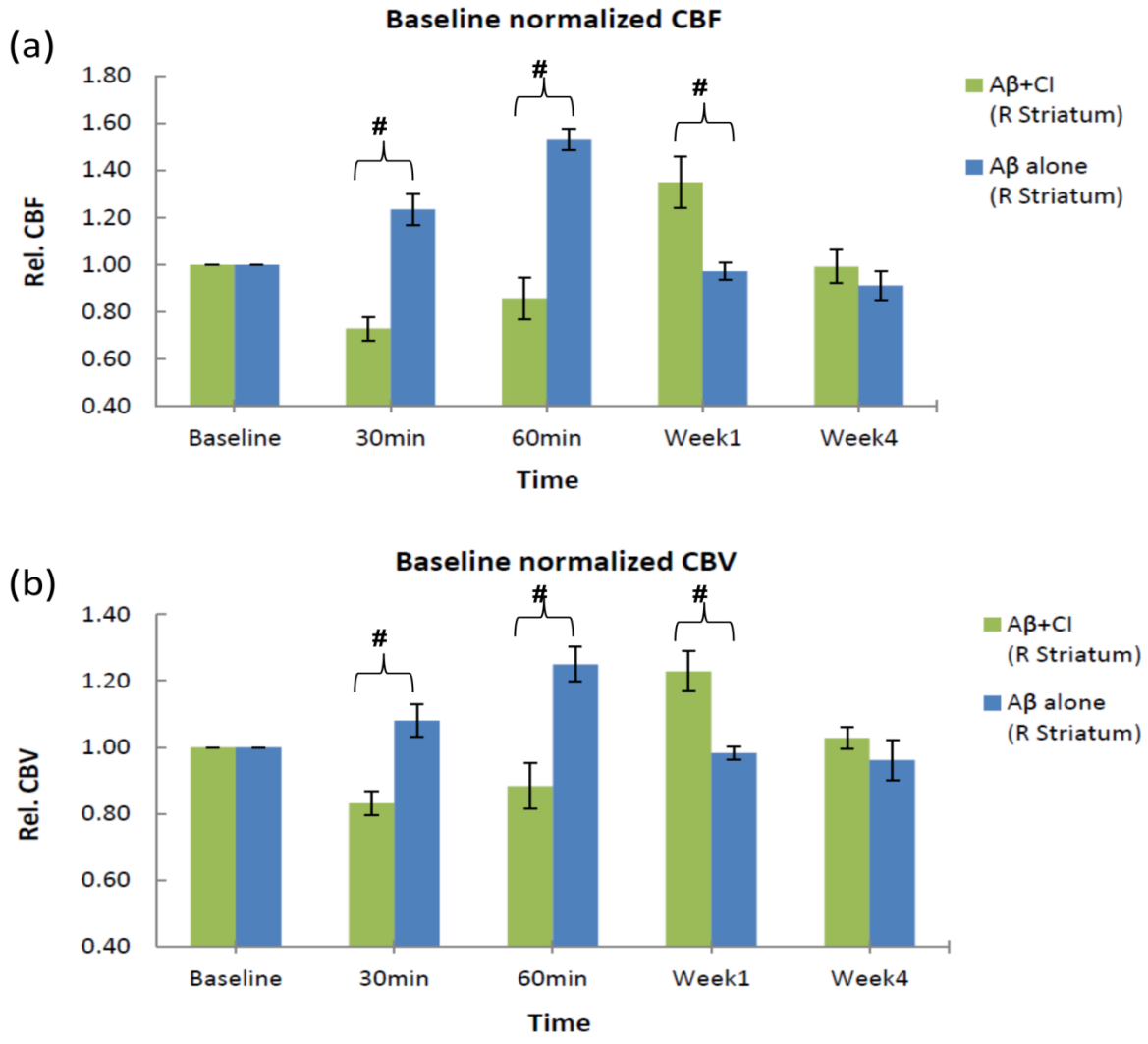

Figure 2-4: **Hemodynamic effects of Aβ+CI and Aβ alone models**. For rats which had combined Aβ and ET injections (n=7) and Aβ only injections (n=6), absolute CBF and CBV in the right (ipsilateral) striatum were normalized with their respective baseline values. Both relative CBF (a) and CBV (b) were significantly different between the Aβ+CI and Aβ alone group at the time points post insult except for week 4 (#, $p<0.01$ for 30-60min, $p<0.05$ for week1). At week 4, rCBF and rCBV in both Aβ+CI and Aβ alone groups dropped to the baseline level.

2.3.4 Vascular pathology after induced CI and Aβ

Viable microvessels assessed by laminin staining was determined in the right (ipsilateral) striatum of control (n=3), CI (n=6) and Aβ+CI (n=6) groups. At week 1, a diffused network of laminin-positive vessels as a result of leakage was detected in the core lesion of CI and Aβ+CI brains. The presence of dilated microvessels (with a diameter greater than 10 μm) was also observed surrounding the lesion epicenter at the striatum in CI and Aβ+CI groups (Figure 2-5, B and C). However, at week 4, laminin immunoreactivity was observed extensively around damaged microvessels in the lesion of CI and Aβ+CI brains (Figure 2-5, E and F), and these brains also had a reduction in dilated vessels. The average number of dilated microvessels per mm^2 in the core of right striatum was 29±2 for CI and 34±3 for Aβ+CI group at week 1, but this number significantly decreased to 3±1 and 5±1 for CI and Aβ+CI, respectively at week 4.

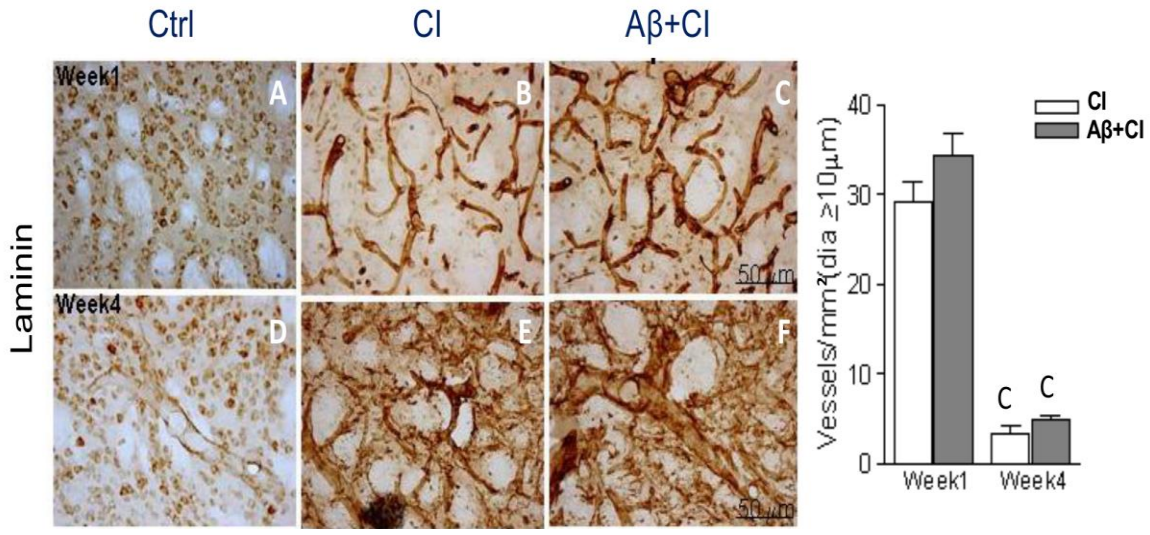

Figure 2-5: **Histology of cerebral microvessels** in control, CI and Aβ+CI groups. Microphotographs showed laminin-stained microvessels in the core of ipsilateral (right) striatum at week 1 (A-C) and week 4 (D-F) post insults. Quantitative analysis of the whole striatal core showed that average density of dilated microvessels (i.e. diameter greater than 10μm) in CI and Aβ+CI groups was significantly higher at week 1 than those at week 4. As induced injury

advanced, at week 4 regular vasculature was almost absent in the Aβ+CI group. Letter "C" indicates significant differences when compared to the control group, $p<0.05$.

2.4 Discussion

The results herein support the hypothesis that the addition of ischemic insult to Aβ pathology leads to greater hemodynamic dysfunction. The major findings are as follows: first, CTP imaging had successfully showed a significant decrease of CBF and CBV in the ipsilateral striatum at the acute phase, followed by a post-ischemic hyperperfusion and hypervolemia at week 1 in Aβ+CI and CI groups. Second, for the two-group comparison between Aβ+CI and Aβ alone model, the ipsilateral striatum affected by Aβ+CI had significant differences in both CBF and CBV compared to that of Aβ alone model from acute phase to week 1. Aβ alone group did not show the hyperperfusion and hypervolemia at week 1, in contrast to the Aβ+CI group. Third, laminin staining showed increased vasodilation at week 1 as a result of reperfusion reaction, which was related to the hyperperfusion in Aβ+CI and CI groups.

Previous work on neurodegeneration has focused on structural alternations, such as brain atrophy and cerebroventricular enlargement using routine CT and MRI (32,33). However, this diagnostic approach is limited by the low sensitivity and specificity to detect early functional changes (33). Conversely, a reduction in glucose metabolism, detected by functional imaging using ^{18}F-FDG PET, has been shown to occur years before onset of clinical symptoms (34-36). Prior to the hypometabolic state, Aβ accumulation in the brain is hypothesized to be the primary driving factor in AD-related pathogenesis (37). Several PET studies have shown that the levels of ^{11}C-PIB (i.e. radiotracer which binds to Aβ aggregates) retention can be used to differentiate

between patients with AD and/or mild cognitive impairment (MCI) and healthy individuals (33,36,38). However, the ability of Aβ imaging to diagnose early AD rests upon the assumption that Aβ plays a central role in the progression of the disease. Some subjects exhibit typical Aβ pathology without clinical symptoms, similarly 25-35% of healthy individuals over the age of 75 years show cortical ^{11}C-PIB uptake (33,38,39), suggesting that Aβ is not the only crucial driving factor for cognitive impairment. Agreed with this view, variably sized cerebrovascular defects are frequently present with AD-related pathogenesis and cognitive decline (4,32,40). Recent studies show that the evolution of changes in cerebral perfusion does not necessarily corroborate with gross structural changes of the neurodegenerative brain (9,23). Brain hypoperfusion and endothelial dysfunction likely precede the hypometabolic and neurodegenerative state observed in MCI and AD (9-11,14,16). As such, CTP imaging may be used to characterize these changes of causative cerebral hemodynamics.

A hyper-acute decrease, followed by an increase in CBF and CBV in the brains of the Aβ+CI group may reflect a dynamic transition from normal cognition/perfusion to a compensatory brain mechanism which attempts to revive the impaired neurovascular functionality prior to substantial neurodegeneration and amyloid deposition. For both Aβ+CI and CI groups, CBF and CBV parameters showed a similar decreasing trend within 60 minutes after the injection, indicative of successful CI induction by ET. Hyperperfusion and hypervolemia were present in the right striatum at week 1 for both Aβ+CI and CI groups, possibly due to release of vasodilators elicited by CI. There were no significant inter-group differences found between the Aβ+CI and CI group at the acute state and week 1-4, indicating that at this phase of disease progression, CI acted as a dominant driving factor in causing hemodynamic dysfunction. This result is supported by a previous investigation which indicates that the development of

pathological changes, changes in infarct size, or even cognitive deficits do not fully develop until 3 weeks after the insult (30). With more prolonged interaction between Aβ pathology and CI, only the Aβ+CI group demonstrated significant intra-group CBF and CBV differences between week 4 and its baseline level, a trend not observed in the control and CI groups.

The presence of soluble Aβ proteins could further increase cellular stress and reduce vascular tone via the inflammatory cascade when CI coexists (29,30). Focal CI has also been shown to produce larger infarcts in transgenic mice overexpressing APP (41,42). Aβ-induced vascular dysregulation, which may increase the propensity for ischemic damage, threatens overall cerebral perfusion (43). This is partially consistent with our findings in which reactive hypervolemia appears at the first week as a post-ischemic reperfusion response in the Aβ+CI model. Recent clinical studies using ASL or PW-MRI also revealed similar states of hyperperfusion in the hippocampus, cingulate gyrus, amygdala and striatum of patients with MCI and mild AD (44-46). Our histopathology data showed that an increase in microvessel diameter, distributed sporadically throughout the striatal ischemic core at week 1, is consistent with vasodilation to maintain regional cerebral perfusion in response to the drop in CBF and CBV after ischemia was induced in CI and Aβ+CI rats.

We also compared longitudinal hemodynamics of ipsilateral striatum between Aβ+CI and Aβ alone group. For the Aβ alone group, the initial CBF and CBV increase at the acute state and later decrease at week 1 and week 4 may be attributed to an immediate response to the injection, and later followed by a vasoconstriction induced by this soluble Aβ (25,47,48), respectively. However, the moderate amount (50 nmol) of Aβ used in this experiment might not be the optimal dose to maintain the vasoconstrictive effect for four weeks or longer duration than

expected. In contrast, the Aβ+CI group showed the opposite hemodynamic effect. This may suggest that hyperperfusion and hypervolemia after CI were a result of prominent hemodynamic disturbance which was further amplified by the initiation of an Aβ-induced pro-inflammatory response. From week 1 to 4, CBF and CBV within Aβ+CI group declined much faster than those of Aβ-only group, indicating that adding Aβ could greatly attenuate the reactive hypervolemia triggered by CI.

Two main limitations of the study included: first, the size of the rat brain relative to the resolution of the clinical CT scanner might contribute to the variability involved in the map processing and registration. However, in our study a high resolution mode was used during CTP scans and this may help to compensate for that limitation. A small animal phantom scanned under the same mode showed an achievable spatial resolution of 500 μm (data not shown), which should be sufficient in guiding ROI placement in a large anatomic region such as striatum in the rat brain here. The feasibility of CTP in evaluating CI has been validated against PET. CTP-derived CBF measurements have shown a good correlation with PET-derived CBF values (49-51). In addition, CTP imaging can be combined with vasodilatory challenge using acetazolamide to assess cerebrovascular reserve in acute stroke, which may further help to identify penumbra and infarct core (52). In the other hand, dynamic susceptibility contrast MRI (DSC-MRI) or MR perfusion has also been applied in assessment of cerebrovascular reserve using acetazolamide. Although MR perfusion has similar or even higher spatial resolution and larger coverage of the brain than CTP, changes in MR signal intensity are not linearly related to changes in contrast concentration, resulting in difficulty with measurement of absolute perfusion parameters in detecting perfusion defect (52, 53). For the second limitation, as vascular cognitive impairment is

an insidious disease process, a study is needed to elucidate the long-term effect of CI on Aβ. Moreover, the addition of contemporaneous PET-CTP imaging is needed.

2.5 Conclusion

In summary, we showed that the co-existence of CI and Aβ disrupted normal cerebral perfusion and exacerbated post-ischemic injury, when compared to the control or Aβ alone. The observed hyperperfusion and hypervolemia post CI support the assertion that there is a local compensatory brain mechanism which occurs early in the pathological progression. This compensation is further associated with increased amount of dilated microvessels. The subsequent decrease in CBF and CBV reflects the failure of vascular autoregulation after Aβ and CI initiated the inflammatory cascade. Overall, this study demonstrated that CTP-derived CBF and CBV are suitable parameters for quantitatively assessing variable hemodynamic changes in the early stage of cerebral ischemia when neurotoxic Aβ is present.

2.6 References

1. Seshadri S, Beiser A, Kelly-Hayes M, Kase CS, Au R, et al. (2006) The lifetime risk of stroke. *Stroke* 37: 345-350.

2. Breteler M (2000) Vascular involvement in cognitive decline and dementia: epidemiologic evidence from the Rotterdam Study and the Rotterdam Scan Study. *Annals of the New York Academy of Sciences* 903: 457-465.

3. Song IU, Kim JS, Kim YI, Eah KY, Lee KS (2007) Clinical significance of silent cerebral infarctions in patients with Alzheimer disease. *Cognitive and behavioral neurology* 20: 93-98.

4. Vermeer SE, Prins ND, den Heijer T, Hofman A, Koudstaal PJ, et al. (2003) Silent brain infarcts and the risk of dementia and cognitive decline. *New England Journal of Medicine* 348: 1215-1222.

5. White L (2009) Brain lesions at autopsy in older Japanese-American men as related to cognitive impairment and dementia in the final years of life: a summary report from the Honolulu-Asia aging study. *Journal of Alzheimer's Disease* 18: 713-725.

6. Snowdon DA, Greiner LH, Mortimer JA, Riley KP, Greiner PA, et al. (1997) Brain infarction and the clinical expression of Alzheimer disease. *JAMA* 277: 813-817.

7. Heyman A, Fillenbaum GG, Welsh-Bohmer KA, Gearing M, Mirra SS, et al. (1998) Cerebral infarcts in patients with autopsy-proven Alzheimer's disease: CERAD, part XVIII. *Neurology* 51: 159-162.

8. Helzner EP, Luchsinger JA, Scarmeas N, Cosentino S, Brickman AM, et al. (2009) Contribution of vascular risk factors to the progression in Alzheimer disease. *Archives of neurology* 66: 343-348.

9. Austin BP, Nair VA, Meier TB, Xu G, Rowley HA, et al. (2011) Effects of Hypoperfusion in Alzheimer's Disease. *Journal of Alzheimer's Disease* 26: 123-133.

10. Johnson NA, Jahng GH, Weiner MW, Miller BL, Chui HC, et al. (2005) Pattern of cerebral hypoperfusion in alzheimer disease and mild cognitive impairment measured with arterial spin-labeling MR imaging: initial experience. *Radiology* 234: 851-859.

11. Schuff N, Matsumoto S, Kmiecik J, Studholme C, Du A, et al. (2009) Cerebral blood flow in ischemic vascular dementia and Alzheimer's disease, measured by arterial spin-labeling magnetic resonance imaging. *Alzheimer's and Dementia* 5: 454-462.

12. Zaknun JJ, Leblhuber F, Schucktanz H (2008) Value of cerebral blood flow quantification in the diagnosis of dementia. *Nuclear medicine communications* 29: 260-269.

13. Hirao K, Ohnishi T, Hirata Y, Yamashita F, Mori T, et al. (2005) The prediction of rapid conversion to Alzheimer's disease in mild cognitive impairment using regional cerebral blood flow SPECT. *Neuroimage* 28: 1014-1021.

14. Kogure D, Matsuda H, Ohnishi T, Asada T, Uno M, et al. (2000) Longitudinal evaluation of early Alzheimer's disease using brain perfusion SPECT. *Journal of nuclear medicine* 41: 1155-1162.

15. Pakrasi S, O'Brien JT (2005) Emission tomography in dementia. *Nuclear medicine communications* 26: 189-196.

16. Alsop DC, Dai W, Grossman M, Detre JA (2010) Arterial spin labeling blood flow MRI: its role in the early characterization of Alzheimer's disease. *Journal of Alzheimer's Disease* 20: 871-880.

17. Hiltunen M, Makinen P, Peraniemi S, Sivenius J, van Groen T, et al. (2009) Focal cerebral ischemia in rats alters APP processing and expression of A-beta peptide degrading enzymes in the thalamus. *Neurobiology of disease* 35: 103-113.

18. Shi J, Yang SH, Stubley L, Day AL, Simpkins JW (2000) Hypoperfusion induces overexpression of β-amyloid precursor protein mRNA in a focal ischemic rodent model. *Brain research* 853: 1-4.

19. Pluta R, Amek MU (2008) Brain ischemia and ischemic blood-brain barrier as etiological factors in sporadic Alzheimer's disease. *Neuropsychiatric disease and treatment* 4: 855-864.

20. Clifford PM, Zarrabi S, Siu G, Kinsler KJ, Kosciuk MC, et al. (2007) Aβ peptides can enter the brain through a defective blood-brain barrier and bind selectively to neurons. *Brain research* 1142: 223-236.

21. Bell MA, Ball MJ (1981) Morphometric comparison of hippocampal microvasculature in ageing and demented people: diameters and densities. *Acta neuropathologica* 53: 299-318.

22. Brown WR, Thore CR (2011) Review: cerebral microvascular pathology in ageing and neurodegeneration. *Neuropathology and applied neurobiology* 37: 56-74.

23. de la Torre JC (2002) Alzheimer disease as a vascular disorder: nosological evidence. *Stroke* 33: 1152-1162.

24. Dietrich HH, Xiang C, Han BH, Zipfel GJ, Holtzman DM (2010) Soluble amyloid-β, effect on cerebral arteriolar regulation and vascular cells. *Molecular neurodegeneration* 5: 15-27.

25. Suo Z, Humphrey J, Kundtz A, Sethi F, Placzek A, et al. (1998) Soluble Alzheimers β-amyloid constricts the cerebral vasculature in vivo. *Neuroscience letters* 257: 77-80.

26. de la Torre JC (2008) Pathophysiology of neuronal energy crisis in Alzheimer's disease. *Neurodegenerative diseases* 5: 126-132.

27. Miles KA (2010) Molecular imaging with dynamic contrast-enhanced computed tomography. *Clinical radiology* 65: 549-556.

28. d'Esterre CD, Fainardi E, Aviv RI, Lee TY (2012) Improving Acute Stroke Management with Computed Tomography Perfusion: A Review of Imaging Basics and Applications. *Translational Stroke Research* 3: 205-220.

29. Whitehead SN, Hachinski VC, Cechetto DF (2005) Interaction Between a Rat Model of Cerebral Ischemia and β-Amyloid Toxicity:Inflammatory Responses. *Stroke* 36: 107-112.

30. Whitehead SN, Cheng G, Hachinski VC, Cechetto DF (2007) Progressive increase in infarct size, neuroinflammation, and cognitive deficits in the presence of high levels of amyloid. *Stroke* 38: 3245-3250.

31. Cenic A, Nabavi DG, Craen RA, Gelb AW, Lee TY (1999) Dynamic CT measurement of cerebral blood flow: a validation study. *AJNR* 20: 63-73.

32. O'Brien JT, Erkinjuntti T, Reisberg B, Roman G, Sawada T, et al. (2003) Vascular cognitive impairment. *The Lancet Neurology* 2: 89-98.

33. Villemagne VL, Rowe CC (2011) Amyloid imaging. *International Psychogeriatrics* 23: S41-S49.

34. Mosconi L, Berti V, Glodzik L, Pupi A, De Santi S, et al. (2010) Pre-clinical detection of Alzheimer's disease using FDG-PET, with or without amyloid imaging. *Journal of Alzheimer's Disease* 20: 843-854.

35. Mosconi L, Mistur R, Switalski R, Tsui WH, Glodzik L, et al. (2009) FDG-PET changes in brain glucose metabolism from normal cognition to pathologically verified Alzheimer's disease. *European journal of nuclear medicine and molecular imaging* 36: 811-822.

36. Nordberg A, Rinne JO, Kadir A, Långström B (2010) The use of PET in Alzheimer disease. *Nature Reviews Neurology* 6: 78-87.

37. Jantaratnotai N, Ryu JK, Schwab C, McGeer PL, McLarnon JG (2011) Comparison of Vascular Perturbations in an Aβ-Injected Animal Model and in AD Brain. *International Journal of Alzheimer's Disease* 2011: 1-8.

38. Wolk DA, Klunk WE (2009) Update on amyloid imaging: from healthy aging to Alzheimer's disease. *Current neurology and neuroscience reports* 9: 345-352.

39. Pike KE, Savage G, Villemagne VL, Ng S, Moss SA, et al. (2007) β-amyloid imaging and memory in non-demented individuals: evidence for preclinical Alzheimer's disease. *Brain* 130: 2837-2844.

40. Riekse RG, Leverenz JB, McCormick W, Bowen JD, Teri L, et al. (2004) Effect of Vascular Lesions on Cognition in Alzheimer's Disease: A Community Based Study. *Journal of the American Geriatrics Society* 52: 1442-1448.

41. Koistinaho M, Kettunen MI, Goldsteins G, Salminen A, Ort M, et al. (2002) Beta-Amyloid precursor protein transgenic mice that harbor diffuse Aβ deposits but do not form plaques show increased ischemic vulnerability: role of inflammation. *PNAS* 99: 1610-1615.

42. Zhang F, Eckman C, Younkin S, Hsiao KK, Iadecola C (1997) Increased susceptibility to ischemic brain damage in transgenic mice overexpressing the amyloid precursor protein. *The Journal of neuroscience* 17: 7655-7661.

43. Lewis H, Beher D, Cookson N, Oakley A, Piggott M, et al. (2006) Quantification of Alzheimer pathology in ageing and dementia: age-related accumulation of amyloid-beta (42) peptide in vascular dementia. *Neuropathology and applied Neurobiology* 32: 103-118.

44. Alsop DC, Casement M, de Bazelaire C, Fong T, Press DZ (2008) Hippocampal hyperperfusion in Alzheimer's disease. *NeuroImage* 42: 1267-1274.

45. Dai W, Lopez OL, Carmichael OT, Becker JT, Kuller LH, et al. (2009) Mild Cognitive Impairment and Alzheimer Disease: Patterns of Altered Cerebral Blood Flow at MR Imaging. *Radiology* 250: 856-866.

46. Luckhaus C, Flüß MO, Wittsack HJ, Grass-Kapanke B, Janner M, et al. (2008) Detection of changed regional cerebral blood flow in mild cognitive impairment and early Alzheimer's dementia by perfusion-weighted magnetic resonance imaging. *NeuroImage* 40: 495-503.

47. Paris D, Humphrey J, Quadros A, Patel N, Crescentini R, et al. (2003) Vasoactive effects of Aβ in isolated human cerebrovessels and in a transgenic mouse model of Alzheimer's disease: role of inflammation. *Neurol Res* 25: 642-651.

48. Townsend KP, Obregon D, Quadros A, Patel N, Volmar CH, et al. (2002) Proinflammatory and vasoactive effects of Aβ in the cerebrovasculature. *Annals of the New York Academy of Sciences* 977: 65-76.

49. Nariai T, Suzuki R, Hirakawa K, Maehara T, Ishii K, et al. (1995) Vascular reserve in chronic cerebral ischemia measured by the acetazolamide challenge test: comparison with positron emission tomography. *AJNR* 16: 563-570.

50. Bisdas S, Nemitz O, Berding G, Weissenborn K, Ahl B, et al. (2006) Correlative assessment of cerebral blood flow obtained with perfusion CT and positron emission tomography in symptomatic stenotic carotid disease. *European radiology* 16: 2220-2228.

51. Kudo K, Terae S, Katoh C, Oka M, Shiga T, et al. (2003) Quantitative cerebral blood flow measurement with dynamic perfusion CT using the vascular-pixel elimination method: comparison with $H_2{}^{15}O$ positron emission tomography. *AJNR* 24: 419-426.

52. Wintermark M, Sesay M, Barbier E, Borbély K, Dillon WP, et al. (2005) Comparative overview of brain perfusion imaging techniques. *Stroke* 36: e83-e99.

53. O'Connor JPB, Tofts PS, Miles KA, Parkes LM, Thompson G, et al. (2011) Dynamic contrast-enhanced imaging techniques: CT and MRI. *Br J Radiol* 84: S112-S120

Chapter 3

Breakdown of Blood-Brain Barrier and Neuroinflammation in a Rat Model of Combined Focal Cerebral Ischemia and Amyloid Protein Toxicity: A Longitudinal CT and PET Study

This chapter is adapted from the original research manuscript entitled "Breakdown of Blood-Brain Barrier and Neuroinflammation in a Rat Model of Combined Focal Cerebral Ischemia and Amyloid Protein Toxicity: A Longitudinal CT and PET Study" submitted to *Frontiers in Aging Neuroscience* by J. Yang, L. Morrison, L. Wang, N. Cockburn, D.F. Cechetto and T.Y. Lee.

3.1 Introduction

Stroke and Alzheimer's disease (AD) are the most common contributors to cognitive impairment in the population greater than 65 years of age (1). Stroke and AD pathology not only coexist in the brain, but also interact with each other. The presence of ischemic lesions or silent infarcts (e.g. subcortical infarcts, lacunes and microbleeds) in AD individuals is associated with a greater decline in cognition (2-5). Therefore, cerebral ischemia (CI) may accelerate AD disease progression.

Animal studies have shown that CI can stimulate mRNA expression of amyloid precursor protein (APP) and APP proteolytic processing to β-amyloid protein (Aβ) (6-9), a central neuro-toxic/degenerative factor in AD pathogenesis. Disruption of the blood-brain-barrier (BBB) caused by CI may also increase the extravasation of soluble Aβ and its precursor APP into the

brain parenchyma (10-12), and then induce inflammatory cytokines, leading to a neuroinflammatory reaction (13-15). In turn, Aβ accumulation over the long term can reduce brain capillary density and disrupt the BBB integrity (16, 17). Morphologically, the basement membrane of microvessels becomes thicker and overall capillary length is reduced in AD brains with coexisting cerebrovascular pathology (17-19). These morphological changes of cerebral microvasculature are commonly associated with subcortical ischemic lesions and/or white matter abnormality, which are often seen in elderly AD subjects (2, 17, 20). Therefore, investigation of BBB breakdown after CI in the brain with coexisting Aβ toxicity may reveal the early pathogenesis of the disease, and provide guidance for post-ischemia management in minimizing the contribution from BBB dysfunction.

CT perfusion (CTP), a functional imaging modality involving intravenous injection of contrast agent, is currently used for the diagnosis of both acute stroke and brain tumors (21). CTP not only measures tissue perfusion but also vascular permeability surface product, an indicator of BBB integrity (22, 23). Positron emission tomography (PET) imaging with ^{18}F-FEPPA (24), which binds to activated microglia, can provide in-vivo information about location and extent of the neuroinflammation and related neuronal damages.

We used a previously established animal model of combined focal CI and Aβ toxicity (14, 25). CTP imaging was performed to study temporal changes of BBB permeability, cerebral blood flow (CBF) and blood volume (CBV), and neuroinflammation was revealed by ^{18}F-FEPPA over the first 3 months post CI and Aβ insult. Immunohistochemistry was used for examining BBB damage and activated microglia.

3.2 Methods and Materials

3.2.1 Animals and surgery

Male Wistar rats, weighing 550-600g, were obtained from Charles River (Montreal, Quebec). They were housed in separated cages in a room maintained at 23℃ with light from 7:00 to 19:00 hr, and had free access to food and water. The surgical procedure was described in the protocol of the previous study (14). Briefly, rats were anesthetized with 2-2.5% isoflurane/medical air during surgery. A stereotaxic frame was used for all surgeries and body temperature was maintained at 37℃. Rats were divided into three groups: (1) CI model: unilateral injection of 200pmol vasoconstrictor, endothelin-1 (ET) (Sigma-Aldrich, Oakville, ON) into the right striatum; (2) CI+Aβ model: injection of 150nmol $A\beta_{25-35}$ peptide (Bachem, Torrance, CA) into the right lateral ventricle followed by the same ET injection into the right striatum; (3) Sham-control: unilateral injection of 10μL of 0.9% w/v saline into the right striatum as in the CI model. The injecting needle was left in-situ for 3 minutes before fully retracted. At end of the study, all animals were euthanized by administration of pentobarbital overdose (80 mg/kg). A total of 16 rats were used for CTP studies, 10 rats for PET studies and 9 rats for histology. All experimental procedures were approved by the Animal Use Subcommittee of the Canadian Council on Animal Care of our institution.

3.2.2 CT perfusion study

CTP studies were performed at pre-surgery baseline, and 60 minutes, 7, 14, 28 (1 month), 56 (2 months) and 90 days (3 months) post surgery on anesthetized rats (1.5-2% isoflurane). Each CTP study started with an injection of iodinated contrast agent (Bracco Diagnostics, Princeton,

NJ) at a dose of 2.5mL/kg body weight into a tail vein at an infusion rate of 8mL/min while a clinical CT scanner (GE Healthcare, Waukesha, WI) continuously scanned coronal sections of the rat brain. A two-phase CTP scanning protocol was used: 24 scans acquired every second, and 12 scans acquired every 14.6 seconds. BBB permeability surface product (BBB-PS), CBF and CBV maps were generated using the delay insensitive CT Perfusion software (GE Healthcare, Waukesha, WI) based on the modified Johnson-Wilson model (23, 26).

3.2.3 PET study

PET studies were performed at 7, 14, 28, 56 and 90 days post surgery using a micro-PET scanner (GE Healthcare, Waukesha, WI). Anesthesia was induced for all animals with 1.5-2% isoflurane. At the beginning of each PET scan, the rat's tail vein was used for intravenous administration of the radiotracer, ^{18}F-FEPPA (at specific activity of 1-3 Ci/μmol and radiochemical purity >96%). Each rat received about 18.5 MBq of ^{18}F-FEPPA and was scanned for 60 minutes. The list mode emission data were sorted into a series of 10 time frames (1min x 5 frames, 10mins x 4 frames and 15mins x 1 frame) and corrected for scatters and randoms. The images were then reconstructed using FORE/OSEM 2D. The time frame for the last 15 minutes was used for image analysis because FEPPA uptake was the highest at that time. Each PET study was followed by a non-enhanced CT (NECT) scan without moving the rat to aid image registration.

3.2.4 Image analysis

The method for registration of CTP maps across time points was described in our previous study (25). Using similar method with Analyze v11.0 software (Mayo Clinic, Rochester, MN), the PET images were also manually 3D-registered to the corresponding CTP maps for each time point via the NECT images acquired with each PET study. For the CTP maps, regions of interests (ROIs) were defined in the ipsilateral (right) and contralateral striatum of the brain. The ROI data in the ipsilateral striatum were then normalized with the contralateral values for each time point to obtain relative BBB-PS, CBF and CBV. For the PET images of ^{18}F-FEPPA, ROIs were defined in the areas of increased uptake in the ipsilateral striatum using Analyze. The ipsilateral ROI data were then normalized with the contralateral data to obtain the relative uptake value.

3.2.5 Immunohistochemistry

After the completion of all imaging studies, the rat brain was removed and serial coronal 20μm-thick sections were cut using a Tissue-Tek Cryo3 sliding microtome (Torrance, CA). Sections were stained with IgG (1:1000, goat anti-rat IgG, Vector Laboratories, Burlingame, CA) and OX-6 primary antibody (1:1000, mouse anti-rat OX-6, BD Pharmingen, San Diego, CA). The stained brain sections were then examined using a light microscope (Leica DC-300, Heerbrugg, Switzerland). IgG staining was used to detect and measure BBB leakage (27), and OX-6 staining was used to measure the density of activated microglia (14). The results were expressed as the percentage of IgG-positive area in the striatum and OX-6-positive microglia cells per mm^2.

3.2.6 Statistical analysis

Statistical analyses were performed using SigmaPlot v12.0 (Systat Software, San Jose, CA). The normalized BBB-PS, CBF, CBV, relative ^{18}F-FEPPA uptake and histological data of the three groups were analyzed using Kruskal–Wallis test, and Tukey's post hoc tests for multiple comparisons with a significance level of $p<0.05$ for all time points. All values were presented as mean ± standard error of the mean (SEM).

3.3 Results

3.3.1 Changes in BBB permeability

The relative BBB-PS of the ipsilateral ROIs over 3 months for the three experimental groups is shown (Figure 3-1). At baseline and 60 minutes post insult, no significant BBB-PS differences were detected between groups. At 7 days after the insult, CI+Aβ group (n=6) had a significantly higher BBB-PS than saline-injected sham group (n=4, $p<0.05$) but not CI group (n=6). However, there were no significant differences in BBB-PS between groups at day 14 and month 1, although both CI and CI+Aβ groups had a trend of elevated BBB-PS above the sham group. In the chronic phase at month 2 and 3, CI+Aβ group showed significantly higher BBB-PS than both CI and sham groups ($p<0.05$). There were no significant BBB-PS differences between CI and sham at all time points. In addition, intra-group comparison showed that BBB-PS in the CI+Aβ group significantly increased at day 7, month 2 and month 3 compared to the baseline level ($p<0.05$), while this was not seen in the other groups. The BBB-PS maps (Figure 3-2) clearly revealed the evolution of BBB-PS over time in the three groups. Both CI+Aβ and CI rats showed

focal patches of high BBB-PS at day 7. However, at month 2 and 3 only CI+Aβ rat still had the elevated BBB-PS in the ipsilateral hemisphere.

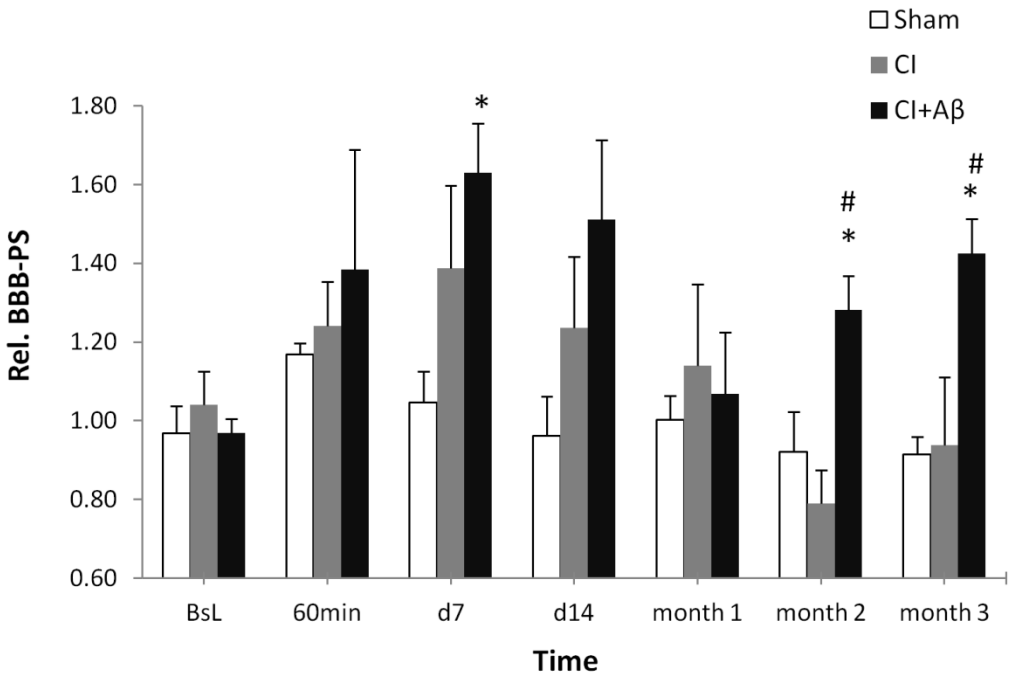

Figure 3-1: **Relative BBB-PS in the ipsilateral striatum of the three groups over the first 3 months**. There were no significant differences between groups for the pre-surgery baseline BBB-PS. At day 7 after the insult, CI+Aβ group showed a significantly higher BBB-PS than the sham, but non-significantly higher BBB-PS than the CI group. At later times, CI+Aβ group had a significantly higher BBB-PS than both sham and CI groups at month 2 and 3. * CI+Aβ (n=6) vs Sham (n=4), # CI+Aβ vs CI (n=6), $P<0.05$ for all.

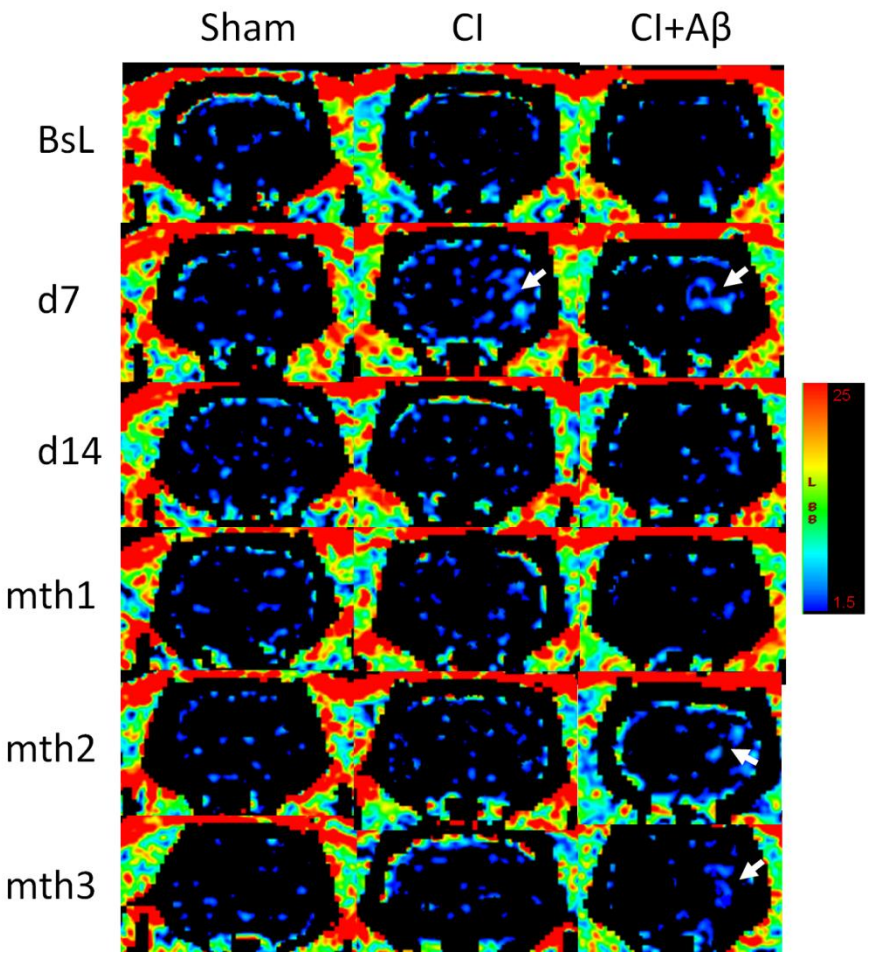

Figure 3-2: **Quantitative BBB-PS maps displayed in rainbow scale** (mL/min/100g). Bright blue patches in the brain indicate elevated BBB-PS of a leaky microvasculature. BBB-PS in the ipsilateral (right) side of the brain increased (white arrows) in the CI+Aβ and CI animals at day 7. The high BBB-PS was only presented in the CI+Aβ animal at month 2 and 3, but not seen in the sham and CI animals.

3.3.2 PET imaging of neuroinflammation

In-vivo neuroinflammation was imaged by the radiolabelled ligand, ^{18}F-FEPPA. Relative ^{18}F-FEPPA uptake in the ipsilateral striatum for each group is shown (Figure 3-3). The saline-injected sham animals were imaged only at the first week after the injection. The sham group (n=3) showed no uptake at day 7, whereas both CI+Aβ (n=4) and CI (n=3) groups had

significantly higher FEPPA uptakes at day 7 than the sham group (p<0.05). At day 14, uptake in CI+Aβ group remained significantly higher than both CI and sham groups (p<0.05). For CI+Aβ and CI groups, uptake reached the peak at day 7. At month 1, 2 and 3, only CI+Aβ group still had significantly higher uptake than the sham group (p<0.05). However, uptake in CI+Aβ group at month 1-3 was not significantly different from CI group.

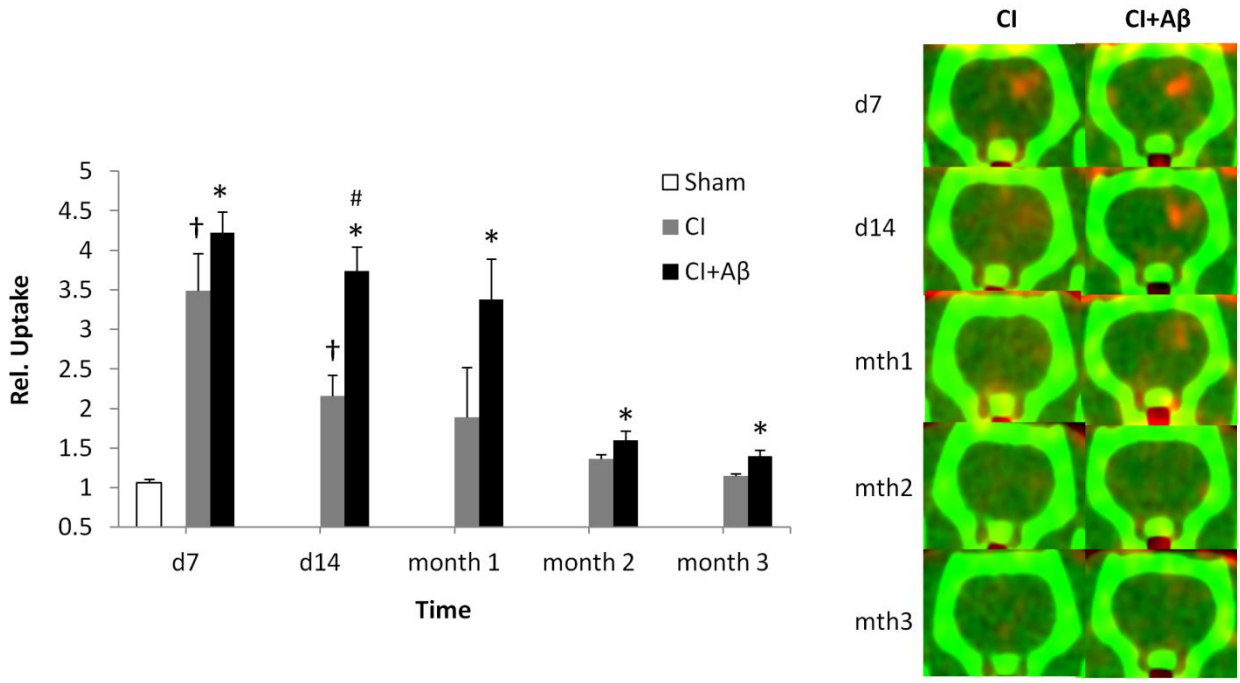

Figure 3-3: **Relative ^{18}F-FEPPA uptake in the ipsilateral striatum**. Relative uptake in the CI+Aβ group was significantly higher than sham group from day 7 to month 3. The CI group showed a significantly higher uptake than sham group, only at day 7 and 14 but not at other times. Uptake in CI+Aβ group was significantly higher than CI group at day 14. Saline-injected sham animals were scanned only at day 7 and showed no uptake. *Sham (n=3) vs CI+Aβ (n=4), † Sham vs CI (n=3), # CI+Aβ vs CI, P<0.05 for all.

3.3.3 Cerebral perfusion

Relative CBF and CBV of the ipsilateral striatum were compared among the three groups over time (Figures 3-4A and 3-4B). At baseline, there were no significant differences in relative CBF and CBV between groups. At 60 minutes after the insult, both CI+Aβ and CI groups showed significant decreases in CBF and CBV as compared to the sham group ($p<0.01$). At day 7, CBF and CBV of the CI+Aβ and CI groups increased significantly compared to the sham group ($p<0.05$), with the highest level in the CI+Aβ animals. At day 14 and month 1, CBV but not CBF in the CI+Aβ and CI groups were still significantly higher than the sham group ($p<0.05$). However, the comparison between CI+Aβ and CI group failed to show any statistical difference for day 7, 14 and month 1. At month 2 and 3, no significant CBF and CBV differences were detected among the three groups.

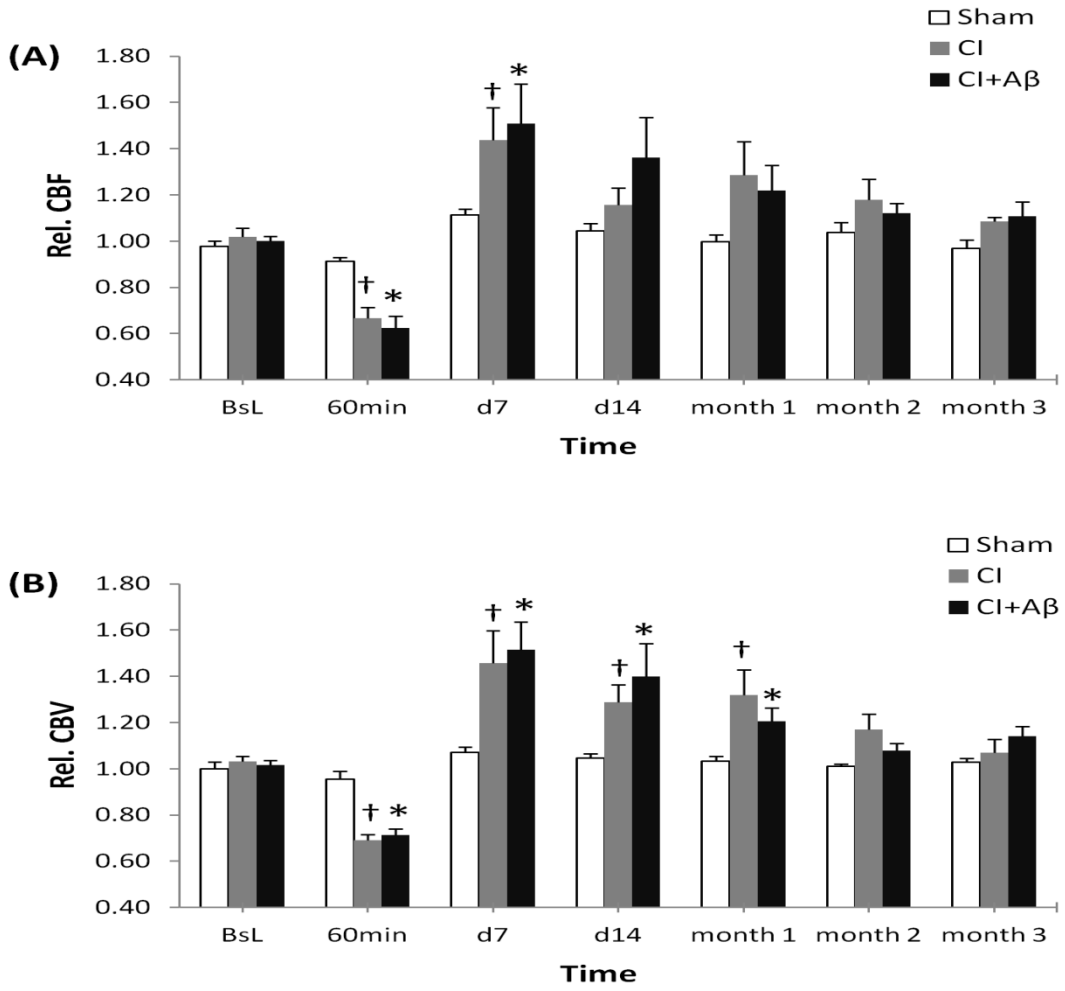

Figure 3-4: **Relative CBF (A) and CBV (B) in the ipsilateral striatum**. At pre-surgery baseline, there were no significant differences in both relative CBF and CBV between groups. Relative CBF and CBV of CI+Aβ and CI groups decreased significantly compared to sham group at 60 minutes post insult. At day 7 CBF and CBV of CI+Aβ and CI groups increased significantly (hyperperfusion/hyperemia) compared to the sham group. At day 14 and month 1, CBV but not CBF in CI+Aβ and CI groups remained significantly higher than sham group. There were no significant differences in CBF and CBV between groups at month 2 and 3. *CI+Aβ (n=6) vs Sham (n=4), † CI (n=6) vs Sham, $P<0.05$ for all.

3.3.4 IgG leakage and microglial activation

Immunohistochemical analysis (Figure 3-5) showed the highest IgG extravasation (indicator of BBB leakage) and microglia density (indicator of neuroinflammation) in the lesion of CI+Aβ group (n=3), as compared to CI (n=3, $p<0.05$) and sham (n=3, $p<0.001$) groups. CI group had significantly higher IgG extravasation and microglia density than sham group ($p<0.001$). Histology revealed that about 30% of the area in the ipsilateral striatum was IgG positive, and activated microglia formed a denser colony in the CI+Aβ brain, compared to the minor IgG extravasation and diffused pattern of activated microglia in CI group.

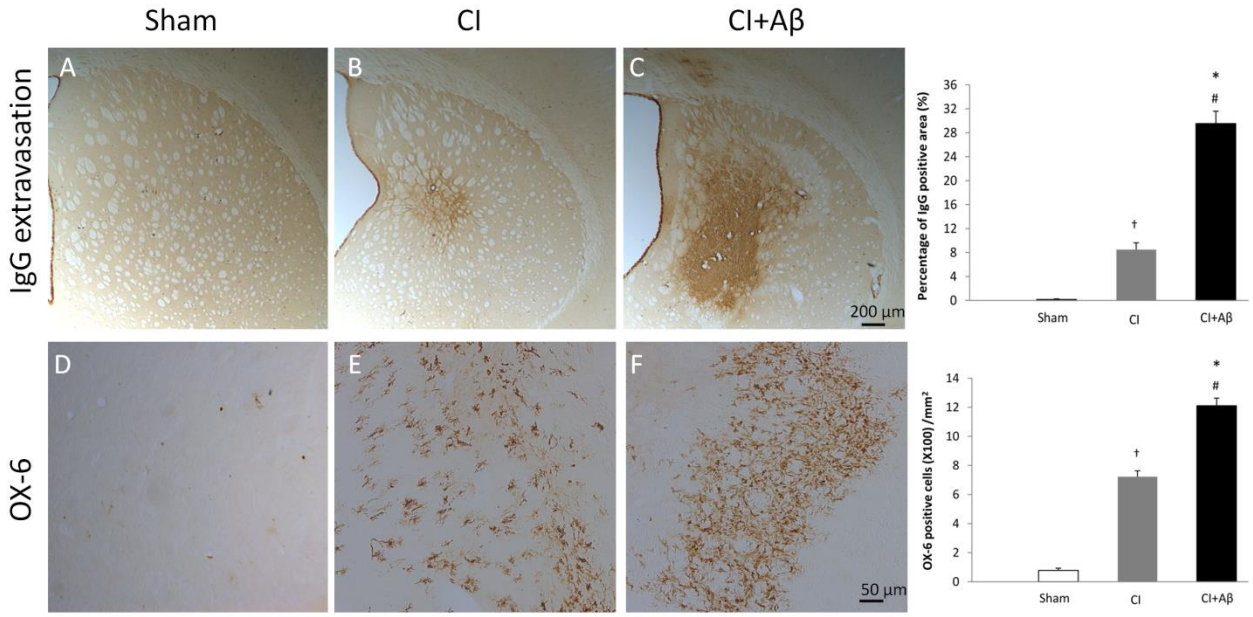

Figure 3-5: **Immunohistochemistry of IgG leakage (A-C) and activated microglia (D-F)**. The data showed a significantly larger IgG-positive region in the ipsilateral (right) striatum of CI+Aβ group compared to CI and sham groups. In the striatal lesion, activated microglia was positively stained with OX-6. CI+Aβ group had the highest density of activated microglia, followed by the moderate amount of activated microglia in the CI group, as compared to the sham. *Sham (n=3) vs CI+Aβ (n=3) at P<0.001, † Sham vs CI (n=3) at P<0.001, # CI+Aβ vs CI at P<0.05.

3.4 Discussion

This imaging study investigated the changes of BBB-PS, neuroinflammation and cerebral hemodynamics over the first 3 months post CI with and without the presence of Aβ. The major findings of the study indicate that BBB-PS in the ipsilateral striatum increased non-significantly at day 7, and significantly at month 2 and 3 in the CI+Aβ group but not the CI group. PET imaging of ^{18}F-FEPPA showed increased levels of neuroinflammation in the striatal lesion of the CI+Aβ brain throughout the 3-month period, with the highest level appeared at day 7 and a smaller sustained increase at month 2 and 3. At day 14, a significantly higher ^{18}F-FEPPA uptake was seen in CI+Aβ group as compared to sham and CI. This is consistent with other reports using similar radiolabeled ligands that bind to translocator protein (TSPO) in activated microglia (28, 29). In addition, CBF and CBV in both CI+Aβ and CI groups showed a decrease at acute phase due to the induced ischemia and a subsequent hyperemic increase at day 7 but no significant changes at month 2 and 3.

For the past several decades, the pathogenic importance of cerebrovascular dysfunction in AD development has been debated. A considerable number of pathological studies, including the well cited Nun study have elucidated the existence and importance of cerebrovascular lesions (particularly subcortical ischemic infarcts and white matter lesions) and microvascular abnormality in AD patients (2, 16, 19). Moreover, reductions in CBF and glucose metabolism have been observed in AD patients in imaging studies using SPECT or PET (30-32). However, it was difficult to interpret the pathogenic importance of these cerebrovascular and metabolic abnormalities because it was not clear whether they were causes or consequences of neurodegeneration. A growing body of epidemiological evidence has indicated that cerebrovascular diseases (e.g. stroke) and AD share common risk factors, suggesting a

pathogenic connection/interaction between them (17, 33). In our study, CTP and PET imaging were used in a rat model of combined subcortical CI and amyloid injury to investigate the contribution of cerebrovascular abnormality and inflammation to the pathogenesis of neurodegeneration. Our previous work on this animal model had shown changes of cerebral hemodynamics in the first month post CI and Aβ induction (25). The present study not only extended the previous investigation but also provided further perspectives on early microglia-related neuroinflammation and chronic breakdown of blood-brain barrier, which is a crucial part of neurovascular unit in regulating local perfusion and traffic of various molecules in and out of the brain.

The CTP imaging showed an increasing trend of the BBB-PS from acute phase to day 7 in CI and CI+Aβ groups, but only CI+Aβ group had significantly higher BBB-PS at day 7 compared to the sham group. This result is consistent with other reports showing the increased BBB permeability/disruption post CI, particularly at day 7 (34, 35). With additive effects of Aβ protein on CI, a greater BBB disruption was expected at day 7 in the CI+Aβ animals. However, a higher but not significant BBB-PS was present in CI+Aβ group compared to CI group at day 7. This may be due to the sample size or BBB disruption/opening that had already reached or approached the maximal degree at day 7, as compared to the other time points. Furthermore, the significantly higher BBB-PS was seen only in the CI+Aβ subjects at month 2 and 3, suggesting a chronic breakdown of BBB/microvascular integrity due to the greater damage caused by combination of CI and Aβ injuries and induced inflammation. The BBB breakdown is consistent with our IgG immunostaining, which showed significantly higher IgG extravasation in the CI+Aβ brain than CI and sham brain. BBB dysfunction caused by ischemia or Aβ can contribute to subcortical and white matter lesions, capillary degeneration and cerebral amyloid angiopathy

(8, 16, 17, 36), all of which would accelerate the neurodegenerative process. Recent studies have shown that increased BBB permeability is an early indication of subcortical ischemic disease and white matter lesion, which are frequently observed in AD and vascular cognitive impairment (VCI) (20, 37-39). In addition, increased level of cerebrospinal fluid albumin was found in suspected elderly subjects prior to the development of AD (37) or VCI (38), suggesting that BBB dysfunction may have a pathogenic role in both diseases. Additionally, Aβ can trigger the release of inflammatory cytokines and mediators, further exacerbating BBB disruption (36, 40, 41). Therefore, the comorbid model of CI and Aβ which mimicks subcortical ischemia in the striatum and infiltration of soluble Aβ to the periventricular region would allow us to study the interaction between CI and Aβ in causing BBB disruption and neuroinflammation.

Neuroinflammation can play a significant role in AD and ischemic injury (42-45). An important hallmark of neuroinflammation in central nervous system is the activation of resident glial cells such as microglia and astrocytes. In this study, in-vivo PET imaging with ^{18}F-FEPPA showed the highest binding to the activated microglia in the ipsilateral striatum of CI+Aβ group, followed by the moderate binding in CI group within the first month post insult. For CI and CI+Aβ groups, FEPPA uptake reached a maximum at day 7, and then gradually decreased over the first month. The same temporal change of activated microglia after CI has been previously reported in several studies using similar TSPO ligands such as ^{11}C-PK11195 and ^{18}F-DPA-714 (28, 29). However, our study extended the previous observations to demonstrate that the synergistic effect of CI and Aβ would lead to a more pronounced activation of microglia than CI alone at day 14 (by ^{18}F-FEPPA imaging) and at month 3 post insult (by immunohistochemical staining with OX-6). Increased levels of activated microglia or neuroinflammation in AD animal models and patients has been observed with histopathology and PET imaging, and has been

associated with neurodegeneration and low cognitive performance (46-49), suggesting a significant role of inflammation in AD development. Under the converging influences of both CI and Aβ demonstrated in our CI+Aβ model, a more severe neuroinflammation can enhance or accelerate the neuronal damage and cognitive deterioration.

CBF and CBV in the ipsilateral striatum decreased significantly in CI and CI+Aβ groups at 60 min post insult, indicating a successful ischemia was induced. At day 7, increased CBF and CBV in CI and CI+Aβ groups represented a post-ischemia hyperperfusion and hypervolemia (hyperemia). These findings are consistent with our previous study (25). Hyperperfusion or hypervolemia were also observed in the CI and CI+Aβ groups up to one month post insult which corresponded with the more pronounced BBB-PS increase and ^{18}F-FEPPA uptake. Some studies have also found the correlation between prolonged hyperperfusion or hyperemia and BBB leakage and irreversible tissue damage (34, 50-52).

The main limitation of this study is the lack of monitoring of cognitive and functional outcomes. This would be useful for investigating the correlation between degree of BBB breakdown or inflammation and severity of cognitive/functional impairment induced by either CI+Aβ or CI alone. Studies have shown the leakage of plasma albumin into cerebrospinal fluid in AD or VCI patients with subcortical ischemic lesions (20). However, the relation of BBB breakdown to the extent of cognitive/functional impairment was not clearly determined at the stage prior to maturation of Aβ and tau pathology as would be the case for our model.

3.5 Conclusion

In summary, CTP imaging showed that CI+Aβ group had significantly higher BBB-PS in the ipsilateral striatum at day 7, and month 2 and 3 than sham and CI groups, suggesting a greater and chronic BBB breakdown in the comorbid group. PET imaging with ^{18}F-FEPPA, as a marker of inflammation, revealed the highest uptake in the lesion of the CI+Aβ group within the first month, especially during the period of day 7-14. The prolonged post-ischemia hyperperfusion/hypervolemia between day 7 and 14 during reperfusion and inflammation could potentiate BBB disruption. Together, these findings suggest that CI+Aβ comorbidity can lead to breakdown of BBB, greater neuroinflammation and hemodynamic disturbances, which may delineate the early pathogenic pattern for the associated neurodegeneration.

3.6 References

1. Seshadri S, *et al.* (2006) The lifetime risk of stroke. *Stroke* 37(2):345-350.

2. Snowdon DA, *et al.* (1997) Brain infarction and the clinical expression of Alzheimer disease. *JAMA* 277(10):813-817.

3. Song IU, Kim JS, Kim YI, Eah KY, & Lee KS (2007) Clinical significance of silent cerebral infarctions in patients with Alzheimer disease. *Cognitive and behavioral neurology* 20(2):93.

4. Vermeer SE, *et al.* (2003) Silent brain infarcts and the risk of dementia and cognitive decline. *New England Journal of Medicine* 348(13):1215-1222.

5. White L (2009) Brain lesions at autopsy in older Japanese-American men as related to cognitive impairment and dementia in the final years of life: a summary report from the Honolulu-Asia aging study. *Journal of Alzheimer's Disease* 18(3):713-725.

6. Hiltunen M, *et al.* (2009) Focal cerebral ischemia in rats alters APP processing and expression of A-beta peptide degrading enzymes in the thalamus. *Neurobiology of disease* 35(1):103-113.

7. Shi J, Yang SH, Stubley L, Day AL, & Simpkins JW (2000) Hypoperfusion induces overexpression of β-amyloid precursor protein mRNA in a focal ischemic rodent model. *Brain research* 853(1):1-4.

8. Kalaria RN (2000) The role of cerebral ischemia in Alzheimer's disease. *Neurobiology of aging* 21(2):321-330.

9. van Groen T, Puurunen K, Mäki H-M, Sivenius J, & Jolkkonen J (2005) Transformation of diffuse β-amyloid precursor protein and β-amyloid deposits to plaques in the thalamus after transient occlusion of the middle cerebral artery in rats. *Stroke* 36(7):1551-1556.

10. Clifford PM, *et al.* (2007) Aβ peptides can enter the brain through a defective blood-brain barrier and bind selectively to neurons. *Brain research* 1142:223-236.

11. Pluta R & Amek MU (2008) Brain ischemia and ischemic blood-brain barrier as etiological factors in sporadic Alzheimer's disease. *Neuropsychiatric disease and treatment* 4(5):855-864.

12. Zlokovic BV (2008) The blood-brain barrier in health and chronic neurodegenerative disorders. *Neuron* 57(2):178-201.

13. Li J, Wang YJ, Zhang M, Fang CQ, & Zhou HD (2011) Cerebral ischemia aggravates cognitive impairment in a rat model of Alzheimer's disease. *Life sciences* 89:86-92.

14. Whitehead SN, Cheng G, Hachinski VC, & Cechetto DF (2007) Progressive increase in infarct size, neuroinflammation, and cognitive deficits in the presence of high levels of amyloid. *Stroke* 38(12):3245-3250.

15. Thiel A, Cechetto DF, Heiss W-D, Hachinski V, & Whitehead SN (2014) Amyloid burden, neuroinflammation, and links to cognitive decline after ischemic stroke. *Stroke* 45(9):2825-2829.

16. de la Torre JC (2002) Alzheimer disease as a vascular disorder: nosological evidence. *Stroke* 33(4):1152-1162.

17. Iadecola C (2010) The overlap between neurodegenerative and vascular factors in the pathogenesis of dementia. *Acta neuropathologica* 120(3):287-296.

18. de la Torre JC (2000) Cerebral hypoperfusion, capillary degeneration, and development of Alzheimer disease. *Alzheimer Disease & Associated Disorders* 14(1):S72-S81.

19. Brown WR & Thore CR (2011) Review: cerebral microvascular pathology in ageing and neurodegeneration. *Neuropathology and applied neurobiology* 37(1):56-74.

20. Farrall AJ & Wardlaw JM (2009) Blood–brain barrier: ageing and microvascular disease–systematic review and meta-analysis. *Neurobiology of aging* 30(3):337-352.

21. Hoeffner EG, *et al.* (2004) Cerebral Perfusion CT: Technique and Clinical Applications 1. *Radiology* 231(3):632-644.

22. Aviv RI, *et al.* (2009) Hemorrhagic Transformation of Ischemic Stroke: Prediction with CT Perfusion. *Radiology* 250(3):867-877.

23. Lee T-Y (2002) Functional CT: physiological models. *Trends in biotechnology* 20(8):S3-S10.

24. Suridjan I, *et al.* (2014) Neuroinflammation in healthy aging: A PET study using a novel Translocator Protein 18kDa (TSPO) radioligand, [18F]-FEPPA. *NeuroImage* 84:868-875.

25. Yang J, d'Esterre CD, Amtul Z, Cechetto DF, & Lee TY (2014) Hemodynamic Effects of Combined Focal Cerebral Ischemia and Amyloid Protein Toxicity in a Rat Model: A Functional CT Study. *PloS one* 9(6):e100575.

26. St. Lawrence K & Lee T-Y (1998) An adiabatic approximation to the tissue homogeneity model for water exchange in the brain: I. Theoretical derivation. *Journal of Cerebral Blood Flow & Metabolism* 18(12):1365-1377.

27. Richmon JD, *et al.* (1998) Induction of heme oxygenase-1 after hyperosmotic opening of the blood-brain barrier. *Brain research* 780(1):108-118.

28. Martín A, *et al.* (2010) Evaluation of the PBR/TSPO radioligand [18F]-DPA-714 in a rat model of focal cerebral ischemia. *Journal of Cerebral Blood Flow & Metabolism* 30(1):230-241.

29. Thiel A & Heiss W-D (2011) Imaging of microglia activation in stroke. *Stroke* 42(2):507-512.

30. Kogure D, *et al.* (2000) Longitudinal evaluation of early Alzheimer's disease using brain perfusion SPECT. *Journal of nuclear medicine* 41(7):1155-1162.

31. Mosconi L, *et al.* (2009) FDG-PET changes in brain glucose metabolism from normal cognition to pathologically verified Alzheimer's disease. *European journal of nuclear medicine and molecular imaging* 36(5):811-822.

32. Zaknun JJ, Leblhuber F, & Schucktanz H (2008) Value of cerebral blood flow quantification in the diagnosis of dementia. *Nuclear medicine communications* 29(3):260-269.

33. Helzner EP, *et al.* (2009) Contribution of vascular risk factors to the progression in Alzheimer disease. *Archives of neurology* 66(3):343-348.

34. Durukan A, *et al.* (2009) Post-ischemic blood–brain barrier leakage in rats: one-week follow-up by MRI. *Brain research* 1280:158-165.

35. Lin C-Y, *et al.* (2008) Dynamic changes in vascular permeability, cerebral blood volume, vascular density, and size after transient focal cerebral ischemia in rats: evaluation with contrast-enhanced magnetic resonance imaging. *Journal of Cerebral Blood Flow & Metabolism* 28(8):1491-1501.

36. Hartz AM, *et al.* (2012) Amyloid-β contributes to blood–brain barrier leakage in transgenic human amyloid precursor protein mice and in humans with cerebral amyloid angiopathy. *Stroke* 43(2):514-523.

37. Skoog I, *et al.* (1998) A population study on blood-brain barrier function in 85-year-olds Relation to Alzheimer's disease and vascular dementia. *Neurology* 50(4):966-971.

38. Taheri S, *et al.* (2011) Blood–brain barrier permeability abnormalities in vascular cognitive impairment. *Stroke* 42(8):2158-2163.

39. Wardlaw JM, *et al.* (2008) Changes in background blood–brain barrier integrity between lacunar and cortical ischemic stroke subtypes. *Stroke* 39(4):1327-1332.

40. Koistinaho M, *et al.* (2002) Beta-Amyloid precursor protein transgenic mice that harbor diffuse Aβ deposits but do not form plaques show increased ischemic vulnerability: role of inflammation. *PNAS* 99(3):1610-1615.

41. Miao J, *et al.* (2005) Cerebral microvascular amyloid β protein deposition induces vascular degeneration and neuroinflammation in transgenic mice expressing human vasculotropic mutant amyloid β precursor protein. *The American journal of pathology* 167(2):505-515.

42. Cameron B & Landreth GE (2010) Inflammation, microglia, and Alzheimer's disease. *Neurobiology of disease* 37(3):503-509.

43. del Zoppo GJ (2009) Inflammation and the neurovascular unit in the setting of focal cerebral ischemia. *Neuroscience* 158(3):972-982.

44. Iadecola C & Gorelick PB (2003) Converging pathogenic mechanisms in vascular and neurodegenerative dementia. *Stroke* 34(2):335-337.

45. Tan Z, *et al.* (2007) Inflammatory markers and the risk of Alzheimer disease The Framingham Study. *Neurology* 68(22):1902-1908.

46. Edison P, *et al.* (2008) Microglia, amyloid, and cognition in Alzheimer's disease: An [11C](R) PK11195-PET and [11C] PIB-PET study. *Neurobiology of disease* 32(3):412-419.

47. Ji B, *et al.* (2008) Imaging of peripheral benzodiazepine receptor expression as biomarkers of detrimental versus beneficial glial responses in mouse models of Alzheimer's and other CNS pathologies. *The Journal of neuroscience* 28(47):12255-12267.

48. Maeda J, *et al.* (2011) In vivo positron emission tomographic imaging of glial responses to amyloid-β and tau pathologies in mouse models of Alzheimer's disease and related disorders. *The Journal of neuroscience* 31(12):4720-4730.

49. Venneti S, *et al.* (2009) PK11195 labels activated microglia in Alzheimer's disease and in vivo in a mouse model using PET. *Neurobiology of aging* 30(8):1217-1226.

50. Shahi V, Fugate J, Kallmes D, & Rabinstein A (2014) Early Basal Ganglia Hyperperfusion on CT Perfusion in Acute Ischemic Stroke: A Marker of Irreversible Damage? *American Journal of Neuroradiology* 35 (9):1688-1692.

51. Yang G-Y & Betz AL (1994) Reperfusion-induced injury to the blood-brain barrier after middle cerebral artery occlusion in rats. *Stroke* 25(8):1658-1664.

52. Shen Q, Du F, Huang S, & Duong TQ (2011) Spatiotemporal characteristics of postischemic hyperperfusion with respect to changes in T1, T2, diffusion, angiography, and blood–brain barrier permeability. *Journal of Cerebral Blood Flow & Metabolism* 31(10):2076-2085.

Chapter 4

Temporal Changes in Blood-Brain Barrier Permeability and Cerebral Perfusion in Lacunar/Subcortical Ischemic stroke

This chapter is adapted from the original research manuscript entitled "Temporal Changes in Blood-Brain Barrier Permeability and Cerebral Perfusion in Lacunar/Subcortical Ischemic stroke" submitted to *BMC Neurology* by J. Yang, C.D. d'Esterre, S. Ceruti, G. Roversi, A. Saletti, E. Fainardi and T.Y. Lee.

4.1 Introduction

Stroke is one of the leading causes of death and long-term disability (1). It is also an important contributing factor to cognitive dysfunction or dementia post stroke, including vascular cognitive impairment (VCI) (2). Around 15-25% of ischemic strokes are lacunar strokes (3), which can manifest as lacunes or subcortical lesions on routine MR and CT images. Recent clinical evidence has suggested that lacunar and subcortical lesion might exert adverse effects on cognition and memory (3-5). Studies have shown that the blood-brain barrier (BBB) becomes more permeable in VCI patients with subcortical lesions and leukoaraiosis (6-8). Contrast-enhanced MRI reveals that BBB permeability increases in patients with lacunar lesions, compared to normal control or cortical stroke (7-10). Moreover, pathological studies report increased level of cerebrospinal fluid (CSF) albumin in patients with lacunar/subcortical lesion or white matter disease (3, 6). Clinically, the primary types of brain lesion in cerebral small vessel-related VCI are lacunar and subcortical lesions, which are caused by ischemia due to arteriolar occlusion (e.g. lenticulostriate arteries, recurrent artery of Heubner and

thalamoperforating arteries). The anatomic regions corresponding to these vascular territories are basal ganglia, thalamus and surrounding white matter (involved in motor movement, cognition, learning, visual memory and signal processing) (11, 12). The ischemic event/occlusion may play as a trigger for the BBB abnormality in the presence of cerebral small vessel disease. Together, the evidence suggests that there is an underlying association between lacunar/subcortical ischemic stroke and cerebral microvascular abnormality, thus longitudinal investigation of subcortical BBB permeability may better demonstrate BBB leakage and microvascular dysfunction in stroke patients with small subcortical ischemic lesions before progressing to VCI. The chronic BBB leakage may act as a contributor and predictor for long-term cognitive impairment and associated pathology.

Recently, CT perfusion (CTP), a physiologic imaging modality requiring intravenous injection of iodinated contrast agent to image blood flow and associated hemodynamic parameters (13), is used for diagnosis of acute ischemic stroke and vasospasm. CTP not only measures tissue perfusion but also vascular permeability surface product (PS), an indicator of BBB integrity and permeability (13, 14). Current CTP technique is more accessible and faster to perform in clinical practice than MRI and xenon-perfusion CT (15), and is ideal for studies at acute and subacute stages of stroke.

In this study we sought to examine the time course of BBB permeability changes measured with CTP in patients from the acute phase to 3 months post stroke to determine whether BBB permeability of the non-infarcted ipsilateral basal ganglia and thalamus is different in patients with and without lacunar/subcortical lesion.

4.2 Methods and Materials

4.2.1 Subjects

Patients with clinically diagnosed acute ischemic stroke were consecutively and prospectively recruited from February 2009 to July 2011 at one institution. All patients were admitted to the Department of Neuroscience of the University of Ferrara within 6 hours of stroke symptom onset. Patients with impaired renal function, contraindications to iodinated contrast agent, intracerebral hemorrhage at admission, brain stem infarct, previous stroke with clear deficits, missing CTP imaging at admission or any follow-up time points (24 hours, 7 days and 3 months), severe motion artifacts in CTP imaging, pregnancy and age < 18 years were excluded. For this study, thirty-one patients who underwent non-enhanced CT (NECT) and two-phase CTP acquisition (2.5 min) at admission and all follow-up exams were included. The study was approved by the Committee for Medical Ethics in Research of the University of Ferrara and informed consent was obtained from all patients enrolled in the study.

All patients were diagnosed by an experienced neurologist (G.R.) who evaluated the clinical stroke symptoms at admission based on the National Institutes of Health Stroke Scale (NIHSS) (16). Clinical outcome was assessed using the modified Rankin scale (mRS) at 3-month post stroke (17) and mRS ≤ 2 and > 2 were defined as good and poor outcome, respectively. Patients having lacunar/subcortical lesion ($\leq$20 mm in diameter) on month-3 NECT images were separated from those without subcortical lesion (i.e. large vessel infarcts primarily in the cortical gray matter). Vascular risk factors including hypertension, diabetes, previous silent infarct, ischemic heart disease and thrombolytic treatment were documented.

4.2.2 CT perfusion acquisition protocol and functional maps

CTP studies were performed at admission, 24 hours, 7 days and 3 months post stroke. Prior to CTP scan, a NECT scan was performed to locate hypodense ischemic lesion. Each CTP scan started with an intravenous injection of 50 mL of iodinated contrast agent (Iomeron 300 mg/ml, Bracco Imaging SpA, Milan, Italy) at the rate of 4 mL/s, followed by 45 mL of saline flush at the same infusion rate. A 20-gauge catheter and cephalic vein were used in peripheral venous access for contrast injection. Each CTP acquisition used a two-phase protocol: eight 5 mm-thick slices covering a 40 mm section of the brain were scanned continuously for 45 s with images reconstructed at 0.5 s intervals and then scanned once every 15 s for another 105 s for a total acquisition time of 2.5 minutes. The scan parameters for both phases were 25 cm FOV, 80 kV, 100 mA, and 1 s per gantry rotation. BBB permeability-surface (BBB-PS), cerebral blood flow (CBF) and cerebral blood volume (CBV) maps were generated with the delay insensitive CT Perfusion software based on the modified Johnson-Wilson model (GE Healthcare, Waukesha, WI) (18, 19).

4.2.3 Image registration and analysis

CTP maps from all follow-up time points and NECT at 3 month of each patient were manually co-registered with the admission maps using Analyze v11.0 software (Mayo Clinic, Rochester, MN). The averages of the source CTP images were used as references for each registration. For lacunar/subcortical stroke, regions of interest (ROIs) were defined in the ipsilateral and contralateral basal ganglia (caudate nucleus, putamen, globus pallidus) and thalamus as well as the infarct using the month-3 NECT (Figure 4-2). Data from the ipsilateral deep gray nuclei excluding the infarct were normalized with contralateral data to obtain relative

CBF (rCBF), CBV (rCBV) and BBB-PS (rBBB-PS) for each time point. The same analysis was used for the cortical stroke group, except that no region of deep gray nuclei was excluded.

4.2.4 Statistical methods

Statistical analyses were performed using SigmaPlot v12.0 (Systat Software, San Jose, CA). The unpaired t-test was used for comparisons of NIHSS score at admission, mRS at month 3 and age between patients with and without lacunar/subcortical lesion. Fisher's exact test was used for demographic data between the two groups. Relative CBF, CBV and BBB-PS in the non-infarcted ipsilateral deep gray nuclei were compared between the two groups, and also between the time points within each group using two-way ANOVA with group and time as independent factors. Tukey's post hoc test was then used for inter-group comparison. Statistical significance was set at $p<0.05$. All CTP-derived data were presented as mean ± SEM.

4.3 Results

4.3.1 Patient data

The 31 patients (18 F, 13 M) included in this study were divided into two groups, 14 patients with lacunar/subcortical infarct and 17 patients with cortical stroke based on month-3 NECT images. Mean proportion of the infarcted area in the basal ganglia or thalamus for the lacunar/subcortical group was small, 11.4 ± 3.6%. There were no significant differences in mean age, gender, hypertension and previous silent infarct between the two groups (Table 4-1). The proportion of the patients who received intravenous thrombolysis was lower but not significant

in the lacunar/subcortical group. The mean NIHSS at admission and mRS at 3 months post stroke were not significantly different between the two groups.

Table 4-1: Characteristics of patients with and without lacunar/subcortical lesion.

Clinical data	Subcortical/lacunar (n=14)	Cortical (n=17)	*p* value
Age*	71 ± 10	69 ± 12	0.50
Female n (%)	9 (64%)	9 (53%)	0.72
Hypertension n (%)	9 (64%)	12 (71%)	1.00
Previous silent infarct n (%)	5 (36%)	7 (41%)	1.00
Thrombolysis n (%)	10 (71%)	14 (82%)	0.67
NIHSS at admission*	15.1 ± 6.2	12.3 ± 6.2	0.21
mRS at month 3*	2.1 ± 1.1	2.2 ± 1.5	0.83

* Age, NIHSS and mRS are represented as mean ± SD

4.3.2 Temporal changes in blood-brain barrier permeability

Mean rBBB-PS (Figure 4-1) in the non-infarcted ipsilateral basal ganglia and thalamus (deep gray nuclei) in the lacunar/subcortical group was significantly higher at day 7 and month 3 ($p<0.01$ at day 7 and $p<0.05$ at month 3), and non-significantly higher at admission and 24 hrs than the cortical group. Particularly, at day 7 the lacunar/subcortical group showed the largest difference in rBBB-PS from the cortical group (2.78 ± 0.64 vs 1.07 ± 0.06). In addition, intra-group comparisons showed that the rBBB-PS within the lacunar/subcortical group at day 7 was significantly higher than those at all other time points ($p<0.05$). This intra-group difference was

not seen in the cortical patients. An example of increased BBB permeability was shown by the enhanced signal in BBB-PS maps (Figure 4-2) in the right basal ganglia (putamen) where the contrast agent leaked into the interstitial space of brain tissue through a compromised BBB.

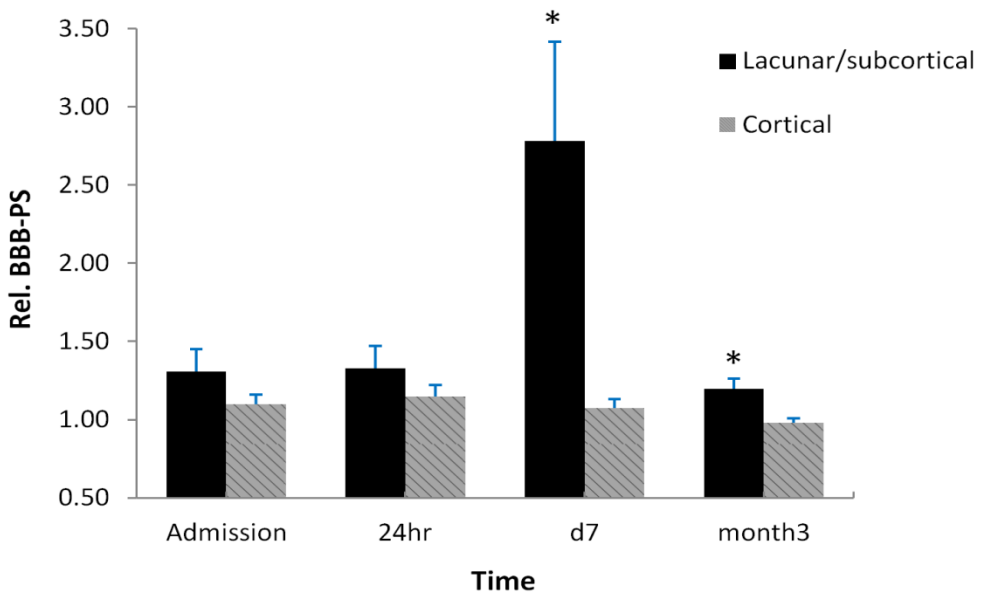

Figure 4-1: Blood-brain barrier (BBB) permeability (PS) in the non-infarcted ipsilateral basal ganglia and thalamus. rBBB-PS was significantly higher in the lacunar/subcortical group compared to the cortical group at 7 days and 3 months after stroke (*, $P<0.01$ at 7 days and $P<0.05$ at 3 months). The largest difference between the two groups occurred at day 7, with about 2.5-fold higher value in the lacunar/subcortical group than the cortical group. In the lacunar/subcortical group, rBBB-PS remained stable between admission and 24hr but significantly increased from 24 hrs to 7 days post stroke ($P<0.05$), and then significantly declined at 3 months ($P<0.05$). No significant intra-group differences in BBB-PS over time were seen in the cortical group.

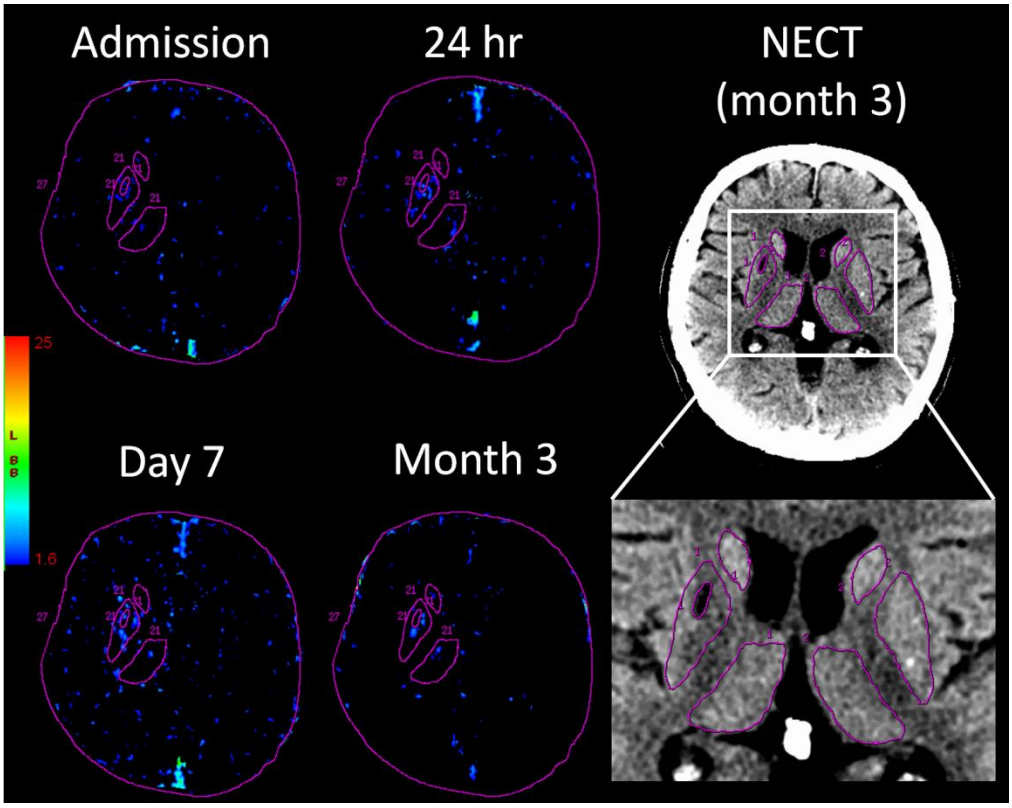

Figure 4-2: BBB-PS maps in a patient with a subcortical infarct in right putamen (as shown on the 3-month NECT). The maps from acute phase to 3 months after stroke were shown. Focally elevated BBB-PS was observed in right putamen at 24 hrs, day 7 and month 3 for the patient. Caudate nucleus, putamen, globus pallidus and thalamus in both ipsilateral and contralateral hemisphere were outlined in red. The infarct in the right putamen shown on the 3-month NECT was also outlined in red (smaller ROI within the right putamen).

4.3.3 Cerebral hemodynamics

Mean rCBF in the non-infarcted ipsilateral basal ganglia and thalamus (Figure 4-3A) was significantly lower in patients with lacunar/subcortical lesions at admission, 0.72 ± 0.05, as compared to the cortical group, 0.86 ± 0.03 (p<0.01). Similarly, mean rCBV in the non-infarcted ipsilateral basal ganglia and thalamus (Figure 4-3B) in the lacunar/subcortical group was significantly lower than the cortical group at admission (0.80 ± 0.05 vs 0.92 ± 0.03, p<0.05).

There were no significant differences in both rCBF and rCBV at 24 hrs, day 7 and month 3 between the two groups, although at day 7 rCBF and rCBV were slightly higher in the lacunar/subcortical group.

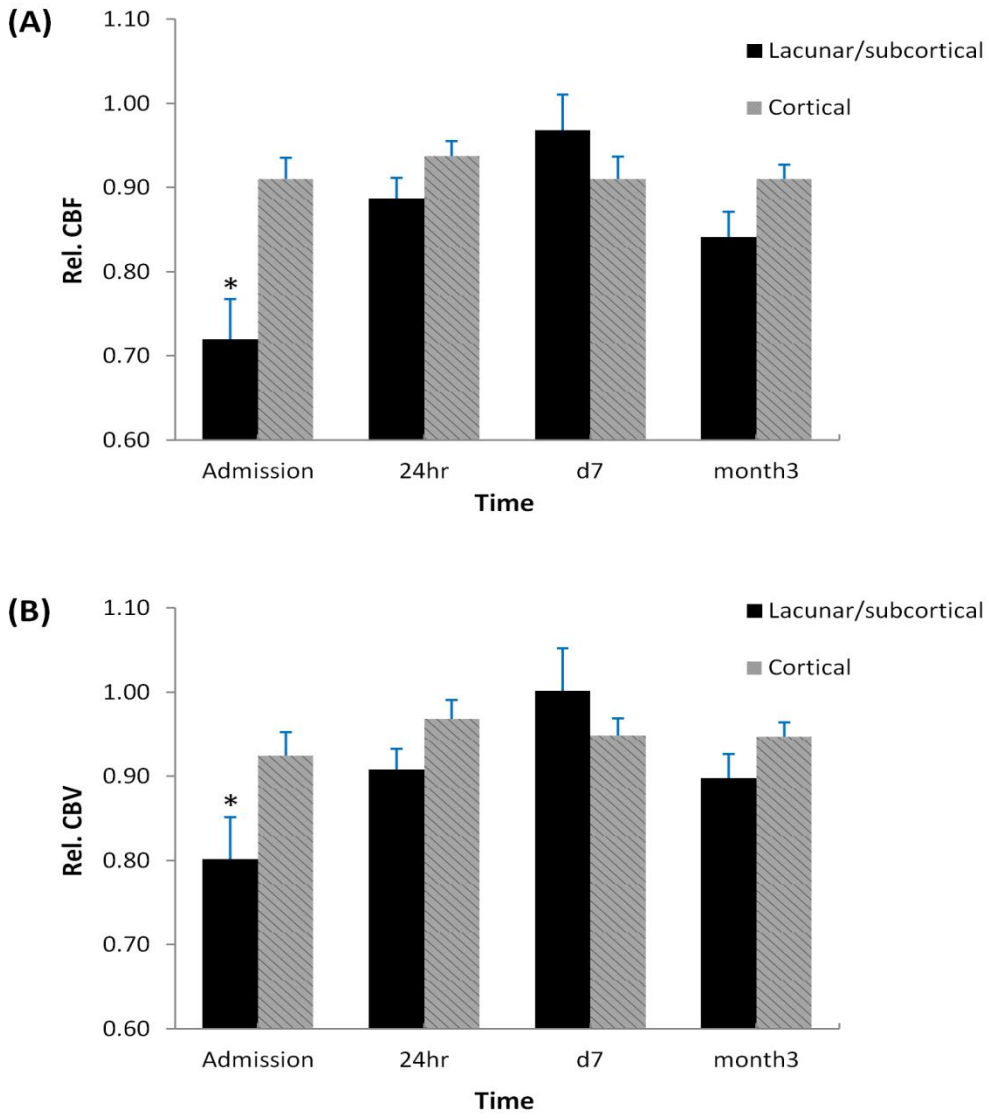

Figure 4-3: (A) CBF and (B) CBV in the non-infarcted ipsilateral basal ganglia and thalamus. Both rCBF and rCBV in the lacunar/subcortical group were significantly lower at admission (*, $P<0.01$ for rCBF and $P<0.05$ for rCBV) and remained lower at 24hrs (no significance) than the cortical group. rCBF and rCBV were higher but not significant in the

lacunar/subcortical group at day 7 compared to the cortical group. At month 3, there was no significant rCBF and rCBV difference between the two groups.

4.4 Discussion

In this study, CTP imaging revealed that patients with lacunar/subcortical lesions had significantly higher BBB-PS in the non-infarcted basal ganglia and thalamus at day 7 and month 3 than patients with cortical stroke. This finding is consistent with previous MRI evidence of increased BBB-PS in lacunar stroke and VCI with subcortical ischemic lesions (6-10, 20). In addition to BBB-PS, at acute phase (admission) CBF and CBV within non-infarcted ipsilateral basal ganglia and thalamus in the lacunar/subcortical patients were significantly lower than the cortical group, suggesting an ischemic influence in the subcortical region.

Lacunar and subcortical lesions, along with white matter lesions (WML), are frequently found in patients with VCI and AD (6). The well cited Nun study found that, in subjects with AD pathology, the presence of subcortical or lacunar infarcts (in the basal ganglia, thalamus and deep white matter) at autopsy was associated with a 20-fold higher risk to develop dementia compared to those without subcortical infarcts (21). Therefore, it is important to understand the pathogenesis of lacunar/subcortical lesion. Some studies report that hypoperfusion (reduced CBF) was found in leukoaraiosis, which is frequently related to cerebral microvascular disturbances in lacunar/subcortical stroke (22, 23). In our study, within the acute phase significantly reduced CBF and CBV was present in the non-infarcted basal ganglia and thalamus of the lacunar/subcortical patients, but not in the cortical patients, indicating the presence of a more severe ischemia in the basal ganglia and thalamus of the lacunar/subcortical group. At day 7, differences in CBF and CBV between the two groups were not significant but CBF and CBV were higher in the lacunar/subcortical group. This is probably due to reactive hyperemia or

compensatory blood supply (reperfusion) from collateral flow to the viable penumbra, similar to the results found in animal model of cerebral ischemia (24). This appeared to be transient since, at month 3, slightly lower CBF and CBV were again detected in the affected region in the lacunar/subcortical group possibly due to compromised vascular reactivity and tissue damage. Several studies show that greater BBB disruption is associated with reperfusion post cerebral ischemia in animal models (24-26). This is consistent with our finding that the greatest BBB disruption (the highest BBB-PS) was observed along with the reperfusion at day 7 in lacunar/subcortical stroke. In addition, the majority of the patients in this study had thrombolytic treatment (tPA) at admission, which has also been associated with increased BBB permeability after reperfusion (as a secondary injury) in previous studies (27, 28). Moreover, other reports indicate that early post-ischemia hyperperfusion may be associated with infarction or impaired BBB at later time (29, 30), which could explain the higher BBB-PS presented at month 3 in the lacunar/subcortical patients.

Hypoperfusion in the basal ganglia and thalamus at acute phase is not the only vascular abnormality of lacunar/subcortical lesion that is associated with cerebral small vessel disease. Additionally, increased BBB permeability (i.e. leaky cerebral microvessels) could be an underlying pathogenic mechanism that is exacerbated by ischemia (9, 10, 20). Pathologically, extravasation of serum proteins such as albumin into CSF, which is an indicator of BBB disruption, has been demonstrated in VCI and AD patients, particularly in those with lacunar/subcortical ischemic lesion or WML (6, 7, 31). In our study, BBB-PS in the basal ganglia and thalamus of the lacunar/subcortical patients was significantly elevated and peaked at day 7, compared to that of cortical group. This reflects a dynamic transition of BBB abnormality from acute phase to a maximum opening/disruption of BBB at subacute phase for

lacunar/subcortical lesion. At month 3, BBB-PS of the non-infarcted basal ganglia and thalamus in the lacunar/subcortical group was still significantly higher than in the cortical group, but at a lower level than at day 7. This suggests that after an ischemic insult BBB in the viable area of the lacunar/subcortical group remained more affected and vulnerable than the cortical group. All these observations, to some extent, may explain early BBB-PS changes of cerebral microvascular disease, especially in the affected subcortical regions such as basal ganglia and thalamus, where about 31% and 12% of lacunar infarcts are located respectively (11). Recent perfusion MRI studies found significantly increased BBB permeability in the basal ganglia, CSF and deep white matter in subjects with VCI and lacunar/subcortical ischemic vessel disease (6-10, 20), which is consistent with our findings. This increased BBB permeability observed from our and other studies posits a link between cerebral small vessel disease and lacunar/subcortical lesions. All of the above evidence strongly supports cerebral microvascular dysfunction as an important contributing vascular mechanism for lacunar/subcortical lesions.

In comparison with previous studies (8-10), the strengths of this study include: (1) multiple time points post stroke at acute and subacute phase over the first 3 months to better identify early changes of BBB-PS, a biomarker of cerebral microvascular dysfunction. In addition, we registered CTP maps for all different time points to ensure measurements are from the same region; (2) multiple parameters such as CBF, CBV and BBB-PS can be produced at the same time for each CTP scan, increasing the chance to detect not only initial (acute) ischemic deficits with viable penumbra but also BBB disturbances at acute and subacute period; (3) in contrast to MRI, changes in CT signal intensity (attenuation) are linearly related to changes in contrast agent concentration, resulting in better measurements of perfusion parameters in detecting defects (14, 32).

The limitations of the study are the small size of the sample population and limited coverage of the brain with relatively thick slices which diminished our ability in detecting some small lacunar/subcortical lesions. The radiation dose is another concern. In our study, no patients showed acute radiation-related complications. The effective radiation dose in a typical CTP study is about 2 mSv (at 100-150 mA and 80 kV), which is significantly lower than xenon-perfusion CT and SPECT (15). With advancement of new iterative reconstruction techniques (33), radiation dose of a CTP study can be reduced to fraction of the background radiation dose (34). This would allow repeated examinations for suspected VCI patients with cerebral small vessel disease to monitor BBB permeability over time.

4.5 Conclusion

This study demonstrated that with serial CTP imaging, a more profound decrease in CBF and CBV at acute phase and a higher BBB-PS in the non-infarcted basal ganglia and thalamus at subacute phase and month 3 in patients with lacunar/subcortical lesions, compared to patients with cortical stroke. These findings suggest that ischemic insult can exacerbate vascular abnormalities, especially subcortical BBB permeability in the presence of cerebral small vessel disease.

4.6 References

1. Thom T, *et al.* (2006) Heart disease and stroke statistics—2006 update a report from the American Heart Association Statistics Committee and Stroke Statistics Subcommittee. *Circulation* 113(6):e85-e151.
2. Selnes OA & Vinters HV (2006) Vascular cognitive impairment. *Nature Clinical Practice Neurology* 2(10):538-547.
3. Wardlaw J, Sandercock P, Dennis M, & Starr J (2003) Is breakdown of the blood-brain barrier responsible for lacunar stroke, leukoaraiosis, and dementia? *Stroke* 34(3):806-812.
4. Norrving B (2003) Long-term prognosis after lacunar infarction. *The Lancet Neurology* 2(4):238-245.
5. Wen HM, *et al.* (2004) Effect of white matter changes on cognitive impairment in patients with lacunar infarcts. *Stroke* 35(8):1826-1830.
6. Farrall AJ & Wardlaw JM (2009) Blood–brain barrier: ageing and microvascular disease–systematic review and meta-analysis. *Neurobiology of aging* 30(3):337-352.
7. Taheri S, *et al.* (2011) Blood–brain barrier permeability abnormalities in vascular cognitive impairment. *Stroke* 42(8):2158-2163.
8. Topakian R, Barrick T, Howe F, & Markus H (2010) Blood–brain barrier permeability is increased in normal-appearing white matter in patients with lacunar stroke and leucoaraiosis. *Journal of Neurology, Neurosurgery & Psychiatry* 81(2):192-197.
9. Wardlaw JM, *et al.* (2009) Lacunar stroke is associated with diffuse blood–brain barrier dysfunction. *Annals of neurology* 65(2):194-202.
10. Wardlaw JM, *et al.* (2008) Changes in background blood–brain barrier integrity between lacunar and cortical ischemic stroke subtypes. *Stroke* 39(4):1327-1332.
11. Benisty S, *et al.* (2009) Location of lacunar infarcts correlates with cognition in a sample of non-disabled subjects with age-related white-matter changes: the LADIS study. *Journal of Neurology, Neurosurgery & Psychiatry* 80(5):478-483.
12. Gold G, *et al.* (2005) Cognitive consequences of thalamic, basal ganglia, and deep white matter lacunes in brain aging and dementia. *Stroke* 36(6):1184-1188.
13. d'Esterre C, Fainardi E, Aviv R, & Lee T (2012) Improving acute stroke management with computed tomography perfusion: a review of imaging basics and applications. *Translational stroke research* 3(2):205-220.

14. Hoeffner EG, *et al.* (2004) Cerebral Perfusion CT: Technique and Clinical Applications 1. *Radiology* 231(3):632-644.
15. Wintermark M, *et al.* (2005) Comparative overview of brain perfusion imaging techniques. *Stroke* 36(9):e83-e99.
16. Brott T, *et al.* (1989) Measurements of acute cerebral infarction: a clinical examination scale. *Stroke* 20(7):864-870.
17. Van Swieten J, Koudstaal P, Visser M, Schouten H, & Van Gijn J (1988) Interobserver agreement for the assessment of handicap in stroke patients. *Stroke* 19(5):604-607.
18. Lee T-Y (2002) Functional CT: physiological models. *Trends in biotechnology* 20(8):S3-S10.
19. St. Lawrence K & Lee T-Y (1998) An adiabatic approximation to the tissue homogeneity model for water exchange in the brain: I. Theoretical derivation. *Journal of Cerebral Blood Flow & Metabolism* 18(12):1365-1377.
20. Wardlaw JM, *et al.* (2013) Blood–Brain Barrier Permeability and Long-Term Clinical and Imaging Outcomes in Cerebral Small Vessel Disease. *Stroke* 44(2):525-527.
21. Snowdon DA, *et al.* (1997) Brain infarction and the clinical expression of Alzheimer disease: the Nun Study. *Jama* 277(10):813-817.
22. Markus H, Lythgoe D, Ostegaard L, O'sullivan M, & Williams S (2000) Reduced cerebral blood flow in white matter in ischaemic leukoaraiosis demonstrated using quantitative exogenous contrast based perfusion MRI. *Journal of Neurology, Neurosurgery & Psychiatry* 69(1):48-53.
23. O'sullivan M, *et al.* (2002) Patterns of cerebral blood flow reduction in patients with ischemic leukoaraiosis. *Neurology* 59(3):321-326.
24. Lin C-Y, *et al.* (2008) Dynamic changes in vascular permeability, cerebral blood volume, vascular density, and size after transient focal cerebral ischemia in rats: evaluation with contrast-enhanced magnetic resonance imaging. *Journal of Cerebral Blood Flow & Metabolism* 28(8):1491-1501.
25. Durukan A, *et al.* (2009) Post-ischemic blood–brain barrier leakage in rats: one-week follow-up by MRI. *Brain research* 1280:158-165.
26. Yang G-Y & Betz AL (1994) Reperfusion-induced injury to the blood-brain barrier after middle cerebral artery occlusion in rats. *Stroke* 25(8):1658-1664.

27. Kaur J, Tuor UI, Zhao Z, & Barber PA (2011) Quantitative MRI reveals the elderly ischemic brain is susceptible to increased early blood–brain barrier permeability following tissue plasminogen activator related to claudin 5 and occludin disassembly. *Journal of Cerebral Blood Flow & Metabolism* 31(9):1874-1885.
28. Yepes M, Roussel BD, Ali C, & Vivien D (2009) Tissue-type plasminogen activator in the ischemic brain: more than a thrombolytic. *Trends in neurosciences* 32(1):48-55.
29. Shahi V, Fugate J, Kallmes D, & Rabinstein A (2014) Early Basal Ganglia Hyperperfusion on CT Perfusion in Acute Ischemic Stroke: A Marker of Irreversible Damage? *American Journal of Neuroradiology* 35(9):1688-1692.
30. Shen Q, Du F, Huang S, & Duong TQ (2011) Spatiotemporal characteristics of postischemic hyperperfusion with respect to changes in T1, T2, diffusion, angiography, and blood–brain barrier permeability. *Journal of Cerebral Blood Flow & Metabolism* 31(10):2076-2085.
31. Wallin A, *et al.* (1990) Blood brain barrier function in vascular dementia. *Acta neurologica scandinavica* 81(4):318-322.
32. O'Connor JPB, *et al.* (2011) Dynamic contrast-enhanced imaging techniques: CT and MRI. *The British Journal of Radiology* 84(S2):S112-S120.
33. Hara AK, *et al.* (2009) Iterative reconstruction technique for reducing body radiation dose at CT: feasibility study. *American Journal of Roentgenology* 193(3):764-771.
34. Murphy A, *et al.* (2014) Low dose CT perfusion in acute ischemic stroke. *Neuroradiology* 56(12):1055-1062.

Chapter 5

Conclusion and Future Work

5.1 Summary

The introduction of this thesis provides an overview of vascular abnormality of cerebral ischemia and clinical background of coexistence of ischemic and AD pathology. As described in the previous chapters, the main goals of this thesis were to investigate the underlying interaction between CI and Aβ, and to elucidate the contribution of post-ischemia vascular disturbances to the early pathogenesis of AD or subcortical ischemic disease. The coexistence of ischemic and AD pathology has been found in many studies, but few mechanisms have been advanced in the literature to facilitate the understanding of vascular abnormalities occurring at early stage of the comorbidity. This may be due to the lack of an appropriate animal model that has both ischemic and AD-related injuries before substantial pathology such as Aβ plaques and tau tangles becomes mature in advanced neurodegeneration. The animal model used for this thesis combines both ischemic and Aβ injuries before formation of substantial Aβ plaques and tau tangles. With CTP and PET imaging, in-vivo biomarkers such as BBB-PS, CBF, CBV, and activated microglia were measured to study the mechanism of early vascular and cellular abnormalities in the comorbidity. In addition to the animal studies, this thesis also explored temporal changes of BBB permeability and cerebral perfusion in patients with small subcortical ischemic stroke, which is closely related to AD and vascular dementia.

In this chapter, major findings of my research and clinical implications will be discussed. Furthermore, a future direction will also be included for the possible investigations that may help

in understanding the relationship between cerebrovascular abnormalities and neurodegeneration in progression of cognitive impairment.

5.2 Disturbances of cerebral perfusion

Clinical evidence indicates that cerebral ischemic lesions and infarcts are frequently present with AD pathology and cognitive decline. Reductions in CBF and glucose metabolism have also been found in elderly AD patients, but could be consequences rather than the causes of neurodegeneration. Therefore, the role of cerebral ischemia needs to be elucidated at early stage post ischemia with coexisting amyloid toxicity. Chapter 2 revealed disturbances in CBF and CBV from acute phase to the first month post ischemia and chapter 3 extended the investigation of chapter 2 to three months in our animal comorbid model of CI and amyloid injuries. Chapter 2 showed that the coexistence of CI and Aβ disrupted normal cerebral hemodynamics and exacerbated post-ischemia injury, as compared to the sham or Aβ alone. The major driving factor of hemodynamic dysfunction in the first month was ischemia. At 7 and 14 days post ischemia, hyperperfusion and hypervolemia in CI and CI+Aβ groups represented a reperfusion-related compensatory phenomenon. However, this prolonged hyperperfusion/hypervolemia may also be associated with inflammation and increased BBB leakage as demonstrated in chapter 3. Our observations suggest the yang (good) and the yin (bad) of prolonged hyperperfusion/hypervolemia post ischemia. A few important questions remain to be addressed: whether there is a long-term hypoperfusion in our animal model after 3 months; and whether hypoperfusion correlates with inflammation and BBB leakage, and precedes or follows neurodegeneration and cognitive decline.

5.3 Changes in BBB permeability/integrity

The local exchange of molecules in and out of the brain is tightly regulated by an intact BBB, thus BBB permeability surface (BBB-PS) can be an important indicator for BBB integrity. In chapter 3, BBB-PS, a functional biomarker of microvascular permeability derived from a CTP study, increased in CI+Aβ animals relative to CI or sham group at day 7, month 2 and 3. This suggests that CI can trigger a greater and chronic BBB disruption in the presence of amyloid toxicity. This may be associated with enhanced inflammatory reaction induced by combination of ischemic and amyloid injuries, which was demonstrated by PET imaging with ^{18}F-FEPPA. The initial pathogenic event at the prodromal stage of AD-related neurodegeneration must be a chronic and minimal perturbation to the central nervous system in order not to cause significant clinical symptoms. The opening or disruption of BBB after focal ischemia can be one of the driving causes leading to this chronic perturbation. The chronic BBB disruption observed in our animal model is similar to the elevated BBB-PS observed in stroke patients with lacunar/subcortical ischemic lesions at 7 days and 3 months post ischemia (chapter 4), because in our animal model CI was also induced in the subcortical location (striatum). Therefore, both animal and clinical studies suggest subcortical CI is highly related to BBB breakdown. The limitation of the studies in chapter 3 and 4 is the lack of investigation for the relationship between long-term cognitive/functional impairment and BBB leakage that we observed.

5.4 Activation of microglia and neuroinflammation

This thesis used in-vivo PET imaging of activated microglia to investigate inflammation in the animal comorbid model (chapter 3). PET imaging with ^{18}F-FEPPA revealed that activation of

microglia reached maximum at 7 days post insult in CI and CI+Aβ groups, with more activated microglia in CI+Aβ group. A significantly higher ^{18}F-FEPPA uptake was found in CI+Aβ group at 14 days as compared to both CI and sham groups. These findings demonstrate that neuroinflammation in CI+Aβ/comorbid group is more severe than that in CI group, suggesting a synergistic effect of CI and Aβ insult on triggering inflammatory reaction. This result is consistent with previous studies that showed enhanced neuroinflammation, associated neuronal damage (e.g. larger infarcted area) and cognitive decline in animal models and patients with such comorbidity (1-6). Under the converging influences of both CI and Aβ demonstrated in our comorbid model, inflammation can accelerate neuronal damage, potentially leading to cognitive deterioration.

5.5 Clinical relevance and implications

Past imaging studies of AD or cognitive impairment have focused on hypoperfusion or hypometabolism, which appears after onset of clinical symptoms from extensive neurodegeneration. Therefore, these studies might miss the initial causes responsible for hypoperfusion/hypometabolism and neuronal dysfunction. In contrast, the studies in this thesis demonstrated the contribution of cerebrovascular injury from ischemia to the pathogenesis of neurodegeneration and subcortical ischemic disease. Our animal CTP-PET studies successfully demonstrated the pathogenic mechanism and temporal profiles of vascular abnormalities and neuroinflammation at early stage post ischemic insult in the presence of amyloid toxicity. The in-vivo CTP-PET studies described in this thesis can be used in clinical research to identify suspected patients having cerebrovascular pathology, particularly those with increased BBB-PS and neuroinflammation in subcortical regions, which can contribute to and accelerate AD

development (7-10). In addition, PET imaging of inflammatory microglia offers a mean to detect disease progression and to monitor efficacy of therapy over time. Moreover, cerebral small vessel disease, a risk factor for vascular cognitive impairment, can result in elevated BBB-PS in small ischemic lesions in the basal ganglia, thalamus and surrounding white matter (11, 12), thus BBB-PS may be used as an indicator for management of BBB dysfunction or a predictor for progression of cognitive impairment.

5.6 Future work

The work of this thesis has provided a better understanding of hemodynamic and vascular abnormalities caused by cerebral ischemia, and investigated synergistic mechanism of ischemic and Aβ insults in contributing to neurodegeneration. However, some questions still remain unclear. The following section will outline possible research directions that may help answer these questions.

5.6.1 Examination of cognitive performance

Although increased BBB-PS, hemodynamic dysfunction and microglia activation were found in the animal comorbid model, our study did not monitor cognitive/functional impairment along with BBB breakdown and neuroinflammation over time. To address this question, future studies should perform animal cognitive testing using radial-arm maze (2) or Morris water maze (13) over the first 3 months or even longer term post insult. These cognitive tests are able to assess spatial learning and memory. The cognitive testing data may help in determining

correlation between our CTP-PET biomarkers and severity of cognitive impairment. The imaging biomarkers can then be used to monitor disease progression.

5.6.2 Amyloid or tau imaging

The pathological features of AD brain are amyloid aggregates and tau tangles. Recent development of PET radiotracers binding to amyloid and tau proteins points out a new direction for imaging neurodegeneration. With the coexistence of ischemic and amyloid injuries, the accelerated neurodegeneration may be correlated with increased levels of amyloid and/or tau pathology. Therefore, PET imaging of amyloid or tau proteins may be useful in investigating progression of these pathologies and related neurodegeneration. In addition, amyloid or tau imaging can also be used to determine whether there is a relation between BBB breakdown or cognitive impairment and increased levels of amyloid and/or tau pathology.

Furthermore, another method can also be used to study correlation between BBB breakdown and extravasation of blood-borne soluble Aβ into the brain. Fluorescent or radio-labeled amyloid proteins can be injected into the bloodstream after cerebral ischemia, and then near-infrared fluorescence camera or PET can be used to determine whether there is extravasation of those labeled Aβ through the leaky BBB caused by ischemia. This imaging study can facilitate our understanding of exogenous source of amyloid pathology when there is ischemia-induced BBB breakdown.

5.6.3 Long-term cognition and imaging study for patients with subcortical/lacunar lesions

In chapter 4, we have performed a longitudinal CTP study over the first 3 months post ischemic event, but this is not sufficient to determine underlying association between BBB dysfunction of subcortical lesions or WMLs and cognitive dysfunction. To address this question, a long-term imaging and cognition study focusing on cognitive changes in patients with small subcortical lesions and/or WMLs up to 1~2 years post initial stroke should be done. Neurocognitive assessments such as Mini Mental State Examination (MMSE), Alzheimer's Disease Assessment Scale-cognitive subsection (ADAS-cog) or Clinical Dementia Rating Scale (CDR) can be performed, and cognitive status of patients can be correlated with follow-up CTP results. In addition, MRI can also be included for follow-up imaging to investigate WMLs, atrophy, microbleeds or other abnormalities. Recurrent stroke and newly formed infarcts can also be documented via CT/MRI examinations. With this long-term imaging and cognition study, chronic changes of BBB permeability/dysfunction of subcortical lesions and WMLs can be correlated with long-term cognitive impairment to answer the question - does BBB dysfunction predict cognitive decline?

5.7 References

1. Amtul Z, *et al.* (2014) Comorbid Aβ toxicity and stroke: hippocampal atrophy, pathology, and cognitive deficit. *Neurobiology of aging* 35(7):1605-1614.
2. Iwasaki K, *et al.* (2006) Cerebral ischemia combined with β-amyloid impairs spatial memory in the eight-arm radial maze task in rats. *Brain research* 1097(1):216-223.
3. Lee MJ, *et al.* (2014) Synergistic effects of ischemia and β-amyloid burden on cognitive decline in patients with subcortical vascular mild cognitive impairment. *JAMA psychiatry* 71(4):412-422.
4. Li J, Wang YJ, Zhang M, Fang CQ, & Zhou HD (2011) Cerebral ischemia aggravates cognitive impairment in a rat model of Alzheimer's disease. *Life sciences* 89:86-92.
5. Whitehead SN, Cheng G, Hachinski VC, & Cechetto DF (2007) Progressive increase in infarct size, neuroinflammation, and cognitive deficits in the presence of high levels of amyloid. *Stroke* 38(12):3245-3250.
6. Snowdon DA, *et al.* (1997) Brain infarction and the clinical expression of Alzheimer disease: the Nun Study. *JAMA* 277(10):813-817.
7. Erickson MA & Banks WA (2013) Blood–brain barrier dysfunction as a cause and consequence of Alzheimer's disease. *Journal of Cerebral Blood Flow & Metabolism* 33(10):1500-1513.
8. Wardlaw J, Sandercock P, Dennis M, & Starr J (2003) Is breakdown of the blood-brain barrier responsible for lacunar stroke, leukoaraiosis, and dementia? *Stroke* 34(3):806-812.
9. Venneti S, Wiley CA, & Kofler J (2009) Imaging microglial activation during neuroinflammation and Alzheimer's disease. *Journal of Neuroimmune Pharmacology* 4(2):227-243.
10. Heneka MT, *et al.* (2015) Neuroinflammation in Alzheimer's disease. *The Lancet Neurology* 14(4):388-405.
11. Farrall AJ & Wardlaw JM (2009) Blood–brain barrier: ageing and microvascular disease–systematic review and meta-analysis. *Neurobiology of aging* 30(3):337-352.
12. O'Brien JT, *et al.* (2003) Vascular cognitive impairment. *The Lancet Neurology* 2(2):89-98.
13. Vorhees CV & Williams MT (2006) Morris water maze: procedures for assessing spatial and related forms of learning and memory. *Nature protocols* 1(2):848-858.

Appendix A: Animal Ethics Approval for the work contained within Chapter 2

Western

12.01.10
***This is the 2nd Renewal of this protocol**
*A Full Protocol submission will be required in **2012**

Dear Dr. **Cechetto**

Your Animal Use Protocol form entitled:

Mechanisms of Vascular Cognitive Impairment and Prevention of Stroke and its Consequences

has had its yearly renewal approved by the Animal Use Subcommittee.

This approval is valid from **12.01.10 to 12.01.11**

The protocol number for this project remains as **2008-113**

1. This number must be indicated when ordering animals for this project.
2. Animals for other projects may not be ordered under this number.
3. If no number appears please contact this office when grant approval is received.
   If the application for funding is not successful and you wish to proceed with the project, request that an internal scientific peer review be performed by the Animal Use Subcommittee office.
4. Purchases of animals other than through this system must be cleared through the ACVS office. Health certificates will be required.

REQUIREMENTS/COMMENTS
Please ensure that individual(s) performing procedures on live animals, as described in this protocol, are familiar with the contents of this document.
The holder of this *Animal Use Protocol* is responsible to ensure that all associated safety components (biosafety, radiation safety, general laboratory safety) comply with institutional safety standards and have received all necessary approvals. Please consult directly with your institutional safety officers.

c.c. Z. Amtul, W. Lagerwerf

***The* University *of* Western Ontario**
Animal Use Subcommittee / University Council on Animal Care
Health Sciences Centre, ● London, Ontario ● CANADA – N6A 5C1
PH: 519-661-2111 ext. 86770 ● FL 519-661-2028 ● www.uwo.ca / animal

Appendix B: Animal Ethics Approval for the work contained within Chapter 3

Western

AUP Number: 2012-067
AUP Title: Investigation of early functional and physiological changes of cerebral ischemia and amyloid-beta protein in a rat model of vascular cognitive impairment by using dynamic contrast-enhanced CT and PET imaging
Yearly Renewal Date: 06/01/2014

The YEARLY RENEWAL to Animal Use Protocol (AUP) 2012-067 has been approved, and will be approved for one year following the above review date.

1. This AUP number must be indicated when ordering animals for this project.
2. Animals for other projects may not be ordered under this AUP number.
3. Purchases of animals other than through this system must be cleared through the ACVS office. Health certificates will be required.

REQUIREMENTS/COMMENTS
Please ensure that individual(s) performing procedures on live animals, as described in this protocol, are familiar with the contents of this document.

The holder of this Animal Use Protocol is responsible to ensure that all associated safety components (biosafety, radiation safety, general laboratory safety) comply with institutional safety standards and have received all necessary approvals. Please consult directly with your institutional safety officers.

Submitted by: Kinchlea, Will D
on behalf of the Animal Use Subcommittee

The University *of* Western Ontario
Animal Use Subcommittee / University Council on Animal Care
Health Sciences Centre, ● London, Ontario ● CANADA – N6A 5C1
PH: 519-661-2111 ext. 86768 ● FL 519-661-2028
Email: auspc@uwo.ca ● http://www.uwo.ca/animal/website/

Appendix C: Human Ethics Approval for the work contained within Chapter 4

SERVIZIO SANITARIO REGIONALE
EMILIA-ROMAGNA
Azienda Ospedaliero - Universitaria di Ferrara

università di ferrara

SERVIZIO SANITARIO REGIONALE
EMILIA- ROMAGNA
Azienda Unità Sanitaria Locale di Ferrara

VERBALE n. 5 / 2012

SEDUTA COMITATO ETICO PROVINCIALE DEL 24/05/2012

In data giovedì 24 maggio 2012 dalle ore 14,30 alle ore 15,45 si è riunito, presso l'Aula Arlotti dell'Azienda Ospedaliero Universitaria "S,. Anna" di Ferrara il Comitato Etico della Provincia di Ferrara nelle persone di:

- **Prof.ssa Aurelia GUBERTI - Presidente** (designazione congiunta) - già Direttore del Dipartimento di Emergenza – AOU Ferrara
- **Prof. Francesco Maria AVATO – Coordinatore scientifico** - Direttore Universitario di Medicina Legale (ex officio) - Professore Ordinario di Medicina Legale e delle Assicurazioni - Università degli Studi di Ferrara
- **Dott. Stefano BIANCHI** - Delega del Direttore del Dipartimento Interaziendale del Farmaco (ex officio) - Farmacista Dirigente – U.O. Farmacia - AOU Ferrara
- **Prof. Pier Andrea BOREA** - Direttore Universitario della Sezione di Farmacologia (ex officio) - Direttore Sezione di Farmacologia - Università degli Studi di Ferrara
- **Prof.ssa Maurizia CAPUZZO** - Clinico designato dall'Azienda Ospedaliero Universitaria - Dirigente Medico U.O. Anestesia e Rianimazione Universitaria - AOU Ferrara
- **Prof. Adalberto CIACCIA** - Delega del Preside della Facoltà di Medicina e Chirurgia (ex officio) - Professore ordinario emerito di Malattie dell'Apparato Respiratorio - Università degli Studi di Ferrara
- **Prof. Carlo CONTINI** - Clinico designato dall'Università degli Studi di Ferrara - Professore ordinario Sezione Malattie Infettive - Università degli Studi di Ferrara
- **Dott.ssa Annamaria FERRARESI** - Nomina del Collegio IPASVI - Rappresentante infermieristico
- **Prof. Baldassare PASTORE** - Esperto di Bioetica (designazione congiunta) - Professore Ordinario di Filosofia del Diritto - Università degli Studi di Ferrara
- **Sig. Alberto PRONI** - Nomina dei Comitati Consultivi Misti - Rappresentante del volontariato
- **Dott. Giovanni SESSA** - Delega del Direttore Sanitario dell'Azienda Usl di Ferrara (ex officio) - Direttore U.O. Organizzazione e sviluppo comunicazione formazione qualità e accreditamento – Azienda Usl di Ferrara
- **Dott.ssa Sandra SOTTILI** - Esperto di Biostatistica (designazione congiunta) - Dirigente statistico - AOU S. Orsola-Malpighi Bologna
- **Dott. Natale VITA** - Nomina Azienda Usl di Ferrara - Medico di Medicina Generale
- **Dott. Ulrich WIENAND** - Delega del Direttore Sanitario dell'Azienda Ospedaliero Universitaria (ex officio) - Responsabile Staff Accreditamento Qualità Ricerca Innovazione – AOU Ferrara

Segreteria Amministrativa
Ufficio Ricerca e Innovazione
Staff AcQuaRI
Azienda Ospedaliero Universitaria
T. +39.0532.236.398 – 236.896
F. +39.0532.237.718
f.palara@ospfe.it
m.voci@ospfe.it

Segreteria Scientifica
Sezione di Medicina Legale
e delle Assicurazioni
Università degli Studi di Ferrara
T. +39.0532.455.527 – 455.554
F. +39.0532.455.777

U.O. Farmacologia Clinica
Dipartimento di Medicina
Clinica e Sperimentale
Università degli Studi di Ferrara
T. +39.0532.236.953 – 455.211 - 455209
F. +39.0532.455.205
smm@unife.it

SERVIZIO SANITARIO REGIONALE
EMILIA-ROMAGNA
Azienda Ospedaliero - Universitaria di Ferrara

università di ferrara

SERVIZIO SANITARIO REGIONALE
EMILIA- ROMAGNA
Azienda Unità Sanitaria Locale di Ferrara

COMITATO ETICO DELLA PROVINCIA DI FERRARA

Protocollo n. 53 – 2012

Ferrara, 24 maggio 2012

"Evoluzione dei disturbi emodinamici cerebrali e della barriera emato-encefalica dopo ictus ischemico acuto: uno studio di perfusione TC"

Proponente responsabile:

Dott. E. FAINARDI, Unità Operativa di Neuroradiologia, Dipartimento di Neuroscienza/Riabilitazione, Azienda Ospedaliero-Universitaria Arcispedale "S.Anna", Ferrara.

Staff operativo:

Dott. M. BORRELLI, U.O. di Neuroradiologia del Dipartimento di Neuroscienze/Riabilitazione della Azienda Ospedaliero-Universitaria S.Anna di Ferrara
Dott. F. CALZOLARI, U.O. di Neuroradiologia del Dipartimento di Neuroscienze/Riabilitazione della Azienda Ospedaliero-Universitaria S.Anna di Ferrara
Dott. A. SALETTI, U.O. di Neuroradiologia del Dipartimento di Neuroscienze/Riabilitazione della Azienda Ospedaliero-Universitaria S.Anna di Ferrara
Dott. L. BORGATTI, U.O. di Neuroradiologia del Dipartimento di Neuroscienze/Riabilitazione della Azienda Ospedaliero-Universitaria S.Anna di Ferrara
Dott. S. CERUTI, U.O. di Neuroradiologia del Dipartimento di Neuroscienze/Riabilitazione della Azienda Ospedaliero-Universitaria S.Anna di Ferrara
Dott. C. AZZINI, U.O. di Neurologia del Dipartimento di Neuroscienze/Riabilitazione della Azienda Ospedaliero-Universitaria S.Anna di Ferrara
Dott. A. DE VITO, U.O. di Neurologia del Dipartimento di Neuroscienze/Riabilitazione della Azienda Ospedaliero-Universitaria S.Anna di Ferrara
Dott.ssa P. MILANI, U.O. di Neurologia del Dipartimento di Neuroscienze/Riabilitazione

COMITATO ETICO DELLA PROVINCIA DI FERRARA

della Azienda Ospedaliero-Universitaria S.Anna di Ferrara
Dott. E. PAOLINO, U.O. di Neurologia del Dipartimento di Neuroscienze/Riabilitazione della Azienda Ospedaliero-Universitaria S.Anna di Ferrara
Prof.ssa M. R. TOLA, U.O. di Neurologia del Dipartimento di Neuroscienze/Riabilitazione della Azienda Ospedaliero-Universitaria S.Anna di Ferrara

Ditta/sponsor:	spontaneo
Codice identificativo del piano clinico generale:	/ /
Specialità medicinale (nome o sigla):	/ /
Principio/i attivo/i:	/ /
Codice CAS (ove disponibile):	/ /
Classe farmacologica di appartenenza:	/ /
Codice ATC proposto (secondo codifica OMS):	
Codice ICD:	/ /
Fase della sperimentazione clinica:	/ /
Indicazione proposta:	si tratta di uno studio volto a valutare il profilo temporale dei valori di flusso ematico cerebrale (CBF), volume ematico cerebrale (CBV), tempo medio di transito (MTT) e permeabilità microvascolare (PS) ottenuti con la Tomografia Computerizzata perfusionale (CTP) nei pazienti con ictus ischemico acuto durante le fasi evolutive iperacuta, acuta, subacuta e cronica per verificare le eventuali relazioni fra questi parametri e gli indici clinici e neuroradiologici di severità della malattia e di decadimento cognitivo.
Forma farmaceutica:	/ /

COMITATO ETICO DELLA PROVINCIA DI FERRARA

Via di somministrazione: / /

Durata dello studio: 24 mesi

Schema dello studio: nei paesi industrializzati, l'ictus ischemico rappresenta la terza causa di morte dopo malattie cardiovascolari e tumori ed è una delle principali cause di disabilità. Attualmente, l'unica terapia riconosciuta, approvata e disponibile per la fase acuta dell'ictus ischemico riguarda le lesioni che interessano il territorio di irrorazione dell'arteria cerebrale media (ACM) ed è costituita dalla trombolisi mediante iniezione per via endovenosa della forma ricombinante dell'attivatore del plasminogeno tissutale (rtPA). Al momento, si ritiene che tale trattamento possa rivelarsi efficace solo se somministrato entro 3 ore dall'esordio dei sintomi ed in pazienti selezionati sulla base dei reperti della Tomografia Computerizzata (TC) cerebrale di ammissione eseguita senza somministrazione endovenosa di mezzo di contrasto iodato non-ionico (mdc), anche se recentemente numerosi studi hanno dimostrato la possibilità di ampliare la finestra terapeutica sino a 4.5 ore dall'ictus. I criteri TC utilizzati sono essenzialmente rappresentati dall'assenza di immagini riferibili ad emorragie cerebrali e dalla presenza di segni precoci di infarto e, cioè, di una ipodensità parenchimale e/o di rigonfiamento cerebrale focale di dimensioni superiori ad un terzo della regione di pertinenza della ACM. Infatti, la comparsa di una ipodensità precoce a carico del tessuto cerebrale viene ritenuta compatibile con edema citotossico e, pertanto, indicativa di danno irreversibile.
L'ipodensità precoce, quindi, rappresenterebbe la porzione centrale dell'area ischemica, il cosiddetto "core ischemico", dove il tessuto cerebrale risulta severamente ipoperfuso, non è più vitale né potenzialmente recuperabile in caso di riperfusione ed evolve irrimediabilmente verso l'infarto. Lo stesso significato viene attribuito al rigonfiamento cerebrale focale che si associa quasi inevitabilmente all'ipodensità precoce e si esprime con un appianamento dei solchi emisferici e/o una compressione dei ventricoli cerebrali.
Il metodo più utilizzato per calcolare l'estensione degli eventuali segni precoci di infarto alla TC cerebrale di ingresso è il cosiddetto ASPECTS (Alberta Stroke Program Early CT Score), in cui il territorio della ACM viene valutato su due sezioni TC passanti per i nuclei della base ed i tetti ventricolari, rispettivamente, e risulta suddiviso in 10 zone a ciascuna delle quali viene attribuito un punto. Per ogni area interessata da segni precoci di infarto si sottrae un punto dal conteggio. Se il punteggio finale è superiore a 7 significa che meno di 1/3 del territorio della ACM è danneggiato in modo irreversibile e, perciò, la trombolisi viene eseguita. Se il punteggio finale è inferiore o uguale a 7, invece, il trattamento trombolitico non viene praticato perché il danno irreversibile interessa più di 1/3 del territorio della ACM. Tuttavia, è noto che la ridotta densità parenchimale determinata dall'insulto ischemico diventa completamente visibile alla TC cerebrale solo dopo circa 24 ore dall'esordio dei sintomi, rendendo in questo modo difficoltoso l'esatto riconoscimento dei segni precoci di infarto e, quindi, la valutazione delle reali dimensioni del core ischemico. Inoltre, è stato dimostrato che il rigonfiamento cerebrale focale senza ipodensità concomitante non è indicativo di infarto ma di penombra ischemica o oligoemia. D'altra parte, l'area ipodensa prodotta da un'occlusione vasale non necessariamente è ischemica ma può essere anche iperperfusa. Infine, la TC cerebrale senza mdc non è in grado di fornire alcuna informazione sull'estensione e sull'entità dei disordini perfusionali che si verificano nel contesto della lesione ischemica. In particolare, la TC cerebrale convenzionale non riesce ad identificare la penombra ischemica e, cioè, la zona

periferica dell'area ischemica che contorna il core dove il tessuto cerebrale si dimostra severamente ipoperfuso, danneggiato in modo reversibile, ancora vitale e potenzialmente recuperabile in caso di riperfusione ed a rischio di infarto.

Fra le diverse metodiche perfusionali capaci di dimostrare i disturbi emodinamici caratteristici delle lesioni ischemiche, la Tomografia ad Emissione di Positroni (PET) e le Risonanza Magnetica (RM) pesata in Diffusione (DWI) e Perfusione (PWI) sono attualmente considerate gli strumenti più adeguati per differenziare fra infarto e penombra ischemica. Queste tecniche, però, hanno numerosi limiti fra cui, soprattutto, l'alto costo, le difficoltà organizzative ed il lungo tempo di esecuzione che ne rendono problematica l'applicazione nel paziente con ictus ischemico in fase acuta.

Per tali ragioni, ultimamente l'interesse si è sempre più concentrato sulla TC Perfusionale (CTP), una metodica rapida e di semplice esecuzione che appare in grado di discriminare fra tessuto cerebrale irreversibilmente danneggiato (infarto) e tessuto cerebrale danneggiato in modo reversibile ed a rischio di infarto (penombra). In particolare, è stato ripetutamente provato che la CTP è in grado di identificare il core e la penombra all'interno di un'area ischemica mediante parametri sia qualitativi, che quantitativi. Infatti, con la CTP è possibile generare mappe perfusionali di flusso ematico cerebrale (CBF), di volume ematico cerebrale (CBV) e di tempo medio di transito (MTT), i cui valori vengono espressi in termini assoluti.

Lo studio comporta un'analisi clinico-radiologica longitudinale nel tempo di pazienti affetti da ictus ischemico acuto comprendente: 1) studi con TC cerebrale standard, Angio-TC e CTP programmati all'ammissione e a 24 ore, 7-10 giorni e 3 mesi dall'esordio; 2) il calcolo del punteggio del National Institutes of Health Stroke Scale (NIHSS) previsto negli stessi intervalli temporali; 3) il calcolo del punteggio del Rankin Scale modificato (mRS) pianificato a 3 mesi dall'esordio e l'esecuzione di una batteria di test neuropsicologici stabiliti a 7 giorni, 3 mesi e 12 mesi dall'esordio.

Il fine ultimo della ricerca è quindi quello di accertare l'effettivo ruolo della TC perfusionale come strumento predittivo del destino funzionale del tessuto ischemico in modo da migliorare le capacità di selezione dei pazienti candidati alle terapie di riperfusione e prevedere l'evoluzione clinica dei pazienti colpiti da ictus ischemico acuto in modo da attivare rapidamente tutte le modalità di supporto necessarie per fornire a questi pazienti un adeguato trattamento non solo in fase precoce, ma anche negli stadi tardivi della malattia.

Saranno inclusi nello studio tutti i pazienti con diagnosi clinica di ictus ischemico cerebrale emisferico confermata dall'esame di TC cerebrale che verranno accolti in Neurologia entro le prime 9 ore dall'insorgenza dei sintomi. L'analisi comprenderà sia i pazienti trattati con trombolisi endovenosa e/o intra-arteriosa o con trombectomia per via endovascolare secondo le linee guida attualmente accettate.

Tutti i pazienti arruolati nello studio saranno sottoposti a controlli longitudinali nel tempo di tipo clinico-radiologico programmati all'esordio (entro 9 ore), a 24 ore, 7-10 giorni e 3 mesi dalla comparsa dei sintomi ed a una batteria di test neuropsicologici programmati a 7-10 giorni a 3 mesi e a 12 mesi dall'esordio.

Valutazione clinica.

Tutti i pazienti accettati nello studio (trattati e non trattati con terapie di riperfusione) saranno sottoposti ad esame neurologico completo con calcolo del punteggio NIHSS (National Institutes of Health Stroke Scale) per definire la severità clinica dello stroke in ciascun intervallo temporale stabilito: all'esordio (entro 9 ore) e dopo 24 ore, 7-10 giorni e 3 mesi dall'esordio dei sintomi. A 3 mesi dall'ingresso verrà anche effettuato il calcolo del punteggio

COMITATO ETICO DELLA PROVINCIA DI FERRARA

della scala di Rankin modificata (mRS) per misurare l'evoluzione dell'ictus ischemico in senso prognostico.

Valutazione neuroradiologica.

In ogni periodo di tempo programmato (all'esordio, a 12 ore, 24 ore, 7-10 giorni e 3 mesi dall'ingresso), tutti i pazienti ammessi nello studio (trattati e non trattati con terapie di riperfusione) verranno sottoposti a TC cerebrale standard senza somministrazione e.v. di mezzo di contrasto iodato, Angio-TC con infusione e.v. di mdc (60 ml) e CTP con iniezione e.v. di mdc (40 ml) eseguite mediante un apparecchio TC a rotazione continua con acquisizione a scansione multipla di 64 strati (CT HiSpeed ZX/i; GE Medical System, Milwaukee, Wis).

In ogni paziente ed in ogni intervallo temporale stabilito verranno calcolati i seguenti parametri:

- TC standard: calcolo del volume dell'infarto mediante la misurazione del punteggio ASPECTS all'esordio e tramite metodo planimetrico, che consiste nel moltiplicare l'area della lesione disegnata a mano libera in ciascuna sezione TC per il corrispondente spessore di strato, a 12 ore, 24 ore, 7-10 giorni e 3 mesi dall'ingresso e valutazione dell'eventuale presenza di trasformazione emorragica in accordo con i criteri indicati dalla letteratura.
- Angio-TC: valutazione della sede e del grado di occlusione vasale ed analisi dell'eventuale ricanalizzazione in accordo con i criteri di letteratura attraverso l'utilizzo di ricostruzioni agiografiche di tipo Multiplanar Reconstruction (MPR) e Volume Rendering (VR).
- CTP: valutazione dei disordini perfusionali mediante la generazione delle mappe di CBF, CBV, MTT e PS tramite algoritmi di deconvoluzione e di approssimazione adiabatica del modello di omogeneità tissutale.

La cadenza temporale degli esami TC ed il protocollo TC previsti dallo studio sono esattamente quelli attualmente adottati nel nostro Dipartimento per tutti i pazienti con ischemia cerebrale acuta che presentano le caratteristiche della popolazione studiata. Lo studio, pertanto, non comporta oneri economici aggiuntivi rispetto alla normale pratica clinica.

Valutazione neuropscicologica.

In ciascun intervallo temporale previsto (a 7-10 giorni a 3 mesi e a 12 mesi dall'ammissione), i pazienti inclusi nello studio (trattati e non trattati con terapie di riperfusione) saranno sottoposti ad una batteria di esami neuropsicologici comprendente:

- Mini-Mental State Examination per la valutazione dello stato mentale;
- Verbal Fonological and Semantic Fluency Test per la valutazione delle funzioni esecutive e di linguaggio;
- Babcock's Story for verbal memory per esaminare la memoria a breve e lungo termine
- Picture Cancellation Test (Bells Test) per misurare l'attenzione e l'esplorazione visuo-spaziale
- Beck Depression Inventory per la misurazione del grado di depressione
- Hamilton Anxiety Rating Scale per la misurazione del grado di ansia

Analisi statistica.

L'analisi statistica comprenderà una prima valutazione della distribuzione delle diverse variabili mediante test di Kolmogorov-Smirnov. Successivamente il paragone fra le medie verrà eseguito attraverso test parametrici (ANOVA, ANOVA per misure ripetute, t test) in caso di distribuzione normale o mediante test non parametrici (Kruskal-Wallis, Friedman e Mann-Whitney) in caso di distribuzione non normale. Le correlazione verranno esaminate quindi con la Regressione Lineare nel primo caso e con il test di Spearman nel secondo. I confronti

COMITATO ETICO DELLA PROVINCIA DI FERRARA

fra percentuali verranno eseguiti con il chi-quadro. Un valore di $p < 0.05$ verrà considerato statisticamente significativo.

Eventuale terapia concomitante: / /

AIC in Italia:
all'estero: / /

Indicazioni all'AIC, posologia, vie di somministrazione e forme farmaceutiche autorizzate: / /

Precedenti approvazioni/autorizzazioni alla sperimentazione per la stessa indicazione proposta: / /.

Obiettivo/i dello/degli studio/i:
Primario:

- verificare se la lesione visibile nella mappa di CBV all'esordio, in fase iperacuta, rappresenta veramente il core ischemico mediante il confronto fra l'estensione del deficit CBV calcolato all'ammissione ed il volume dell'infarto finale misurato a 3 mesi dall'ictus e stabilire la possibile correlazione fra valori di permeabilità microvascolare e sviluppo di un declino cognitivo

Secondario:

- valutare la storia naturale dei disordini perfusionali durante le fasi evolutive iperacuta, acuta, subacuta e cronica dell'ictus cerebrale, chiarire se il deficit di permeabilità microvascolare evidenziato all'esordio nella mappa PS è effettivamente in grado di prevedere il successivo infarcimento emorragico della lesione ischemica e esaminare il potere prognostico delle diverse mappe perfusionali utilizzando misure di outcome cliniche e radiologiche.

Tipologia dei soggetti da arruolare (specificare se pazienti o volontari sani): pazienti di ambo i sessi ed età compresa tra i 18 e gli 80 anni con diagnosi clinica di ictus ischemico cerebrale emisferico acuto che soddisfino i criteri di inclusione

Numero dei soggetti da arruolare: 22

Informazione al candidato: mediante scheda informativa nella quale si riporteranno notizie sulla natura, i metodi e scopo dello studio, nonché il rapporto rischio/beneficio.
L'informazione del paziente, in virtù della propedeuticità di tale fase, dovrà essere fornita in un momento formalmente distinto dal recepimento del consenso.

COMITATO ETICO DELLA PROVINCIA DI FERRARA

Si raccomanda che l'avvenuta informazione venga formalizzata su cartella clinica o su scheda personale del paziente (in alternativa su modulo che ne faccia parte integrante), riportando contestualmente data e firma del medico sperimentatore e dell'arruolando stesso.

Recepimento del consenso: mediante apposito modulo

Si raccomanda che il recepimento del consenso/dissenso avvenga in un momento formalmente distinto dalla fase informativa e ad essa successivo e venga formalizzato su cartella clinica o su scheda personale del paziente (oppure su modulo che ne faccia parte integrante).

Criteri di inclusione/esclusione:
criteri di inclusione:

- pazienti di ambo i sessi ed età compresa fra i 18 ed gli 80 anni;
- improvvisa comparsa di manifestazioni neurologiche focali attribuibili ad ictus ischemico acuto nel territorio della ACM;
- epoca di insorgenza dei sintomi chiaramente definita;
- ictus ischemico acuto clinicamente stabile con punteggio NIHSS compreso fra 4 e 20;
- assenza di disordini di tipo afasico;
- esecuzione di TC standard, CTA e CTP all'ingresso;
- presenza di segni precoci di ischemia iperacuta in un'area inferiore a 1/3 del territorio della ACM alla TC standard di ammissione calcolati sulle due sezioni TC indicate dall'ASPECTS.

criteri di esclusione:

- età inferiore ai 18 anni e superiore a 80 anni;
- rapido miglioramento delle manifestazioni neurologiche focali attribuibili ad ictus ischemico acuto nel territorio della ACM o improvvisa comparsa di disturbi neurologici focali di grado lieve ("minor stroke");
- epoca di insorgenza dei sintomi sconosciuta;
- ictus ischemico acuto clinicamente severo con punteggio NIHSS superiore a 20;
- mRS superiore a 1;
- crisi epilettica all'esordio;
- stato di coma;
- presentazione clinica suggestiva di emorragia subaracnoidea (anche in caso di TC standard normale);
- pregressa storia riferibile a emorragia subaracnoidea, aneurismi, malformazioni artero-venose, emorragia intraparenchimale o tumori;
- altro ictus ischemico o trauma cranico grave nei 3 mesi precedenti all'esordio;

COMITATO ETICO DELLA PROVINCIA DI FERRARA

- uso di anticoagulanti orali o tempo di protrombina superiore a 1.7 INR;
- uso di eparina nelle 48 precedenti all'esordio o tempo di tromboplastina parziale superiore a 1.5 rispetto alla norma;
- conta piastrinica inferiore a 100.000/mm^3;
- ematocrito inferiore a 0.25;
- glicemia inferiore a 50 o superiore a 200 mg/dl;
- pressione arteriosa sistolica superiore a 185 mm/Hg o pressione arteriosa distolica superiore a 110 mm/Hg non reponsive alla terapia anti-ipertensiva;
- diatesi emorragica ereditaria o acquisita;
- retinopatia emorragica;
- infarto miocardio acuto nelle 3 settimane precedenti all'esordio;
- emboli settici, endocardite batterica, pericardite;
- pancreatine acuta;
- malattie epatiche di grado severo;
- diabete;
- interventi chirurgici maggiori o trauma grave nei 3 mesi precedenti all'esordio;
- emorragie gastrointestinali o dell'apparato urinario nei 21 giorni precedenti all'esordio;
- presenza di malattie ulcerative gastrointestinali nei 3 mesi precedenti all'esordio;
- presenza di varici esofagee, di aneurismi o di malformazioni artero-venose a livello sistemico;
- puntura arteriosa in una sede non comprimibile nei 7 giorni precedenti all'esordio;
- stato di gravidanza;
- presenza di afasia;
- mancata esecuzione di TC standard e/o CTA e CTP all'ingresso;
- presenza di emorragia cerebrale alla TC standard di ammissione;
- presenza di segni precoci di ischemia iperacuta in un'area superiore a 1/3 del territorio della ACM alla TC standard di ammissione calcolati sulle due sezioni TC indicate dall'ASPECTS;
- riconosciuta sensibilità nei confronti dei mezzi di contrasto iodati.

Sorveglianza clinica: //

Il Comitato Etico esprime parere favorevole allo studio proposto, ove siano soddisfatti i prerequisiti etici nei termini innanzi richiesti.

Si ricorda al proponente responsabile la necessità di comunicare alla Segreteria Tecnico-Scientifica del Comitato Etico la fine dello studio, nonché di trasmettere copia di eventuale/i pubblicazione/i ovvero del report finale.

Si dà atto che il Comitato Etico ha preso visione della seguente documentazione:
- n.1 copia di lettera di intenti datata 4 maggio 2012;
- n.1 copia di richiesta di autorizzazione allo svolgimento dello studio clinico datata 4 maggio 2012;

COMITATO ETICO DELLA PROVINCIA DI FERRARA

- n.1 copia di analisi dell'impatto economico ed organizzativo per studi clinici;
- n.1 copia di protocollo di studio;
- n.1 copia di foglio informativo per il paziente;
- n.1 copia di modulo di consenso per il paziente;
- n.1 copia di lettera per il medico di base;
- n.1 copia di presentazione del progetto a European Network e Canadian Stroke Network;
- n.1 copia di approvazione del finanziamento da parte di European Stroke Network e Canadian Stroke Network.

Il Presidente del Comitato Etico
(dott.ssa Aurelia Guberti)

Appendix D: Copyright Agreement

"Hemodynamic Effects of Combined Focal Cerebral Ischemia and Amyloid Protein Toxicity in a Rat Model: A Functional CT Study" published in *PLoS ONE*. 2014, 9(6): e100575 by J. Yang, C.D. d'Esterre, Z. Amtul, D.F. Cechetto and T.Y. Lee.

Appendix E: Absolute values of CBF and CBV

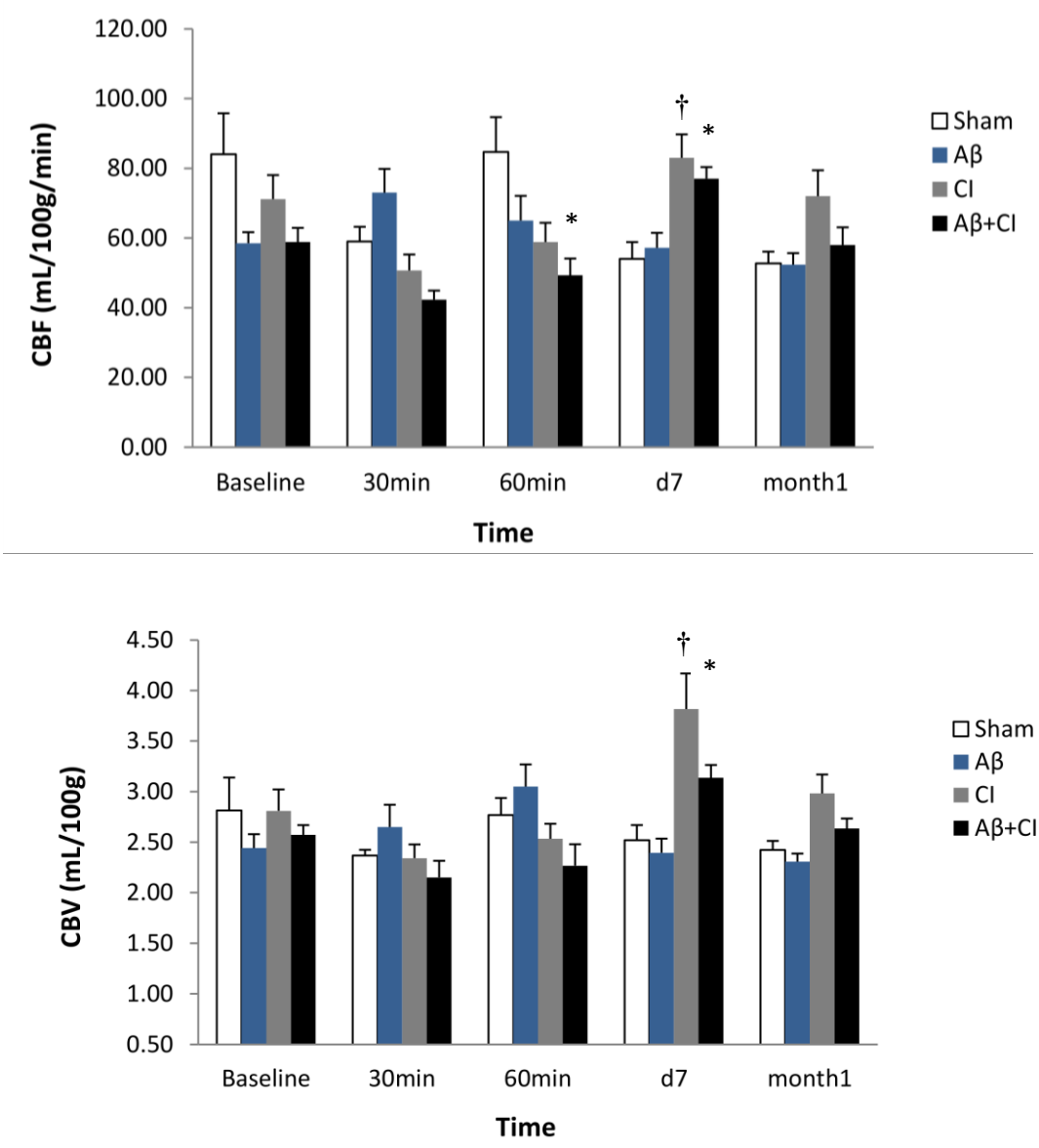

Figure AP-1: Absolute CBF and CBV in the striatal lesions. No significant differences in CBF were shown among four groups at baseline, 30 min and month 1. No significant differences in CBV were shown among four groups at baseline, 30-60 min and month 1. However, Aβ+CI group had a lower CBF at 60 min compared to sham group (*, $p<0.05$). At day 7, higher CBF and CBV (hyperperfusion/hyperemia) were observed in both CI and Aβ+CI groups compared to sham and Aβ († and *, $p<0.05$).

Curriculum Vitae

Jun (Kevin) Yang

Education

Ph.D. Medical Biophysics, 2009 – Present

University of Western Ontario (UWO), London, Ontario, Canada

B.Sc. High Honours, Biology 2005 – 2009

Minor program in Chemistry

Carleton University, Ottawa, Ontario, Canada

Work Experience

Research assistant, Department of Biology, Carleton University, Ottawa, Canada. 2009

Visiting researcher, Institute for Biological science (IBS), National Research Council of Canada (NRC), Ottawa, Canada. 2008

Major Awards

WGRS scholarship, UWO 2009 - 2014

Dean's list award, Carleton University 2007-2008 and 2008-2009

Conferences and Presentations

1. "Preclinical investigation of progressive effects of β-amyloid accumulation and ischemic stroke on vascular cognitive impairment using CT imaging". J. Allyn Taylor International Prize in Medicine, London, Ontario, Canada. November 2010.

2. "Combined hemodynamic effects of β-amyloid protein and cerebral ischemia in a rat model of cognitive impairment: A CT Perfusion study". The 10th Imaging Network Ontario (ImNO), Toronto, Ontario, Canada. February 2012.

3. "Investigation of cerebral hemodynamics in a rat model of combined β-amyloid pathology and ischemic stroke: A CT Perfusion study". London Health Research Day, London, Ontario, Canada. March 2012.

4. "Combined hemodynamic effects of β-Amyloid protein and cerebral ischemia in a rat model of cognitive impairment: A CT Perfusion study". Alzheimer's Association International Conference (AAIC), Vancouver, British Columbia, Canada. July 2012.

5. "Contrast-enhanced CT reveals the early hemodynamic changes of focal cerebral ischemia and amyloid protein toxicity in a rat model". The 12th Imaging Network Ontario (ImNO), Toronto, Ontario, Canada. March 2014.

6. "Dynamic contrast-enhanced CT reveals the early hemodynamic and chronic blood-brain-barrier changes in a rat model of combined focal cerebral ischemia and amyloid protein toxicity". The 23rd European Stroke Conference (ESC), Nice, France. May 2014.

Invited talks

1. "Imaging of blood-brain barrier breakdown and neuroinflammation: CT perfusion and PET". 2015 MB-ON End MS (Multiple Sclerosis) RRTC Educational Program, London, Ontario,

Canada. February 2015.

Publications

1. **Jun Yang**. "Combined hemodynamic effects of β-Amyloid protein and cerebral ischemia in a rat model of cognitive impairment: A CT Perfusion study". *Alzheimer's & Dementia*. 2012, 8(4), S21-22

2. **Jun Yang**, C.D. d'Esterre, Z. Amtul, D.F. Cechetto and T.Y. Lee. "Hemodynamic Effects of Combined Focal Cerebral Ischemia and Amyloid Protein Toxicity in a Rat Model: A Functional CT Study". *PLoS ONE*. 2014, 9(6): e100575

Submitted Manuscripts

1. **Jun Yang**, C.D. d'Esterre, S. Ceruti, G. Roversi, A. Saletti, E. Fainardi and T.Y. Lee. "Temporal changes in blood-brain barrier permeability and cerebral perfusion in lacunar/subcortical ischemic stroke". Accepted by *BMC Neurology*. September 2015

2. **Jun Yang**, L. Morrison, L. Wang, N. Cockburn, D.F. Cechetto and T.Y. Lee. "Breakdown of Blood-Brain Barrier and Neuroinflammation in a Rat Model of Combined Focal Cerebral Ischemia and Amyloid Protein Toxicity: A Longitudinal CT and PET Study". *Frontiers in Aging Neuroscience*, August 2015